TRANSFER PROCESSES

IN

STEADY TWO-DIMENSIONAL SEPARATED FLOWS

by

Akshai Kumar Runchal

Thesis submitted for the degree of
Doctor of Philosophy
in the Faculty of Engineering
University of London.

January 1969

... to a growing realisation
that the future of any
section of mankind is
linked intimately to
the future of mankind
as a whole ...

Abstract

A general solution procedure is described to predict the transport of momentum, enthalpy and matter in steady, two-dimensional, incompressible, laminar or turbulent flows. The procedure is based upon a special 'upwind' difference scheme so as to ensure that the resulting difference equations converge to a solution in an iterative procedure, and that they obey the physical laws of conservation.

To permit prediction of turbulent flows, a modified form of the Kolmogorov-Prandtl hypotheses of turbulence is employed. Also used is a model of a Couette flow for regions close to solid walls where the dependent variables often have steep gradients. The use of this model allows the computer time to be employed more economically.

As a comment on the accuracy, economy, and applicability of the procedure, predictions are obtained for two flow problems: the laminar flow in a square cavity with a moving lid, and the turbulent flow downstream of a sudden enlargement in a circular pipe. These predictions are examined in the light of the available experimental and theoretical information.

Finally, an experimental investigation for the sudden-enlargement problem is reported. Experimental data, obtained for very high Schmidt numbers by the use of 'diffusion-controlled electrolysis' are presented.

Preface

This thesis represents the main result of my research activities during the last three years or so. It describes a general solution procedure for the prediction of steady, two-dimensional imcompressible flows. To the best of my knowledge, it is based upon more secure mathematical foundations than most other methods, and, undoubtedly, has a very wide field of applicability.

At the time of my arrival (October 1965) in the Mechanical Engineering Department of the Imperial College, research activities were being directed towards the use and exploration of the integral profile methods for the solution of the differential equations which govern the transfer processes in the boundary-layer type of flows. It was thought, at the time, that a logical extension of the then existing methods would be their application to separated flows. With this aim in mind, I completed a survey of the integral profile methods. However, during the next few months it became apparent that the parabolic equations of the boundary-layer type were unsuitable for the description of recirculating flows or flows with no dominant direction of velocity. A search for alternative methods immediately centred on the numerical solution of the steady-state Navier-Stokes equations which are of elliptic type and adequately describe the flows mentioned above. Suggestions of Spalding (1966) were incorporated in a numerical procedure by Runchal and Wolfshtein (1966). A modified solution procedure, which to this date has remained essentially unchanged, was later presented by

Runchal, Spalding and Wolfshtein (1967).

Once a reliable solution procedure had been devised, I was able to devote almost my entire attentions to the experimental project. The application of an electrolysis technique to mass-transfer in separated flows at high Schmidt numbers proved, as is usual, frustrating in the initial stages. However, by the end of March 1968, I was able to obtain the required data and learn my lessons about some of the problems posed by separated flows.

Final comparisons of the predictions with the experimental data of other research workers, and with those of mine, were carried out during the summer of 1968. However, the writing-up of this thesis was delayed because of my contribution to the Post-Experience Course in 'Heat and Mass Transfer in Recirculating Flows' held in the Mechanical Engineering Department. The experience gained from this Course has proved very valuable to me in my general understanding of recirculating flows and, in particular, has influenced the presentation of chapters 2, 3 and 8.

Now that it is time for me to acknowledge the training and help that I have received from various individuals, I find it hard to distinguish my contribution from that of Professor Spalding, my supervisor. At almost every stage of my research activities he was very closely involved, sometimes through direct participation, but mostly in an advisory capacity. His optimistic and ambitious attitude did much to prevent me from being dismayed by the initial difficulties involved. At practically every crossroad, he was able to identify the path that led in the direction of

the main goal. At this moment of introspection, I can think of at least a few instances when I lost valuable time by either not heeding, or not seeking, his advice. I also owe a lot to Spalding for his persistent and patient advice on the grammar, the logic and the semantics of the English language. If this thesis is still inadequate in these respects, as is more than probable, all that I can say is that it would have been much worse but for Spalding's constructive criticism. I cannot truthfully say that I always enjoyed his merciless correction of my reports but I can definitely say that I always benefited from his criticism: after all, most medicines are bitter to swallow, but they do good.

Almost all of the work on the basic numerical procedure and the basic computer programme was done in close cooperation with Mikha Wolfshtein. This partnership with him, and his friendship, has been a most helpful influence. The credit for the development of the numerical procedure is shared by him at every level. Suhas Patanker patiently explained the intricacies of the principles of heat transfer and fluid flow in the initial stages of my research programme. David Gosman and Dr. Iribarne made the application of the experimental technique far less painful than it would otherwise have been. The beneficial effects of the discussions during the Sunday-afternoon coffees with David have been too helpful to escape mention. I also wish to thank David Hayes for many helpful discussions and comments.

There are many others to whom my thanks are due. For lack of space, I find myself unable to mention all the individuals by name who have contributed to this thesis in

various capacities. But I wish to mention specifically Bob Curr, Bob King, Krishnan, Rodney Le Feuvre, Norman Mitchell, Dr. Pun and Alan Robinson. My thanks are also due to Miss E. Archer for library services, and to Miss M. P. Steele for help and advice in connection with countless secretarial and administrative problems. The Tea Club in the Heat Transfer Laboratory always provided a welcome distraction during the routine of experimental work.

I find myself unable to express my feelings in words for the active encouragement and support of my parents, Yashoda and Boota Ram, and my sisters, Raksha and Smiti, in my pursual of an engineering career. To a large extent, it is Raksha's active interest which enables me to present this thesis.

Most of the work reported in this thesis was carried out during the tenure of a scholarship from I.C.I. (India) Pvt. Ltd. A generous allocation of computer time by the Centre for Computing and Automation of Imperial College and the development of a contour plotting subroutine by Richard Graham of C.C.A. contributed to the speed of execution of this project.

London, January 1969. A. K. Runchal

Contents

Chapter 1

Prologue

1.1 The problem considered

Flow separation, a commonly encountered engineering phenomenon, may increase or decrease the usefulness of an engineering device. An example of the increase in usefulness is the use of turbulence promoters on the wings of an aeroplane; that of the decrease is the stall of an aerofoil at large angles of incidence.

Separation is caused by an adverse pressure gradient; and in engineering practice its most common cause is an abrupt change in the profile of a solid surface in contact with the fluid - in other words, 'a surface discontinuity'. An example in confined flows is the sudden change in the diameter of a pipe; in unconfined flows it may be caused by a depression in, or a protrusion from, an otherwise smooth surface, such as a step in an open channel.

However, surface discontinuity is not the only cause of separation: there are others. As the present thesis is intended to deal only with steady subsonic flows, some types of separation will not fall within its scope; among these types are the separation due to impulsive motion and that induced by an incident shock-wave. A type of separation which is to be considered is that induced by an adverse pressure gradient even on smooth surfaces without any surface discontinuity. In such cases, the pressure gradient progressively retards the fluid, the effect being more pronounced on the low-momentum fluid near the wall. This fluid is ultimately unable to overcome the opposing

pressure and there results a reversal in the direction of flow: this is termed 'boundary-layer separation'. Perhaps the best known example of such behaviour is the flow separation from the rear of a circular cylinder placed transverse to a stream of fluid.

In spite of their common occurrence and their technical importance, separated flows remain relatively unexplored; they pose a formidable problem for the engineer who is often incapable of evaluating their advantages - such as the increased heat transfer - against their disadvantages - such as the increased pressure loss. This scarcity of information is a result of the mathematical complexity of the system of equations which describe separated flows. For laminar, incompressible, flows the problem is defined by the Navier-Stokes equations (see, e.g., Bird, Stewart & Lightfoot 1960). For steady turbulent flows a common approach is to assume that the flow can be adequately represented by a fluctuating component superimposed on a time-mean flow; this, via the Navier-Stokes equations, leads to what are commonly referred to as the Reynolds equations. Transfer of heat and mass is governed by equations mathematically similar to the hydrodynamic equations.

The magnitude of the mathematical problem can be appreciated by recognizing that the Navier-Stokes (as well as the Reynolds) equations are a set of coupled non-linear second-order partial differential equations. For steady-state flows, these equations are of elliptic nature (see, e.g., Forsythe & Wasow 1960). Even the theory of such linear partial differential equations is in a far from

satisfactory state (e.g. Bramble 1966); that of non-linear equations can only be described as fragmentary (e.g. Ames 1967). A result of their mathematical complexity is that these equations, in the absence of any simplifying assumptions, are impervious to known analytic techniques. For turbulent flows, the Reynolds equations do not even define a closed mathematical system: introduction of the fluctuating components of flow results in the number of unknowns exceeding the number of available equations. One way to make the problem tractable is to supply the additional information in the form of physical hypotheses about the structure of turbulence; the fluctuating components can then be related to the mean components of flow.

Additional mathematical and physical complicacies arise from the evidence that some steady and two-dimensional flows develop unsteady and three-dimensional characteristics after separation. The phenomena associated with the vortex street behind a cylinder provide a striking example of the separation-induced unsteady behaviour of a flow. Three-dimensional and unsteady phenomena have also been noted in certain regions of otherwise steady, two-dimensional flows by, for example, Tani (1958), Abbot & Kline (1962) and Filetti & Kays (1967).

It is no surprise therefore that the analysis of separated flows is still at a primitive stage. Though some methods exist for laminar flows, they are by no means applicable generally; moreover, in practice, most problems involve turbulence.

The basic task, therefore, is to devise a solution procedure for non-linear second-order partial differential equations, such as the Navier-Stokes equations. Within the restrictions imposed, those of steady, incompressible and two-dimensional flows, the solution procedure must be generally applicable to all types of boundary and flow problems; it must, of course, be economical enough to be of use for design purposes. Once the mathematical problem has been successfully tackled, attention can be turned to obtaining and testing the physical information concerning the structure of turbulence and the special phenomena associated with separation.

1.2 Previous knowledge

1.2-1 Numerical solutions of the complete equations

The improbability of obtaining analytical solutions for the complete differential equations has forced a search for alternatives and, of those explored, numerical methods of the finite-difference type have proved to be the most successful.

In 1933, Thom obtained a finite-difference solution for the flow past a circular cylinder. From the Navier-Stokes equations, he obtained a differential equation for the transport of vorticity, and avoided the explicit use of velocities by defining a stream-function. He then used 'central'* finite-differences to obtain algebraic equations for vorticity and stream-function which were solved by an

---

* The reader who is not familiar with the terminology used in connection with the finite-difference methods should refer to some textbook on numerical methods, such as Forsythe & Wasow (1960).

iterative technique. His method was, however, unstable above a certain Reynolds number ($\sim$50) and no solutions could be obtained for higher Reynolds numbers (Thom & Apelt 1961)*. Such was also the experience of Kawaguti (1961) and Simuni (1964) who were dealing with different problems by, essentially, the same method. Thom and Apelt (1961) also reported that the range of Reynolds number could be extended by the use of under-relaxation. Burggraf (1966) made extensive use of under-relaxation and presented solutions, for the confined flow in a cavity, for Reynolds numbers as high as 400. However, his experience demonstrated that under-relaxation exacts severe penalties in computing time and he had to abandon his computations for higher Reynolds numbers. It was therefore realised that if economical solutions were to be obtained, a radically different approach was necessary.

A significant discovery was made by Courant et al. (1952) in connection with numerical solutions of non-linear hyperbolic equations. They found that the stability of their numerical procedure could be improved by the use of an 'upwind' finite-difference scheme. This concept implies that the difference form of the convective terms be caused to depend on the direction of the local flow in contrast to the central finite-difference forms, which do not attach any importance to the direction of flow. Encouraging results were obtained by the use of Courant's

---

* Allen & Southwell (1955) used a similar method and a space transformation to obtain solutions for Reynolds numbers as high as 1000. However, transformations such as theirs are particular to a physical problem and cannot be considered general.

suggestion for a number of problems involving unsteady flow, e.g. by Blair et al. (1957) and by Barakat and Clark (1965).

Incorporating a similar independent suggestion of Spalding (1966), Runchal and Wolfshtein (1966) put forward a method for the prediction of steady, viscous and two-dimensional flows.* In contrast with the earlier methods, such as the one by Burggraf (1966), their method was found to be unconditionally stable for all Reynolds numbers; and the computing times involved were much smaller.

Following another suggestion by Spalding (1967a), the above method was generalised to include non-uniform properties, and was later also modified to improve accuracy. Various stages of development, of which the present thesis forms a part, have been reported by Runchal et al. (1967), Wolfshtein (1967) and Pun and Spalding (1967).

All the finite-difference techniques mentioned above had one common thread: they followed Thom's practice of using the vorticity and stream-function as the dependent variables. The chief advantage is that pressure, usually not a pre-specified function, does not enter into the calculations explicitly. These techniques, therefore, differ sharply from another recent stream of work; this employs velocities and pressure as the dependent variables; and has been applied mainly to unsteady flows. For example, Harlow and Welch (1965) reported an interesting application to the transient flow of a fluid with a free surface.

---

* It seems that by this time a number of workers had been attracted by the suggestion of 'upwind-differences'. For example, Greenspan (1967) independently proposed an identical method. Not surprisingly his findings were in accord with those of Runchal and Wolfshtein.

There is a difference of opinion among numerical analysts about the relative merits of using either the 'vorticity' formulation or the 'velocity' formulation of the equations. Though the use of the latter has the advantage of direct interpretation of the results in terms of velocities, this is of importance only when the results are monitored at intermediate stages. Such a necessity usually arises only for transient flows; on the other hand, it has been observed that the 'velocity' formulation converges to a steady-state only very slowly because of the strong non-linear nature of the pressure equation (Aziz & Hellums 1967). Recently Chorin (1967) reported an alternative formulation for the pressure equation which has not been widely tested as yet. Under these circumstances the only conclusion that can be drawn is that the calculations for pressure are, at the least, an inconvenience.

A large volume of numerical work in recent years has been concerned with the behaviour of transient flows. Much of this work was performed at Los Alamos Scientific Laboratories and has been reported in a number of reports from that source; for example, Fromm & Harlow (1963) presented the numerical solution of the classical problem of the vortex street development behind a cylinder. However, the sole concern in the present thesis is the solution of steady-state problems: therefore, no particular attention has been, nor will be, devoted to the literature dealing with transient flows.

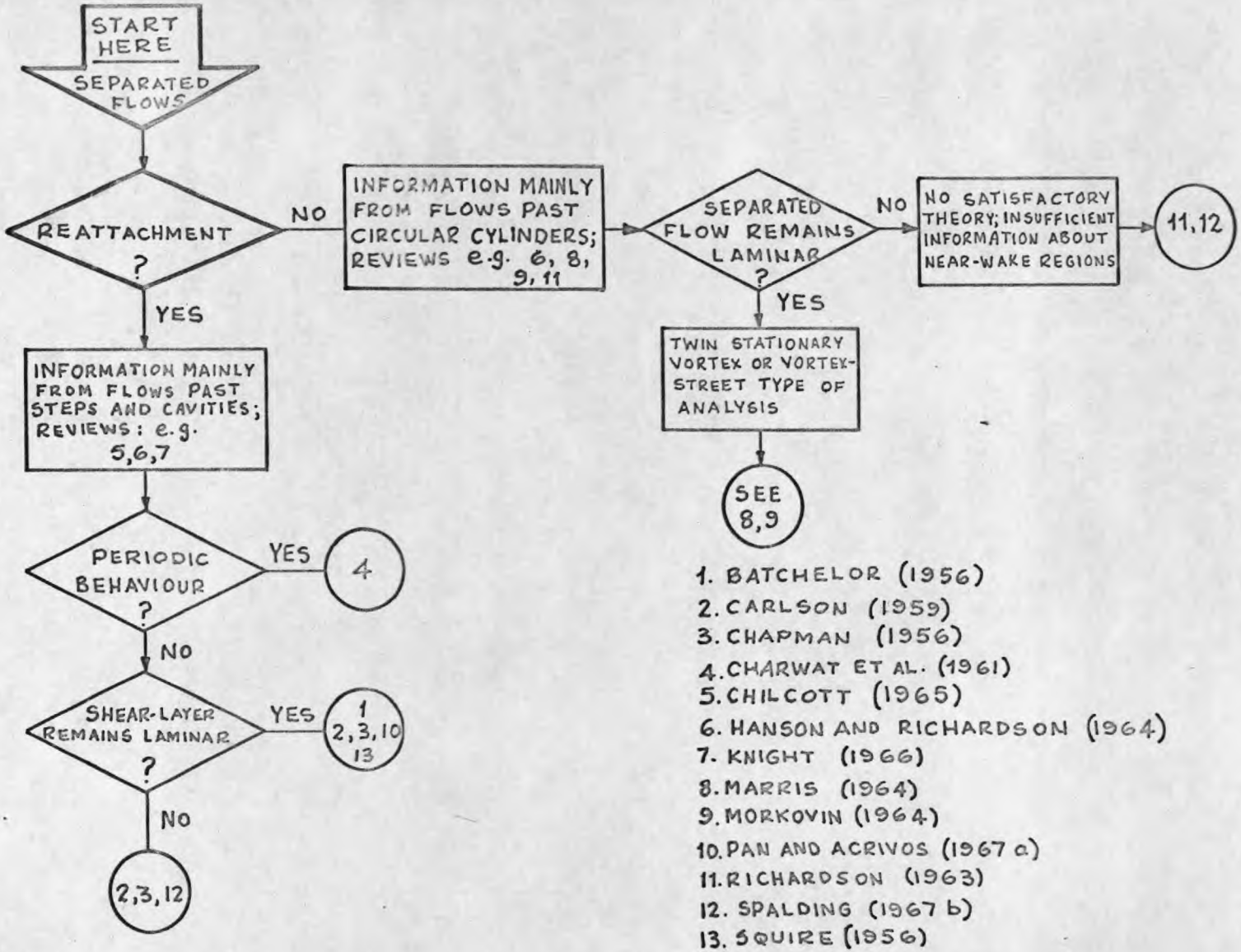

1. BATCHELOR (1956)
2. CARLSON (1959)
3. CHAPMAN (1956)
4. CHARWAT ET AL. (1961)
5. CHILCOTT (1965)
6. HANSON AND RICHARDSON (1964)
7. KNIGHT (1966)
8. MARRIS (1964)
9. MORKOVIN (1964)
10. PAN AND ACRIVOS (1967 a)
11. RICHARDSON (1963)
12. SPALDING (1967 b)
13. SQUIRE (1956)

FIG. 1.2-1 APPROXIMATE THEORIES FOR SEPARATED FLOWS

1.2-2 Approximate theories based upon physical models

A number of theories for separated flows postulate the existence of a particular flow-pattern which is supported by specialised mechanisms for the exchange of mass, momentum and enthalpy etc. The mathematical problem is simplified by assuming that some parts of the flow can be described by equations of the boundary-layer type. Furthermore, such theories are usually particular either to those flows which re-attach to a surface, or to the ones that do not.

Various authors (Hanson & Richardson 1964, Chilcott 1967) have recently prepared detailed surveys of the available literature and it seems pointless here to provide yet another.

Fig. 1.2-1 displays a rough summary of the available information in the form of a flow diagram.* For the sake of clarity, the display has been kept as simple as possible; a look at the representative literature is enough to demonstrate that separated flows are capable of behaving in a much more complex fashion.

The notion that steady separated flows, which re-attach to a surface, can be represented by a core of recirculating fluid surrounded by thin boundary layers, has existed for a long time; in 1956, Batchelor derived an integral condition for the state of laminar fluid in such core regions with closed stream-lines and also proved that, for two-dimensional flows, such a core will consist of uniform-vorticity fluid. Pan and Acrivos (1967a) later

---

* The author gratefully acknowledges the contribution made by Prof. Richardson in drafting this section in general, and Fig. 1.2-1 in particular.

extended this analysis to include heat transfer. If this view is accepted in its general implications, then such separated flows, whether laminar or turbulent (Squire 1956), can be envisaged as a core of recirculating fluid surrounded, in general, by a free shear-layer between the outer main-stream fluid and the core, and a wall boundary layer between the solid surface and the core.

Chapman (1956), on the basis of the above assumption, proposed that the free shear-layer offers the bulk of the resistance to momentum and heat transfer. That such was the case for laminar flows, could be concluded from good agreement between the theory and the experimental evidence; however, the predictions for turbulent flows failed to match the experiments (Larson 1959). Carlson (1959) suggested that the heat transfer process is dominated by the diffusional exchange between the recirculating core and the wall; however, Carlson's analysis also does not stand up to experiments (Scott & Eckert 1966). Inadequacies of the above two models led Charwat et al. (1961) to propose that the transfer processes are a manifestation of the periodic exchange of fluid between the free shear layer and the core. This model was proposed specifically from observations on supersonic flow past cavities, with oscillations in the separating stream-line. Its validity, therefore, is questionable for those flows which do not possess such a behaviour.

Lack of any satisfactory theory is more striking for the case of the flows which do not reattach to a surface, such as the flows behind bluff bodies. In spite of the large amount of effort that has gone into this field, we

know little about the transfer mechanisms in this region. The main reason for this seems to be the strong periodic nature of the flow in the near-wake regions. Hanson and Richardson (1968) state that "the near wakes cannot be adequately represented by a time-independent mean flow with oscillations imposed upon it, in contrast with wakes at remote distances from body."

The flows with Reynolds numbers (for a circular cylinder) of less than about 300 are not of much technical interest and consequently we shall not discuss these: excellent reviews, such as the one by Morkovin (1964), are available. Above a critical Reynolds number, which depends upon the free-stream turbulence, the shear layers separating from the cylinder undergo transition to turbulence before joining the vortex street; at still higher Reynolds numbers ($\sim 2 \times 10^5$) the transition occurs before separation from the cylinder.

The observation that turbulent separated flows behind bluff bodies seem to belong to a class of flows which exhibit similar characteristics, led Richardson (1963) to propose a simple power law - similar to the one for turbulent Reyleigh convection (Malkus 1954) - for the average heat transfer coefficient vs. the Reynolds number. Knight (1966), after examining the experimental data, concluded that a similar dependence also exists for those flows which reattach to a surface.

Recently Spalding (1967b) proposed a theory for heat transfer in steady turbulent flows, with or without reattachment, on the basis of a different concept. One of the characteristic features of separated flows is that

the locations of maximum shear stress are remote from any wall. Thus the turbulence which is generated in the high-shear regions must be conveyed to the vicinity of the wall by the mechanisms of convection and diffusion. Spalding argued that the turbulence intensity, and thus the heat transfer, in the vicinity of a wall is governed by the interaction of these two with the turbulence dissipation. By making further use of a one-dimensional model and the hypotheses of turbulence energy balance, proposed by Kolmogorov (1942) and Prandtl (1945), he obtained a relation for the heat transfer coefficient in terms of other parameters such as Reynolds number, turbulence intensity, etc. Spalding, to the extent of the empirical constants required by the hypotheses, obtained good order-of-magnitude agreement with experimental data for three different problems. Lack of information about the empirical input and the mathematical complexity of the two-dimensional model have, until recently, prevented any further development in this direction.

1.3 The present contribution

1.3-1 An evaluation

The major contribution of the present thesis is in that it presents a general numerical method to deal with the basic mathematical problem - that of solving the complete differential equations. Inadequacies of the approximate theories of section 1.2-2 are all too noticeable in their limited applications; their use for general solution procedures is therefore ruled out. The numerical work reviewed in section 1.2-1 suggests the use of finite-

difference techniques as a cornerstone for general numerical methods: the method presented in this thesis exploits this suggestion. The applicability, economy and accuracy of the method is demonstrated by solving two different problems: one for laminar and one for turbulent flow.

The problem tackled for laminar flow is that of a square cavity with a moving lid. Flows which are similar to that in a cavity are frequently encountered in practice. A common example is the flow past a recess, or a step, in a solid surface. Better understanding of such phenomena will, it is hoped, lead to more efficient designs.

The turbulent-flow problem is that of the abrupt enlargement of a circular pipe. Steps in pipes are either intentional or accidental features of design; and they lead to appreciable differences in local heat-transfer and pressure-loss along the pipe.

For the pipe-enlargement problem an experimental investigation is also reported. The experimental technique is based upon diffusion-controlled electrolysis, and is suitable for measuring mass-transfer rates at high Schmidt numbers. Although the technique is well-established, its application to separated flows is novel. Some of the special problems, which are posed by its application to such flows, are also discussed in the thesis.

Lastly, some progress is reported in the direction of finding an appropriate physical input for turbulent flows. The work is based upon the hypotheses of turbulence-energy balance first proposed by Kolmogorov (1942) and Prandtl (1945).

During the course of the present work some special difficulties were encountered, mostly connected with turbulent flows; these are listed where appropriate, in the hope that they will act as a guide for further research in this field.

1.3-2 An outline

This thesis is divided into three parts.

Part I concerns the theoretical investigation and is further sub-divided into five chapters. Chapter 2 presents the mathematical problem, and chapter 3 a numerical procedure to solve it. For turbulent flows, the mathematical model is made complete by provision of a suitable empirical input in the form of a set of physical hypotheses; this is presented in chapter 4. In the same chapter is also presented a special one-dimensional flow model; this enables anlytic integration to be carried out across thin boundary layers which usually exist close to solid walls. The chief advantage of this model is that it permits economy of computer time. Chapter 5 deals with the results obtained by the application of the numerical procedure to two flow problems: these results are also compared with those available from other sources. The theoretical investigation is reviewed and discussed in chapter 6. Also listed in this chapter are some of the deficiencies in the present state of knowledge; in the light of these some recommendations for future work are made.

Part II is a summary of the experimental investigation and the discussion of the results so obtained.

A listing of the computer programme, and some other information in connection with the computations, is presented in Part III which deals with the computational aspects of the numerical procedure.

Nomenclature and list of references follow Part III.

Part I

THEORETICAL INVESTIGATION

Chapter 2: The mathematical problem

Chapter 3: The numerical procedure

Chapter 4: Two special models of flow

Chapter 5: Flow prediction

Chapter 6: Discussion and conclusions

Chapter 2

The mathematical problem

Differential equations are convenient means of expressing physical laws. The equations that follow in this chapter express the laws of conservation of mass, momentum, enthalpy and other convected properties. The laminar and turbulent flows are described by the same set of equations by postulating 'effective' exchange coefficients for momentum, enthalpy, etc. The mathematical problem is closed by a statement and discussion of the boundary conditions.

2.1 The differential equations

2.1-1 Restrictions

In this chapter are presented the partial differential equations which describe the steady two-dimensional flow of an isotropic fluid in an axisymmetric space. The axis of symmetry may be present in the vicinity of the flow-field, as for the flow in a circular pipe, or it may be located at infinity, as for the flow along a plane surface. The condition of two-dimensionality is imposed by requiring that the flow be completely definable by two mutually orthogonal space directions.

If the flow is turbulent, it will be postulated, following the common practice, that it can be represented by a fluctuating component superimposed on a time-mean

component (see e.g. Hinze 1959). We further postulate that the effect of the fluctuating components can be incorporated by using effective mean diffusional fluxes of momentum, heat and mass-species, etc. For example, the effective diffusional flux of momentum will comprise both the mean stresses and the stresses due to the fluctuating components better known as the Reynolds stresses.

Although the numerical method, to be presented in the next chapter, does not require any further restrictions (Spalding 1967a), for simplicity and clarity of analysis, the field of interest will be further restricted by assuming that the body forces, thermal radiation and swirl velocity are absent. Attention will now be confined to those flow fields which can be adequately described by either a plane cartesian coordinate system, or a cylindrical coordinate system. In the following sub-section we will see how these two coordinate systems can be incorporated into a single system.

2.1-2 The coordinate system

Fig. 2.1-1 shows a part of the coordinate system $x_1 \sim x_2 \sim r$. x_1 and x_2 respectively denote the two mutually orthogonal coordinates to be used to describe the spatial behaviour of the flow. The distance from the axis of symmetry is denoted by the radius r.

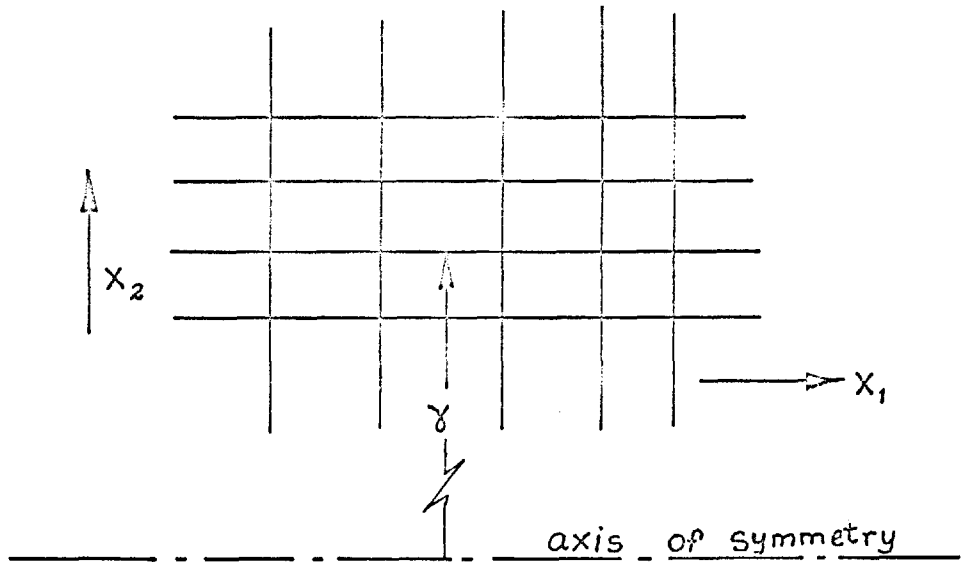

FIG. 2·1-1 THE CO-ORDINATE SYSTEM.

For a cylindrical coordinate system, the origin of the coordinates is on the axis; in such a case $x_2(=r)$ is the radial coordinate and x_1 is the axial coordinate which is more commonly denoted by z.

On the other hand, when $r \to \infty$, x_1 and x_2 represent the familiar plane cartesian coordinates.

2.1-3 The laws of conservation

With the restrictions of section 2.1-1 and the notation of section 2.1-2, the following are the mathematical statements of the respective laws of conservation:

conservation of mass

$$(\partial/\partial x_j)(r.G_j) = 0 \quad , \qquad (2.1\text{-}1)$$

conservation of momentum in direction i

$$(\partial/\partial x_j)(r.G_j.u_i + r.\tau_{ij}) + r.\partial p/\partial x_i = 0 \quad , \qquad (2.1\text{-}2)$$

and conservation of property Ø

$$(\partial/\partial x_j)(r.G_j.\emptyset + r.J_{\emptyset,j}) + r.S_\emptyset = 0 \quad , \qquad (2.1\text{-}3)$$

where,

G_i & u_i are, respectively, the mass velocity and the velocity component in direction i; by definition, $G_i = \rho u_i$ with ρ as the mass-density,

τ_{ij} is the component of the stress tensor in direction j and it operates in the plane which has its normal in the direction i,

p is the fluid pressure,

ϕ is any conserved property such as enthalpy,

$J_{\phi,j}$ is the diffusional-flux component of the property ϕ in the direction j, and

S_ϕ is composed of all the terms which represent the generation or destruction of the property ϕ.

The above representation makes use of the summation convention: a repeated subscript is summed over its all possible values, and a non-repeated subscript takes all its possible values independently. For a two-dimensional flow, the equation:

$$(\partial/\partial x_j)(A_i.B_j) = 0 \quad , \qquad (2.1\text{-}4)$$

represents the following two equations:

$$(\partial/\partial x_1)(A_1.B_1) + (\partial/\partial x_2)(A_1.B_2) = 0 \text{ ,and} \qquad (2.1\text{-}5)$$

$$(\partial/\partial x_1)(A_2.B_1) + (\partial/\partial x_2)(A_2.B_2) = 0 \quad . \qquad (2.1\text{-}6)$$

2.2 Auxiliary information: the diffusional fluxes

Equations such as (2.1-2) and (2.1-3) do not, in themselves, state the mathematical problem completely. This is so because nothing, as yet, has been said about the flux components τ_{ij} and $J_{\phi,j}$.

For laminar Newtonian fluids, the components of the stress tensor τ_{ij} are easily related to the rate-of-strain

tensor (velocity-gradients) via a generalised form of the Newton's law of viscosity (Bird, Stewart and Lightfoot 1960). Similarly, the flux components of enthalpy and mass-species can be related to their respective gradients by the generalised forms of the Fourier's law of heat conduction and the Fick's law of diffusion.

For turbulent flows, the stress tensor cannot be, rigorously, related to the strain tensor; nor, for that matter, can the flux vectors of a conserved property be related to its gradients. Nevertheless, following an early proposal by Boussinesq (1877), for prediction purposes we can postulate the existence of effective exchange coefficients to replace the laminar exchange coefficients in the respective stress and flux laws; thus:

$$\tau_{ij} = -\mu_{eff}(\partial u_j/\partial x_i + \partial u_i/\partial x_j) \quad , \qquad (2.2\text{-}1)$$

and

$$J_{\phi,j} = -\Gamma_{\phi,eff}(\partial \phi/\partial x_j) \quad , \qquad (2.2\text{-}2)$$

where μ_{eff} and $\Gamma_{\phi,eff}$ are respectively the effective viscosity and the effective diffusivity.

We can also postulate that:

$$\Gamma_{\phi,eff} = \mu_{eff}/\sigma_{\phi,eff} \quad , \qquad (2.2\text{-}3)$$

where $\sigma_{\phi,eff}$ is the effective Prandtl/Schmidt number for the property ϕ and, from experimental evidence, is likely to be almost constant.

Thus the unknowns τ_{ij} and $J_{\phi,j}$ have been replaced by the unknowns μ_{eff} and $\sigma_{\phi,eff}$. Fortunately some information about the latter can be obtained from correlation of experimental data for turbulent flows; admittedly, however, the available information leaves much to be desired. In chapter 4 we shall discuss these

matters in more detail; for the time being, we proceed further on the assumption that μ_{eff} and $\sigma_{\phi,eff}$ are determinable.

For laminar flows, of course, μ_{eff} and $\sigma_{\phi,eff}$ are to be replaced by the respective laminar values: the dynamic viscosity μ and the laminar Prandtl/Schmidt number σ_{ϕ}. These are evaluable from many compilations in the form of tabulations or formulae.

2.3 The transformed momentum and continuity equations

2.3-1 The vorticity equation

Equation (2.1-2) contains the gradient of pressure, an unknown of the problem. It is true that the total number of unknowns is equal to the number of equations and that the pressure can be eliminated between equations (2.1-1) and(2.1-2). However, for reasons stated in section 1.2-1, the calculation of pressure is not very desirable from the point of view of numerical solution. We therefore proceed to eliminate the pressure from the above equations by a well-known trick: the introduction of vorticity. For a two-dimensional flow, vorticity ω is defined by:

$$\omega \equiv \partial u_2/\partial x_1 - \partial u_1/\partial x_2 \quad , \qquad (2.3\text{-}1)$$

Now, if we differentiate the direction-1 momentum equation with respect to x_2 and the direction-2 momentum equation with respect to x_1, and subtract the first from the second, we then obtain*:

$$(\partial/\partial x_j)(r.G_j.\omega/r) - r^{-2}.(\partial/\partial x_j)(r^3.(\partial/\partial x_j)(\mu_{eff}.\omega/r)) - r.S_\omega = 0 \quad , \qquad (2.3\text{-}2)$$

---

* A detailed derivation is given by Gosman et al. (1968)

where S_ω is a group of terms containing second derivatives of μ_{eff}; specifically:

$$S_\omega = (\partial^2\mu_{eff}/\partial x_1^2)(\partial u_1/\partial x_2) - (\partial^2\mu_{eff}/\partial x_2^2)(\partial u_2/\partial x_1) + \\ + (\partial^2\mu_{eff}/\partial x_1\partial x_2)(\partial u_2/\partial x_2 - \partial u_1/\partial x_1) \quad .(2.3\text{-}3)$$

2.3-2 The stream-function equation

With the replacement of equation (2.1-2) by (2.3-2), velocity components no longer appear as the dependent variables, but they do still appear as multipliers in equations (2.1-3) and (2.3-2). These can also be eliminated by the introduction of a stream-function ψ, defined by:

$$G_1 \equiv \frac{1}{r}\frac{\partial\psi}{\partial x_2} \quad ; \quad G_2 \equiv -\frac{1}{r}\frac{\partial\psi}{\partial x_1} \; . \qquad (2.3\text{-}4)$$

It is easy to show that, by this definition of the stream-function, the law of conservation of mass, as expressed by equation (2.1-1), is implicitly satisfied.

A consequence of definitions (2.3-1) and (2.3-4) is that:

$$(\partial/\partial x_j)(\rho^{-1}.\, r^{-1}.\partial\psi/\partial x_j) + \omega = 0. \qquad (2.3\text{-}5)$$

This is usually referred to as the stream-function equation. ψ's can be calculated with its aid, and G_j's can then be eliminated from the vorticity and the conserved property equations with the help of (2.3-4): this, we shall proceed to do in the next section.

2.4 The general form of the differential equations

Equations (2.1-3), (2.3-2) and (2.3-5) redefine the mathematical problem with ω/r and $\emptyset$ as the primary dependent variables and ψ as the supporting variable.

All these equations may be represented by a single general equation:

$$\alpha.(\partial/\partial x_j)(r.G_j.\phi) - \beta.(\partial/\partial x_j)(r.\Gamma.\partial(\delta.\phi)/\partial x_j) = r.S_\phi = 0 \quad , \qquad (2.4\text{-}1)$$

where ϕ now stands for any one of the previous variables, ω/r, ψ or ϕ.

This equation, in full, in terms of the gradients of the stream-function, is:

$$\alpha.(\partial/\partial x_1)(\partial\psi/\partial x_2.\phi) - \alpha.(\partial/\partial x_2)(\partial\psi/\partial x_1.\phi) -$$
$$- \beta.(\partial/\partial x_1)(r.\Gamma.\partial(\delta.\phi)/\partial x_1) -$$
$$- \beta.(\partial/\partial x_2)(r.\Gamma.\partial(\delta.\phi)/\partial x_2) = r.S_\phi = 0 \quad , \qquad (2.4\text{-}2)$$

where the various coefficients and S_ϕ's are given in table 2.4-1.

ϕ	Name	α	β	Γ	δ	S_ϕ	Remarks
ψ	stream-function	0	1	$\rho^{-1}r^{-2}$	1	ω/r	see equation (2.3-5)
ω/r	vorticity ÷ radius	1	r^{-2}	r^2	μ_{eff}	equation (2.3-3)	S_ϕ neglected for computations because of uncertain nature of μ_{eff}; see section 4.1-4.
T	temperature	1	1	$\Gamma_{T,eff}$	1	0	S_ϕ for a flow with i) low velocity, ii) negligible mass transfer, iii) no generation or dissipation of enthalpy.
m	mass of a chemical species in unit mass of the mixture	1	1	$\Gamma_{m,eff}$	1	0	S_ϕ for a flow with i) small mass transfer rates, ii) no generation or destruction of the species
k	kinetic-energy of turbulence	1	1	$\Gamma_{k,eff}$	1	equations (4.1-4) (4.1-7)	S_ϕ depends on turbulence-hypotheses; see section 4.1 and equation (4.1-3).

Table 2.4-1 Some particular forms of the general differential equation (2.4-2).

It must be stressed here that the S_{ϕ}'s given in the Table 2.4-1 are by no means general: but they are the ones which apply to the problems discussed in chapter 5 of the present thesis.

2.5 The boundary conditions

The application of equation (2.4-2) to any particular problem needs the specification of boundary conditions. In the mathematical literature, equation (2.4-2) is referred to as an elliptic equation (e.g. Forsythe & Wasow 1960). Such equations require that, for each dependent variable, a boundary condition be specified along a closed curve bounding the region of interest. This boundary condition may be the value of the variable itself or that of its normal gradient at the boundary. Of course, a boundary condition of the third type, a combination of the above two, may also be specified.

The boundaries encountered in practice can usually be accommodated by one of the following four categories: a) Inlet sections, b) Outlet sections, c) Axes (or planes) of symmetry, and d) Solid walls. We will discuss the boundary conditions for each of these individually.

a) Inlet sections: The conditions of the entering fluid are supplied as part of the problem-specification. For example, in a typical case, it may be the distributions of velocity, temperature, composition, and the intensity of turublence which are given. The dependent variables of the general equation (2.4-2) are normally calculable from this information; for example, the stream-function can be obtained from the velocity distribution via equation (2.3-4).

b) Outlet sections: The fluid condition at an outlet section is not always known in advance. Nevertheless, a boundary condition for each variable must be specified in order that the calculations may proceed.

At high Reynolds numbers, the effect of the outlet boundary condition on the upstream fluid is small. This follows from the observation that, in the type of flow being considered, diffusion is the only mechanism capable of transmitting upstream the effects of the downstream boundary condition; this mechanism is understandably weak at high Reynolds numbers. This fact can often be exploited in the specification of boundary conditions at an outlet section. For example, the gradients of the dependent variables along the stream-lines may be taken as zero; the stream-lines, in turn, may be assumed to intersect the outlet boundary at, say, right angles. In some cases, it may be possible to calculate the position of the stream-lines from a given, or assumed, velocity-distribution.

c) Axes* of symmetry: In an axisymmetrical flow, no fluid can cross the axis of symmetry; the stream-function along the symmetry axis must, therefore, be a constant.

Although the vorticity, ω, at an axis of symmetry is zero, the dependent variable ω/r, is not necessarily zero. A boundary condition for ω/r can be derived by considering the restraints on the variation of the axial velocity, u_1, in the proximity of the symmetry axis. For reasons of symmetry:

* The boundary conditions for a plane of symmetry are derived in a similar manner to that for an axis except that r is to be treated as a constant.

$$\underset{r \to 0}{Lt} \quad \partial u_1/\partial r = 0 \quad . \qquad (2.5\text{-}1)$$

Since u_1 itself tends to a finite value, say U, at the axis, it follows that the first two terms in a polynomial expansion for u_1 are:

$$\underset{r \to 0}{Lt} \quad u_1 = U + C.r^2 + \ldots \quad . \qquad (2.5\text{-}2)$$

A boundary condition for w/r can now be obtained from:

$$\underset{r \to 0}{Lt} \quad w/r = -r^{-1}.\partial u_1/\partial r = -2C \quad . \qquad (2.5\text{-}3)$$

The coefficient C can be evaluated by reference to the value of u_1 at a small value of r where (2.5-2) may be assumed to hold.

The boundary condition for other variables, such as temperature, takes the form of the vanishing normal gradient at the axis. For example, for any conserved property $\emptyset$, $\partial\emptyset/\partial r$ will be specified as zero at the symmetry axis.

d) Solid walls: For a wall impermeable to matter, it is an implication of equation (2.3-4) that the stream-function along the wall must be a constant. The value of this constant can be obtained from the data of the problem. For a permeable wall, given the rate of injection through the wall, the stream-function can be calculated from equation (2.3-4).

Vorticity is composed of the gradients of velocity, and it is rare for these to be pre-specified. A boundary condition for vorticity can, however, be obtained from the 'no-slip' condition. For purposes of illustration, let us consider a simple case: that of an impermeable, stationary

wall situated far away from the axis of symmetry. In most cases, near a wall, the gradients of the variables in the direction parallel to the wall may be neglected in comparison with those in the normal direction. The vorticity equation (2.3-2) for this case may be written as:

$$(\partial^2/\partial x_n^2)(\mu_{eff}.\omega) = 0 \quad , \qquad (2.5\text{-}4)$$

where x_n is the distance normal to the wall.

From this equation we obtain:

$$\omega = (C_1.x_n + C_2)/\mu_{eff} \quad , \text{ and} \qquad (2.5\text{-}5)$$

$$\omega_S = C_2/\mu_{eff} \quad , \qquad (2.5\text{-}6)$$

where C_1 and C_2 are the constants of integration and the subscript S refers to the value at the wall.

A relation for the constants of integration can be obtained by reference to the stream-function equation (2.3-5) which, for this case, may be written as:

$$(\partial^2/\partial x_n^2)(\psi) + \rho.r.(C_1.x_n + C_2)/\mu_{eff} = 0 \quad . \qquad (2.5\text{-}7)$$

This equation, with the help of 'no-slip' condition ($(\partial\psi/\partial x_n)_S = 0$), yields:

$$\psi - \psi_S = -\rho.r.\int_0^{x_n}\int_0^{x} (C_1.x + C_2)/\mu_{eff}.dx.dx_n \quad . \qquad (2.5\text{-}8)$$

If a μ_{eff}~x_n relation is available, C_1 and C_2 may be evaluated by reference to ψ and ω values a short distance away from the wall. For example, if μ_{eff} is a constant,

$$\omega_S = C_2/\mu_{eff} = -\omega_C/2 - 3(\psi_C-\psi_S)/(\rho.r.x_{n,C}^2) \quad , \qquad (2.5\text{-}9)$$

where C refers to a point within the flow field at a distance of $x_{n,C}$ from the wall.

For turbulent flows μ_{eff} may vary sharply near a wall. In such cases, equation (2.5-8) should be integrated with proper assumptions about the variation of μ_{eff}; one such set of assumptions is discussed in chapter 4.

Chapter 3

The numerical procedure

In chapter 2 we started from the laws of conservation and succeeded in formulating a general differential equation applicable to all conserved properties. However, the designer wants an answer not in terms of the differential equations but in terms of numbers and formulae which he can use for design purposes. In this chapter is outlined a numerical procedure to help achieve this aim.

3.1 The choice and fundamentals of the technique

There are many numerical methods for solving partial differential equations. Of all these, none has been able to rival finite-differences in ease and universality of application. This technique has proved its worth in practically every branch of science and technology involving differential equations. Thom, in 1933, found its application extremely laborious, but the development of high-speed computers greatly reduces the labour involved. What took Thom months to solve, would have taken hours in the early 1950's; it takes but seconds on modern machines.

The essential principle of the finite-difference technique is to replace the differentials of a variable by the differences taken over finite intervals. The field of interest, which is a continuum, is therefore replaced by a net of grid lines spread over it. The points of intersection of the grid are termed the 'nodes'

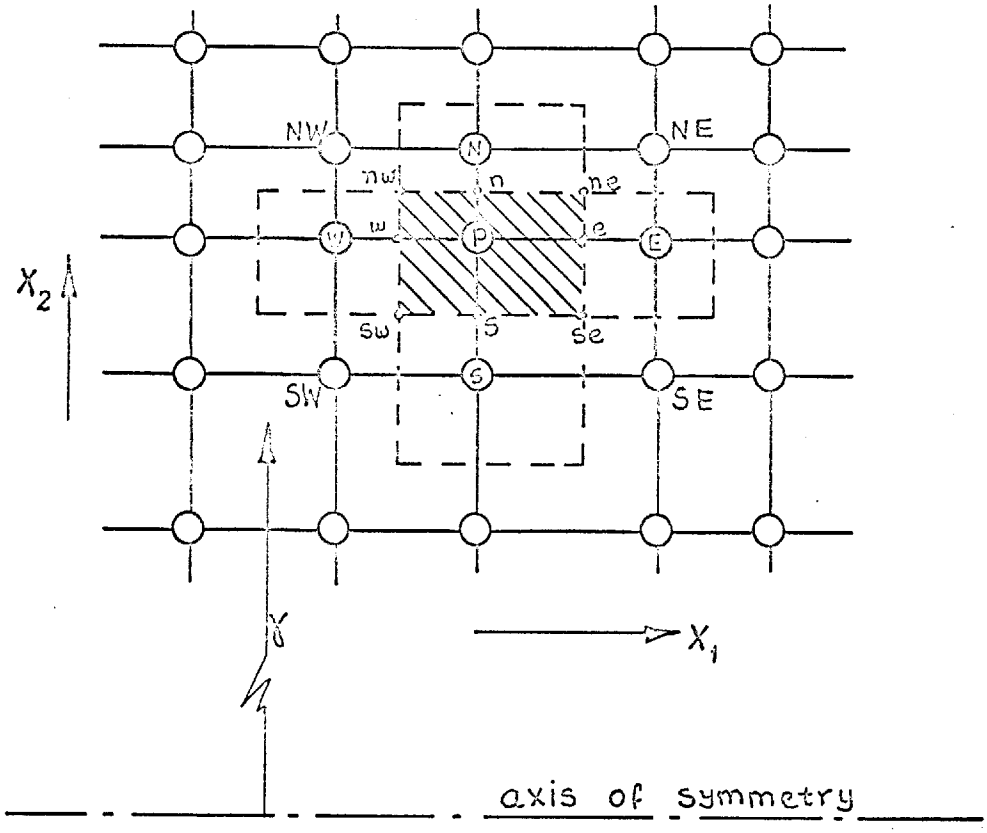

FIG. 3-2-1. THE FINITE-DIFFERENCE GRID.

and it is with these nodes as the foci of attention that the differential equation (2.4-2) is to be integrated.

There are, of course, some questions raised by this 'discretization' of the continuum problem; such as: does the solution in the discrete space represent the solution in the continuum? or, how many grid lines should be chosen for a given problem and what is the best way to distribute them? Questions like these will be deferred to the end of this chapter; for the time being, let us concentrate on deriving a finite-difference analogue to the differential equation (2.4-2).

3.2 The finite-difference equation

There are many ways in which the grid may be spread over the field of interest (Forsythe & Wasow 1960); we choose one of the simplest: that in which the grid lines are the coordinate lines at discrete intervals of the coordinates x_1 and x_2, as in fig. 3.2-1. No restrictions are to be placed on the spacing between the grid lines; it may be non-uniform.

Let P denote a typical node of the grid, with the nodes E,N,W,S and NE,NW,SW and SE surrounding it. Let us now restrict our attention to the shaded rectangle, ne-nw-sw-we, of fig. 3.2-1, the sides of which lie midway between the neighbouring grid-lines. It is over each such rectangle, individually, that the differential equation (2.4-2) is to be integrated. To this extent our approach is unconventional in that the attention is focussed on the integral values of the differential terms rather than on their local values. Thus, equation (2.4-2) is to be replaced by the integral equation:

$$\int_{x_{2,s}}^{x_{2,n}} \int_{x_{1,w}}^{x_{1,e}} \alpha.\left[\frac{\partial}{\partial x_1}\left(\frac{\partial \psi}{\partial x_2}.\phi\right) - \frac{\partial}{\partial x_2}\left(\frac{\partial \psi}{\partial x_1}.\phi\right)\right].dx_1.dx_2 -$$

CONVECTION TERMS

$$- \int_{x_{2,s}}^{x_{2,n}} \int_{x_{1,w}}^{x_{1,e}} \beta.\left[\frac{\partial}{\partial x_1}\left\{r.\Gamma.\frac{\partial}{\partial x_1}(\delta.\phi)\right\} + \frac{\partial}{\partial x_2}\left\{r.\Gamma.\frac{\partial}{\partial x_2}(\delta.\phi)\right\}\right].dx_1.dx_2 +$$

DIFFUSION TERMS

$$- \int_{x_{2,s}}^{x_{2,n}} \int_{x_{1,w}}^{x_{1,e}} r.S_\phi.dx_1.dx_2 = 0 \quad . \qquad (3.2\text{-}1)$$

SOURCE TERMS

3.2-1 The convection terms

Let I_{Con} denote the integral of the convective terms in the equation (3.2-1), i.e.,

$$I_{Con} \equiv \int_{x_{2,s}}^{x_{2,n}} \int_{x_{1,w}}^{x_{1,e}} \alpha.\left\{\frac{\partial}{\partial x_1}\left(\frac{\partial \psi}{\partial x_2}.\phi\right) - \frac{\partial}{\partial x_2}\left(\frac{\partial \psi}{\partial x_1}.\phi\right)\right\}.dx_1.dx_2 \quad . \qquad (3.2\text{-}2)$$

Since α is a constant, by integrating once formally, we obtain

$$I_{Con} = \alpha \int_{x_{2,s}}^{x_{2,n}} \left\{\overline{\left|\frac{\partial \psi}{\partial x_2}.\phi\right|}_e - \overline{\left|\frac{\partial \psi}{\partial x_2}.\phi\right|}_w\right\}.dx_2 -$$

$$- \alpha \int_{x_{1,w}}^{x_{1,e}} \left\{\overline{\left|\frac{\partial \psi}{\partial x_1}.\phi\right|}_n - \overline{\left|\frac{\partial \psi}{\partial x_1}.\phi\right|}_s\right\}dx_1 \quad , \qquad (3.2\text{-}3)$$

where the quantities under the '$\overline{\ }$' symbols are to be evaluated along the side of the rectangle denoted by the

subscript, e.g. $\big]_e$ denotes along the side se - ne. To evaluate such quantities, let us take one of the convective terms,

$$I_C \equiv \alpha \int_{x_{2,s}}^{x_{2,n}} \frac{\partial\psi}{\partial x_2} . \phi \Big|_e . dx_2 \quad . \qquad (3.2\text{-}4)$$

If both ψ and ϕ are well-behaved functions in x_2, then there exists an average value ϕ_e, such that:

$$\phi_e \equiv \int_{x_{2,s}}^{x_{2,n}} \frac{\partial\psi}{\partial x_2} . \phi \Big|_e . dx_2 \Big/ \int_{x_{2,s}}^{x_{2,n}} \frac{\partial\psi}{\partial x_2} \Big|_e . dx_2 \quad ; \qquad (3.2\text{-}5)$$

but

$$\int_{x_{2,s}}^{x_{2,n}} \frac{\partial\psi}{\partial x_2} \Big|_e . dx_2 = \psi_{ne} - \psi_{se} \quad , \qquad (3.2\text{-}6)$$

where subscripts ne and se refer to the corners of the shaded rectangle in fig. 3.2-1. Therefore, from (3.2-4), (3.2-5) and (3.2-6),

$$I_C = \alpha . \phi_e . (\psi_{ne} - \psi_{se}) \quad . \qquad (3.2\text{-}7)$$

Since ϕ_e, ψ_{ne} and ψ_{se} do not represent the values at the nodes of the grid, equation (3.2-7) cannot be used directly in the finite-difference procedure: I_C must be expressed in terms of the values at suitable nodes of the grid; this we do by making an assumption which in the literature has been referred to as the assumption of 'upwind differences' (see e.g. Richtmeyer 1962). For equation (3.2-7), it states that ϕ_e is equal to that value of ϕ which is representative of the rectangle lying immediately upstream of the side e. The implications of

this assumption are readily perceived if we note that the gradients of stream-function, and hence terms such as $(\psi_{ne} - \psi_{se})$ are connected to the direction, and magnitude, of the mass velocities via the defining equation (2.3-4). In particular, if $(\psi_{ne} - \psi_{se})$ is positive, the direction of the flow is from the node P towards the node E; therefore the above assumption implies that ϕ_e is equal to the representative value of the rectangle surrounding the node P; we will take this value to be ϕ_P. If, on the other hand, $(\psi_{ne} - \psi_{se})$ is negative, the implication is that ϕ_e is equal to ϕ_E, since the flow direction is now from E to P.

The above arguments can be incorporated into equation (3.2-7) by expressing it as

$$I_C = \alpha.\phi_P.\ [(\psi_{ne} - \psi_{se}) + |\psi_{ne} - \psi_{se}|]/2 + \\ + \alpha.\phi_E.\ [(\psi_{ne} - \psi_{se}) - |\psi_{ne} - \psi_{se}|]/2 \quad . \qquad (3.2\text{-}8)$$

In the above equation, one of the terms in the square brackets will always be zero and we will be left with the term which represents the contribution from the <u>upstream rectangle</u> only.

Equation (3.2-8) may be rearranged to

$$I_C = \alpha.(\phi_P - \phi_E).[(\psi_{se} - \psi_{ne}) + |\psi_{se} - \psi_{ne}|]/2 - \alpha.\phi_P.(\psi_{se} - \psi_{ne}) \quad . \qquad (3.2\text{-}9)$$

Our task is not yet complete; we must now express ψ_{se} and ψ_{se} in terms of the ψ values at the nodes of the grid. To this intent, we make the simple assumption that <u>the value of the stream function at any particular corner of the rectangle is equal to the arithmetic mean of the stream-function values at its four immediate neighbours</u>.

Thus,

$$\psi_{se} = (\psi_{SE} + \psi_E + \psi_P + \psi_S)/4 \quad . \qquad (3.2\text{-}10)$$

With,

$$A_E \equiv \alpha.[(\psi_{se} - \psi_{ne}) + |\psi_{se} - \psi_{ne}|]/2$$
$$= \alpha.[(\psi_{SE}+\psi_S-\psi_{NE}-\psi_N) + |\psi_{SE}+\psi_S-\psi_{NE}-\psi_N|]/8 \quad , \qquad (3.2\text{-}11)$$

$$I_C = (\phi_P-\phi_E).A_E - \alpha.\phi_P(\psi_{se} - \psi_{ne}) \quad . \qquad (3.2\text{-}12)$$

In a similar way, and by noting that the second term on the R.H.S. of equation (3.2-12) vanishes under summation, we rewrite the integral in the equation (3.2-3) as

$$I_{Con} = (\phi_P-\phi_E).A_E + (\phi_P-\phi_W).A_W +$$
$$+ (\phi_P-\phi_N).A_N + (\phi_P-\phi_S).A_S \quad . \qquad (3.2\text{-}13)$$

The A's are given by expressions such as (3.2-11); we will later list all the A's together when reassembling the complete difference equation in section 3.2-4.

It is to be noted here that the A's can never become negative; but they may fall to zero. We draw attention to this point because, later, we will see that this is one of the features which makes the present finite-difference scheme stable and convergent.

3.2-2 The diffusion terms

Let I_{Dif} denote the integral of the diffusion terms in equation (3.2-1); then,

$$I_{Dif} \equiv \int_{x_{2,s}}^{x_{2,n}} \int_{x_{1,w}}^{x_{1,e}} \beta.\left[\frac{\partial}{\partial x_1}\left\{r.\Gamma.\frac{\partial}{\partial x_1}(\delta.\phi)\right\}+\frac{\partial}{\partial x_2}\left\{r.\Gamma.\frac{\partial}{\partial x_2}(\delta.\phi)\right\}\right]dx_1.dx_2 \quad .$$

(3.2-14)

As β is a constant for all the equations except the one for vorticity (cf. table 2.4-1), we will proceed with formal integration by replacing β with a representative value β_P; thus:

$$I_{Dif} = \beta_P \int_{x_{2,s}}^{x_{2,n}} \left[\overline{r.\Gamma.\frac{\partial}{\partial x_1}(\delta.\emptyset)}\Big|_e - \overline{r.\Gamma.\frac{\partial}{\partial x_1}(\delta.\emptyset)}\Big|_w \right].dx_2 + \\ + \beta_P \int_{x_{1,w}}^{x_{1,e}} \left[\overline{r.\Gamma.\frac{\partial}{\partial x_2}(\delta.\emptyset)}\Big|_n - \overline{r.\Gamma.\frac{\partial}{\partial x_2}(\delta.\emptyset)}\Big|_s \right].dx_1 \quad , \tag{3.2-15}$$

where the notation is the same as for (3.2-3).

Consider one of the diffusion terms,

$$I_D \equiv \beta_P \int_{x_{2,s}}^{x_{2,n}} \overline{r.\Gamma.\frac{\partial}{\partial x_1}.(\delta.\emptyset)}\Big|_e .dx_2 \quad . \tag{3.2-16}$$

By assumptions similar to the one expressed by (3.2-5) the above may be rewritten as:

$$I_D = \beta_P.r_e.\Gamma_e.\overline{\frac{\partial}{\partial x_1}(\delta.\emptyset)}\Big|_e .(x_{2,n} - x_{2,s}) \quad . \tag{3.2-17}$$

I_D can be further expressed in terms of the values at the nodes by:

$$I_D = \beta_P.\frac{r_E+r_P}{2}.\frac{\Gamma_E+\Gamma_P}{2}.\frac{\delta_E.\emptyset_E-\delta_P.\emptyset_P}{x_{1,E}-x_{1,P}}.\frac{x_{2,N}-x_{2,S}}{2} \quad . \tag{3.2-18}$$

The assumptions between (3.2-17) and (3.2-18), of course, imply that the variations of different quantities between E and P can be considered linear.

Thus, the total integral of (3.2-14) may be expressed as:

$$I_{Dif} = (\delta_E \cdot \phi_E - \delta_P \cdot \phi_P) \cdot B_E + (\delta_W \cdot \phi_W - \delta_P \cdot \phi_P) \cdot B_W +$$

$$+ (\delta_N \cdot \phi_N - \delta_P \cdot \phi_P) \cdot B_N + (\delta_S \cdot \phi_S - \delta_P \cdot \phi_P) \cdot B_S \quad , \qquad (3.2\text{-}19)$$

where B's can be deduced from equation (3.2-18). Like the A's of convective terms, the B's are also always positive and these will be listed later in section 3.2-4.

3.2-3 The source terms

The final integral to be evaluated in equation (3.2-1) is

$$I_{Sor} \equiv \int_{x_{2,s}}^{x_{2,n}} \int_{x_{1,w}}^{x_{1,e}} r \cdot S_\phi \cdot dx_1 \cdot dx_2 \quad . \qquad (3.2\text{-}20)$$

Because the form of the source terms is not fixed, unlike the convective and diffusive terms, it is not possible to make any general assumptions; nevertheless, for purposes of illustration only, let S_ϕ be assumed constant over the domain of integration. Then

$$I_{Sor} = S_{\phi,P} \cdot V_P \quad , \qquad (3.2\text{-}21)$$

where

$$V_P \equiv r_P \cdot (x_{1,E} - x_{1,W}) \cdot (x_{2,N} - x_{2,S})/4 \quad , \qquad (3.2\text{-}22)$$

is equal to the volume swept by the rectangle when it is rotated through an angle of one radian about the axis of symmetry.

3.2-4 The complete difference equation

We are now in a position to obtain a complete finite-difference analogue for our general differential equation (2.4-2). From (3.2-1), (3.2-13), (3.2-19) and (3.2-21) we deduce:

$$(\phi_P-\phi_E).A_E + (\phi_P-\phi_W).A_W + (\phi_P-\phi_N).A_N + (\phi_P-\phi_S).A_S +$$
$$+ (\phi_P.\delta_P-\phi_E.\delta_E).B_E + (\phi_P.\delta_P-\phi_W.\delta_W).B_W +$$
$$+ (\phi_P.\delta_P-\phi_N.\delta_N).B_N + (\phi_P.\delta_P-\phi_S.\delta_S).B_S = S_{\phi,P}.V_P = 0 \quad . \qquad (3.2\text{-}23)$$

This equation is the major outcome of our efforts so far; it provides an algebraic relationship between the values of the variable at a particular node P and those at the surrounding nodes E, N, etc.

There will, of course, be one such equation for <u>each dependent variable</u> at <u>each node</u> of the grid. Thus the number of these algebraic equations can indeed be very large; moreover, ϕ's are usually interdependent, and therefore a simultaneous solution is required. Inversion of such a large matrix can pose problems - such as those of storage space - even for modern electronic computers and we are forced to search for alternatives. The only practicable way of a solution is an iterative procedure; we, therefore, now recast equation (3.2-23) as a successive-substitution formula.

Thus by rearrangement:

$$\phi_P = \phi_E.C_E + \phi_W.C_W + \phi_N.C_N + \phi_S.C_S + S \quad , \qquad (3.2\text{-}24)$$

where, for I respectively equal to E, W, N and S,

$$C_I \equiv (A_I + B_I.\delta_I)/\Sigma_{AB} \quad ,$$

$$\Sigma_{AB} \equiv \sum_{\text{All } I} (A_I + B_I.\delta_P) \quad ,$$

$$S \equiv S_{\phi,P}.V_P/\Sigma_{AB} \quad , \text{ and}$$

$$V_P \equiv r_P.(x_{1,E}- x_{1,W}).(x_{2,N}- x_{2,S})/4 \quad . \qquad (3.2\text{-}25)$$

A's are given by,

$$A_E \equiv \alpha.[(\psi_{SE}+\psi_S-\psi_{NE}-\psi_N) + |\psi_{SE}+\psi_S-\psi_{NE}-\psi_N|]/8 \quad ,$$

$$A_W \equiv \alpha.[(\psi_{NW}+\psi_N-\psi_{SW}-\psi_S) + |\psi_{NW}+\psi_N-\psi_{SW}-\psi_S|]/8 \quad ,$$

$$A_N \equiv \alpha.[(\psi_{NE}+\psi_E-\psi_{NW}-\psi_W) + |\psi_{NE}+\psi_E-\psi_{NW}-\psi_W|]/8 \quad ,$$

$$A_S \equiv \alpha.[(\psi_{SW}+\psi_W-\psi_{SE}-\psi_E) + |\psi_{SW}+\psi_W-\psi_{SE}-\psi_E|]/8 \quad , \qquad (3.2\text{-}26)$$

and B's are given by,

$$B_E \equiv \beta_P.[(r_P+r_E).(\Gamma_P+\Gamma_E).(x_{2,N}-x_{2,S})/(x_{1,E}-x_{1,P})]/8 \quad ,$$

$$B_W \equiv \beta_P.[(r_P+r_W).(\Gamma_P+\Gamma_W).(x_{2,N}-x_{2,S})/(x_{1,P}-x_{1,W})]/8 \quad ,$$

$$B_N \equiv \beta_P.[(r_P+r_N).(\Gamma_P+\Gamma_N).(x_{1,E}-x_{1,W})/(x_{2,N}-x_{2,P})]/8 \quad ,$$

$$B_S \equiv \beta_P.[(r_P+r_S).(\Gamma_P+\Gamma_S).(x_{1,E}-x_{1,W})/(x_{2,P}-x_{2,S})]/8 \quad . \qquad (3.2\text{-}27)$$

It is equation (3.2-24), together with its supporting equations, which is to form the core of our computational procedure. And, now that we have a set of algebraic equations to replace the differential equations of chapter 2, we must begin to examine the properties of these algebraic equations. This is the subject matter for the following section.

3.3 Some properties of the numerical procedure

3.3-1 Convergence

It was stated in section 3.2-4 that the difference equations are to be solved by an iterative procedure. In such a procedure, a new solution is obtained by substituting an initial guess into a successive-substitution formula; this solution is then used as the new guess, and so on. It is necessary, if the procedure is to be useful,

that the iterative solution progressively approaches the exact solution of the difference equations. In line with this idea, the condition that the iterative solution of the difference equations should approach their exact solution with successive iterations is defined as the requirement of convergence.

Not all iterative procedures lead to convergence. Unfortunately, rigorous methods to investigate convergence exist only for linear equations with constant coefficients; whereas equation (3.2-24) has variable coefficients which change from iteration to iteration. Nevertheless, practical experience has shown that the criteria for the former can often be successfully employed for equations with variable coefficients (Lax & Richtmeyer 1956; Richtmeyer 1962).

Let us consider a set of linear algebraic equations with constant coefficients:

$$\phi_i = \sum_{\text{All. } j} (a_{ij}\phi_j + b_i) \quad , \quad i = 1,2,3,..... \quad . \quad (3.3\text{-}1)$$

The matrix theory states that this set of equations will, in an iterative procedure, converge to its exact solution if the matrix a_{ij} is 'diagonally dominant' (Forsythe & Wasow 1960). This condition can be expressed as:

$$\sum_{\text{all } j} |a_{ij}| \leqslant 1 \quad \text{(for all i)} \quad ,$$

$$\text{with strict inequality for at least one i} \quad . \quad (3.3\text{-}2)$$

Experience has shown that this condition is often sufficient, but not always necessary for convergence; it may be mildly contravened without serious effect.

That equation (3.2-24) will satisfy the above condition is easily proved if S be considered independent* of ϕ. In that equation, A's, B's and δ's are all positive; therefore:

$$\sum_{\text{all I}} |C_I| = \sum_{\text{all I}} C_I$$

$$= \sum_{\text{all I}} (A_I+B_I.\delta_I) / \sum_{\text{all I}} (A_I+B_I.\delta_P) \quad . \quad (3.3\text{-}3)$$

Thus the condition that $\sum C_I \leqslant 1$ is:

$$\sum_{\text{all I}} \{B_I.(\delta_I-\delta_P)\} \leqslant 0 \quad . \quad (3.3\text{-}4)$$

This condition is obviously satisfied when δ is a constant; this is the case for all equations listed in table 2.4-1 with one exception only - the vorticity equation with non-uniform viscosity. As mentioned earlier, condition (3.3-2), in some cases, may be over-stringent. It seems that in many practical cases, the variations of viscosity are such that inequality (3.3-4) is not seriously contravened; one such example follows in chapter 5 (see also Gosman et al. 1968).

To prove diagonal dominance, we now have to show that strict inequality (3.3-2) is observed for, at least, one set of coefficients. Consider the boundary condition

$$\phi = C \quad , \quad (3.3\text{-}5)$$

where C is not a function of ϕ.

For such a boundary condition, with the notation of (3.3-1),

$$\Sigma |a_{ij}| = 0 \quad . \quad (3.3\text{-}6)$$

---

* See Gosman et al. (1968) for the effect of a variable S on convergence.

For almost all practical problems this type of boundary condition is always specified for at least a part of the boundary.

Thus we see that the difference equations are stable according to this criterion; of course, there are other criteria which could be used. Barakat and Clark (1965) have discussed some of the common criteria; their experience, and that of the other research workers, indicates that simple criteria such as (3.3-2) are usually sufficient to ensure convergence.

3.3-2 Accuracy and economy

The difference between the numerical solution of the difference equations and the exact solution of the differential equations is the overall numerical error; * our discussions of accuracy will refer to this error. Economy, in this context, will refer to the actual cost of the machine-time required to procure the numerical solution by iterative means.

The overall numerical error is composed of three components: a) the round-off error, b) the iterative error, and c) the discretization error.

a) The round-off error: This error is a result of the limitations on a computing machine to perform all arithmetic operations with a finite number of digits. In practice, the round-off error is reduced to negligible

---

* It is being assumed that a unique solution of the differential equations exists, and that another unique solution to the difference equations also exists.

proportion of the overall error by using a sufficiently large number of digits; experience suggests that 8-digit numbers, available as a standard option on many computing machines, are accurate enough for most practical purposes.

b) The iterative error: The iterative error is the difference between the iterative numerical solution and the exact solution of the difference equations. It is a reflexion of the fact that, ultimately, the total number of iterations must be limited for reasons of economy; for, the computing time increases in direct proportion to the number of iterations. A compromise is sought in that the iterative error is reduced to a small acceptable value by performing a sufficiently large number of iterations.

For a convergent algorithm, a convenient practical measure for termination of computations (and an indirect measure of the iterative error) is the index of convergence, λ, defined as:

$$\lambda \equiv \max_{(\text{all nodes})} \left| (\phi^{I} - \phi^{I-1})/\phi_{ref} \right| \quad . \qquad (3.3\text{-}7)$$

In this relation I and I-1 denote the ϕ-values from two successive iterations and ϕ_{ref} is a suitable reference value. ϕ_{ref} may be set equal to ϕ^{I}, or it may be replaced by a representative value, such as the maximum, in whole of the field. Computations are terminated when λ falls below a prespecified limit λ_{ref}. The actual magnitude of λ_{ref} is dictated by reasons of economy and the acceptable level of the iterative error.

c) The discretization error: The difference between the exact solution of the difference equations and that of the differential equations is termed the discretization error. It is a consequence of solving the difference equations at a discrete number of points in space instead of solving the differential equations in a continuum. In other words, this error is composed of the errors entailed by the assumptions for the respresentative values of ϕ and its gradients along the cell boundaries and by the formulae for ψ_{ne} etc. In many cases this error forms almost whole of the overall numerical error; the errors from the other two sources having been made negligible by a judicious selection of the number of digits and the number of iterations. The accuracy of the numerical solution is therefore intimately related to this error. Unfortunately, this is also the error about which the least is known. In general, it cannot be reliably predicted, as the requisite theoretical knowledge is not yet available; reliance has to be placed on empirical information. It seems that two of the factors which influence the magnitude and nature of this error are the size of the grid and the local gradients of the variables*. One obvious remedy, of course, is to use a large number of grid nodes with consequently small grid size. However, considerations of economy** and the

---

* This statement can be justified from rigorous reasoning, by Taylor-series analysis, if the solution is assumed to behave as a polynomial in space-coordinates.

** Computing-time per iteration increases in direct proportion to the number of nodes. Moreover, in general, the total number of iterations required to reduce the iterative error to a prespecified level, also increases with the number of nodes.

size (storage space) of the computing machine usually limit the total number of grid-nodes. Fortunately, having chosen the grid-nodes, one can distribute these to obtain a better accuracy than that which would be obtainable from a uniform distribution. No hard and fast rules are available for the distribution of nodes. An empirical suggestion is to place the nodes closer where the gradients of the variables are large; for example, near a solid wall. On the other hand, the nodes may be spaced farther apart when these gradients are small without any appreciable loss of accuracy. Some illustrations of the use and advantages of non-uniform grids are given in chapter 5.

From the foregoing discussion on accuracy and economy, it is clear that, at least for the present, the relevant information can be obtained only empirically; whatever theoretical knowledge exists can help us little. In this regard, analysis of numerical solutions will be of special value; in chapter 5 the accuracy and economy of the numerical solutions to two problems will be discussed.

Chapter 4

Two special flow-models

The prediction of turbulent flows requires some information regarding the physics of the phenomena; specifically, it is necessary to account for the intense mixing caused by turbulence. The first part of this chapter describes a model of turbulence based on the Kolmogorov-Prandtl hypotheses. The second part uses this model to formulate a Couette-flow model which allows analytic integration for regions close to a wall; the need for a fine grid to account for steep-gradients near a wall is thus eliminated, and the solution procedure is made more economical.

4.1 Kolmogorov-Prandtl model of turbulence

4.1-1 The purpose

There are two current approaches to the analysis and prediction of turbulent flows. One of these concerns itself with the description of the mean flow only and allows for the effect of turbulence by postulating various similarity hypotheses. In contrast, the second approach attempts a description of both the nature and the effect of turbulence and usually makes extensive use of various statistical correlations to deal with the mathematical problem. For want of any better terminology, we will call these approaches, respectively, 'phenomenological' and 'statistical'.

Because of its mathematical complexity, the statistical approach has been successful in dealing with only the simplest of the practical situations; whereas most of the engineering information has originated in the less sophisticated, but mathematically simpler, phenomenological approach.

Probably the most significant practical contribution to the phenomenological approach to turbulence has been Boussinesq's concept of an 'effective viscosity'. Together with Prandtl's 'mixing-length' hypothesis, it has made possible the predictions of a large number of turbulent problems, especially in the field of boundary-layer flows. However, in recent years, it has become increasingly evident that Prandtl's concept of a 'mixing-length' must give way to more realistic assumptions.

Kolmogorov (1942) and Prandtl (1945) proposed a model of turbulence in which they introduced the kinetic energy of the fluctuating motion. This model, though still too simple, goes some way to characterise the nature of turbulence and is more promising than Prandtl's 'mixing-length'model. It has already succeeded in predicting the behaviour of some flows for which the 'mixing-length' model was found inadequate (e.g. Emmons 1945; Spalding 1967b). It is this model which forms the basis of the present section.

4.1-2 The basic hypotheses

The kinetic energy of turbulence, k, is defined as:

$$k \equiv (1/2).\overline{u_i'.u_i'} = (1/2).(\overline{u_1'^2}+\overline{u_2'^2}+\overline{u_3'^2}), \qquad (4.1\text{-}1)$$

where over-bars denote time-averages, and u_i', the fluctuating component of velocity in direction i, is related to the instantaneous total velocity U_i, and the mean velocity u_i by:

$$U_i = u_i + u_i' \quad . \qquad (4.1\text{-}2)$$

A differential equation for the balance of k can be derived from the Navier-Stokes equations with the help of definitions such as (4.1-2); such equations have been derived by a number of authors (e.g. Wolfshtein 1967) and we will make use of their derivations.

For a two-dimensional axisymmetrical flow, the equation for the balance of k is:

$$(\partial/\partial x_j)(r.G_j.k)-(\partial/\partial x_j)(r.\Gamma_{k,eff}.\partial k/\partial x_j)-r.(P-D) = 0, \qquad (4.1\text{-}3)$$

where $\Gamma_{k,eff}$ is the effective exchange coefficient for k; P and D are the production and dissipation terms, respectively. The rest of the notation follows section 2.1-3. Furthermore, for incompressible flows, the production term may be expressed as:

$$P \equiv \mu_t.(\partial u_i/\partial x_j)(\partial u_i/\partial x_j+\partial u_j/\partial x_i), \qquad (4.1\text{-}4)$$

μ_t being the turbulent viscosity.

Equation (4.1-3) fits into the general pattern outlined in sect. 2.4; therefore, given suitable expressions for $\Gamma_{k,eff}$, μ_t, and D, this equation may be solved for k by the numerical procedure of chapter 3. Following Emmons (1954), Spalding (1967b) and others, we may postulate that $\Gamma_{k,eff}$, μ_t, and D are all dependent only on k, the kinetic energy of turbulence and l, a turbulence length scale. Dimensional considerations (e.g. Emmons)

then lead to:

$$\Gamma_{k,eff} = C_{\mathcal{D}} \cdot \rho \cdot k^{\frac{1}{2}} \cdot l \quad , \qquad (4.1\text{-}5)$$

$$\mu_t = C_\mu \cdot \rho \cdot k^{\frac{1}{2}} \cdot l \quad , \qquad (4.1\text{-}6)$$

$$D = C_D \cdot \rho \cdot k^{3/2} \cdot l \quad , \qquad (4.1\text{-}7)$$

where $C_{\mathcal{D}}$, C_μ, and C_D are constants and ρ is the mass density.

$\sigma_{k,eff}$, the effective 'Prandtl number' for k is given by:

$$\sigma_{k,eff} = C_\mu / C_{\mathcal{D}} \cdot \qquad (4.1\text{-}8)$$

The determination of l and C's is of prime importance if this model of turbulence is to be employed for predictions: this is the topic of discussion for the following sections.

4.1-3 The length scale

The length scale, l, is most readily visualized as a representative of the local mean eddy size. It affects the generation, diffusion and dissipation of the kinetic energy of turbulence; and, of course, through turbulent viscosity, it affects the flow field and the distribution of all other dependent variables. In the Kolmogorov-Prandtl model of turbulence, the length scale is thus one of the most important factors; yet the information available about it is meagre. Starting from the Navier-Stokes equations, Rotta (1951) succeeded in deriving a differential equation which may be interpreted as an equation for the length scale; but, except for very simple cases, it has not been possible to solve this equation. Recently some progress has been reported by Spalding (1967c) and Harlow & Nakayama (1967); nevertheless, it

will be some time before this equation can be solved for general cases.

In the absence of quantitative information, qualitative information prevails. It can be shown that, under some circumstances, a proportionality exists between the length scale and Prandtl's 'mixing-length' (Spalding 1967d); at present it is convenient to assume the proportionality to be generally true. Then for flows close to a wall, the length scale may be considered proportional to the distance from the wall and for flows away from a wall, it may be considered a constant. For the definitions of sect. 4.1-2, the proportionality constant for the regions near a wall may be taken as unity, i.e. the length scale is equal to the distance from the wall. Since Prandtl's 'mixing-length' near a wall is generally taken as 0.4 times the distance from the wall (Schlichting 1960), from this result Spalding (1967d) suggested that the length scale, as defined here, should be taken as about 2.5 times the Prandtl's 'mixing-length' everywhere.

In fact, it seems more than likely that the above qualitative deductions are gross over-simplifications. A closer look at Rotta's equation for the length scale shows that, like all ohter dependent variables, the length scale may be interpreted as being convected, diffused, generated and dissipated. Hence, for a general problem, if the differential equation were solved, the distribution is certain to be much more complex. To solve the equation is the task of the future; for the present, we would accept the implications of the above-mentioned qualitative information.

4.1-4 The effective exchange coefficients

The turbulent viscosity μ_t may be evaluated from expression (4.1-6); it has now to be related to the effective viscosity and the effective diffusivity of section 2.2-1.

Following Spalding (1967d), it may be assumed that for highly turbulent regions,

$$\mu_{eff} = \mu + \mu_t, \text{ and} \qquad (4.1\text{-}9)$$

$$\Gamma_{\phi,eff} = \mu/\sigma_\phi + \mu_t/\sigma_{\phi,t} \; . \qquad (4.1\text{-}10)$$

Usually for such flows turbulent viscosity is orders of magnitude larger than the laminar viscosity and it is a common practice to retain only the second term on the R.H.S. of (4.1-9) and (4.1-10) unless the laminar Prandtl/Schmidt number is very small.

For flows which are not fully turbulent, such as in the regions close to a wall, following a suggestion by Spalding (1968), (4.1-6) may be generalized by assuming C_μ to be a function of the 'Reynolds number of turbulence',

$$R_t = \rho . k^{\frac{1}{2}} . l/\mu \; ; \qquad (4.1\text{-}11)$$

and then

$$C_\mu = C_\mu\{R_t\} \; , \qquad (4.1\text{-}12)$$

where $\{\ \}$ denotes 'a function of'.

As R_t tends to infinity, the laminar viscosity ceases to have any noticeable influence on the transfer processes and C_μ may then be assumed a constant. On the other hand, when R_t tens to zero, the flows become laminar and C_μ tends to $1/R_t$, No proven proposal has yet emerged for the intermediate ranges of R_t though some suggestions have been put forward (e.g. Spalding 1967d, Wolfshtein 1967).

The uncertainty which prevails about μ_{eff} under some circumstances, prevails to a smaller extent about the value of $\sigma_{\phi,eff}$. For turbulent flows remote from walls, both $\sigma_{T,eff}$ and $\sigma_{m,eff}$ are commonly taken as 0.5 for plane flows (Abramovich 1963) and 0.7 for round-sectioned jets (Forstall & Shapiro 1950). For turbulent flow in a pipe the review of heat transfer data by Kestin and Richardson (1963) suggests a value of 0.8 for $\sigma_{T,eff}$, whereas Jayatillaka (1966) recommended a value of 0.9 for both $\sigma_{T,eff}$ and $\sigma_{m,eff}$ in turbulent pipe flows.

Very close to a smooth impermeable wall the value of $\sigma_{\phi,eff}$ remains uncertain and no definite recommendations can be made (Spalding 1967d). After Jayatillaka and Spalding (1965), a convenient practice is to express the extra resistance offered by such regions in terms of a separate integral which is a function of $\sigma_{\phi}/\sigma_{\phi,t}$; the use of this concept will be illustrated in sect. 4.2-3.

4.1-5 The empirical constants

The constants $C_{\mathcal{J}}$, C_{μ} and C_{D} can be deduced from experimental data on turbulent flows. Such deductions have been made by a number of research workers; for details of derivation the reader may consult one of the references cited in the preceding sections (e.g. Spalding (1967d).

The following values, used for the predictions presented in the next chapter, were derived by Spalding (1967b):

$$
\begin{aligned}
C_{\mathcal{D}} &= 0.130 \ , \\
C_{\mu} &= 0.200 \ , \\
C_{D} &= 0.313 \ , \text{ and} \\
\sigma_{k,eff} &= 1.540 \ .
\end{aligned}
\qquad (4.1\text{-}13)
$$

4.2 The Couette model of flow

4.2-1 The purpose

The stimulus to the following analysis is the fact that often the dependent variables change steeply close to a wall. To obtain good accuracy with the finite-difference formulae described above, the grid would have to be very fine, with consequent expense of computer time. This shortcoming can be obviated by the use of Couette-flow assumptions which, under certain circumstances, allow analytic integrations near a wall. Thus, the whole of the flow field is broken down into two regions: a thin one close to the wall, where a Couette-flow solution is obtained, and the major part of the flow where the solution is obtained for the complete equations. These two are then matched at the intermediate 'boundary' with the Couette-flow solution serving as the 'boundary condition' for the finite-difference solution of the complete equations. Patankar and Spalding (1967) and Wolfshtein (1967) have already demonstrated the advantages of such an approach.

4.2-2 The differential equations

Close to an impermeable wall, the velocity along the wall starts to decrease rapidly and, thus, in a thin region adjacent to the wall, the longtitudinal convection

terms can be neglected altogether. The resulting flow is commonly known as a Couette flow and the previously described partial differential equations reduce to ordinary differential equations for this flow. With appropriate assumptions, these equations can be integrated once-for-all to relate the fluxes at the wall, such as the Stanton number, to other flow-parameters, such as the Reynolds number.

Let us consider the Couette flow along an impermeable wall which lies on the x_1-axis of the coordinate system; because of the thinness of the region of interest we will not account for the variations of the radius r. The resulting differential equations can be deduced from equations (2.1-2) and (2.4-2). They are:

<u>for momentum</u>:

$$(d/dy_*)(\mu_* . du_*/dy_*) - p_* = 0 \quad , \qquad (4.2\text{-}1)$$

<u>for enthalpy</u>:

$$(d/dy_*)(\mu_*/\sigma_{T,eff} . dT_*/dy_*) = 0 \quad , \qquad (4.2\text{-}2)$$

<u>and for turbulent kinetic energy</u>:

$$(d/dy_*)(\mu_*/\sigma_{k,eff} . dk_*/dy_*) + P_* - D_* = 0 \quad , \qquad (4.2\text{-}3)$$

where, with subscript S denoting the conditions at the wall and C those at the outer edge of the Couette layer,

$$\begin{aligned} y_* &= x_2/x_{2,C} \quad , \\ k_* &= k/k_C \quad , \\ u_* &= u_1/u_{1,C} \quad , \\ T_* &= (T-T_S)/(T_C-T_S) \quad , \\ \mu_* &= \mu_{eff}/(\rho k^{\frac{1}{2}} x_2)_C \quad , \\ p_* &= (dp/dx_1) . (x_2/(\rho k^{\frac{1}{2}} u_1)_C) \quad . \end{aligned} \qquad (4.2\text{-}4)$$

P_* and D_* represent, respectively, the non-dimensional production and dissipation terms which will be given later.

It should be noted that equation (4.2-2) is valid only for low velocity flows as it neglects both viscous dissipation and kinetic heating; also, under these circumstances, the equation for the transport of chemical-species, m, is identical to the enthalpy equation, as long as the rate of mass-transfer is small enough not to affect the fluid properties. A more general case of Couette-flows has been considered by Spalding (1967d).

For ease of interpreting results, let us define the following non-dimensional parameters:

Skin-friction coefficient: $s = \tau_S/(\rho u_1^2)_C$,

Stanton number: $St = \dot{q}''_S/(c_p.(T_C-T_S)(\rho u_1)_C)$, (4.2-5)

Reynolds number: $Re = (\rho u_1 x_2/\mu)_C$,

and,

Turbulence Reynolds number: $R_t = (\rho k^{\frac{1}{2}} x_2/\mu)_C$;

where τ_S is the wall shear-stress, $\dot{q}''_S$ is the wall heat-flux, and c_p is the specific heat of the fluid.

Equations (4.2-1) and (4.2-2) can now be integrated to obtain:

$$s = (R_t/Re)(\int_0^1 \mu_*^{-1}.dy_*)^{-1}.(1-p_*\int_0^1 y_*.\mu_*^{-1}.dy_*) \quad , \quad (4.2\text{-}6)$$

$$St = (R_t/Re).(\int_0^1 \sigma_{T,eff}.\mu_*^{-1}.dy_*)^{-1} \quad . \quad (4.2\text{-}7)$$

The evaluation of the integrals in these equations would enable us to calculate the skin friction and the Stanton number. However, before these integrals can be obtained, the relationships connecting μ_* and $\sigma_{T,eff}$ with y_* must be available.

a) Evaluation of the effective viscosity: Since μ_* is linked, by the Kolmogorov-Prandtl hypothesis, to the kinetic energy of turbulence, we first turn our attention to equation (4.2-3). This equation cannot be integrated without a recourse to additional assumptions about P_*, D_*, $\sigma_{k,eff}$, and μ_*. Neglecting the existence of a transition region, let us assume that the Couette flow can be divided into two distinct regions: a laminar sub-layer close to the wall, and a fully turbulent region in the outer part. Inconsistencies of such an assumption can be tolerated for the present because of the uncertain nature of the empirical input, and, to some extent, also because they simplify the mathematical problem considerably.

If the junction of the laminar and the fully turbulent regions is denoted by the subscript J, then the implications of the two-layer-Couette-flow assumption, together with the Kolmogorov-Prandtl hypotheses, can be expressed as in the following table 4.2-1:

State of fluid	$k_*^{\frac{1}{2}} y_*$	μ_*	P_*	D_*
Laminar	R_{t*}	R_t^{-1}	0	$2k_*/(y_*^2 R_t \sigma_{k,eff})$
Turbulent	R_{t*}	$C_\mu k_*^{\frac{1}{2}} y_*$	$\mu_*(du_*/dy_*)^2$	$C_D k^{3/2}/y_*$

Table 4.2-1 Various terms in the equation for the kinetic energy of turbulence.

In this table R_{t*} is defined as:

$$R_{t*} \equiv R_{t,J}/R_t \quad . \tag{4.2-8}$$

D_*, in the above table, has been deduced from dimensional reasoning and the constant $2/\sigma_{k,eff}$ allows a particularly simple solution for the laminar region. Details of the deduction have been given by Spalding (1967d).

At this stage we make one further assumption: that the kinetic-energy profile in the fully turbulent region can be represented by a power law of the form:

$$k_* = y_*^q \qquad (4.2\text{-}9)$$

The exponent q can be determined by substituting (4.2-8) into the parent equation (4.2-3) and matching it at the J-surface with the solution for the laminar region. The resultant expression is:

$$q = (2(C_D - P_* y_*^{1-1.5q})/(3C_{\mathcal{J}}))^{\frac{1}{2}} \quad . \qquad (4.2\text{-}10)$$

Not surprisingly, the exponent q turns out to be a function of y_*. Therefore, in general, any selection of q allows the differential equation to be satisfied at only one point across the flow. In the absence of any better guide, we will choose this point to be the outer edge of the Couette flow where y_* equals unity. Then:

$$q = (2/3 \cdot (C_D - P_*)/C_{\mathcal{J}})^{\frac{1}{2}} \quad . \qquad (4.2\text{-}11)$$

μ_* can now be obtained from table 4.2-1 and equation (4.2-8).

b) Evaluation of the skin-friction coefficient: The skin-friction coefficient can be evaluated from equation (4.2-6) with the help of the integrals:

$$I_1 = \int_0^1 \mu_*^{-1}\, dy_* \quad , \text{ and}$$
$$I_2 = \int_0^1 \mu_*^{-1}\, y_* dy_* \quad , \qquad (4.2\text{-}12)$$

where, for:

$$q = 0,\ I_1 = R_{t,J} - C_\mu^{-1} \ln R_{t*} \quad ,$$
$$q \neq 0,\ I_1 = (R_{t,J} + 2C_\mu^{-1} q) \cdot R_{t*}^{-q/(q+2)} - 2C_\mu^{-1} q \quad ,$$
$$q = 2,\ I_2 = R_{t,J}/2 - 2C_\mu^{-1} \ln R_{t*} \quad , \qquad (4.2\text{-}13)$$
$$q \neq 2,\ I_2 = (R_{t,J}/2 - 2C_\mu^{-1}(2-q)^{-1}) \cdot R_{t*}^{(2-q)/(2+q)} +$$
$$+ 2C_\mu^{-1} (2-q)^{-1} \quad .$$

$R_{t,J}$ is given by:

$$R_{t,J} = 2.5(C_\mu C_D)^{-1/4}(\ln(R_{t,J}(C_\mu C_D)^{-1/4}) + 2.2) \quad . \quad (4.2\text{-}14)$$

For the empirical constants suggested in section 4.1-5 the value of $R_{t,J}$ is 23.3.

c) Evaluation of the Stanton number: To evaluate the Stanton number, following the practice of Spalding and Jayatillaka (1965), let us split the integral in equation (4.2-7),

$$I_3 \equiv \int_0^1 \sigma_{T,eff}\mu_*^{-1}\, dy_* \quad , \quad (4.2\text{-}15)$$

into two parts so that:

$$I_3 = \sigma_{T,t}\int_0^1(\sigma_{T,eff}/\sigma_{T,t} - 1)\mu_*^{-1}\, dy_* + \sigma_{T,t}\int_0^1\mu_*^{-1}dy_* \quad (4.2\text{-}16)$$

As explained in section 4.1-4, for the fully turbulent region $\sigma_{T,eff}$ tends to a constant $\sigma_{T,t}$; therefore, the above may be approximated by:

$$I_3 = \sigma_{T,t}\,(I_1 + I_1) \quad , \quad (4.2\text{-}17)$$

where

$$I_1 \equiv \int_0^1(\sigma_{T,eff}/\sigma_{T,t} - 1)\mu_*^{-1}\, dy_* \quad . \quad (4.2\text{-}18)$$

I_1 expresses the extra resistance of the semi-laminar transitional layer to heat (or mass) transfer: it is only when $\sigma_{T,eff}$ is different from $\sigma_{T,t}$ that it contributes to the total resistance I_3.

For high values of the laminar Prandtl number σ_T, and with the use of (4.1-10), it can be shown the I_1 is given by(Spalding 1967d):

$$I_1 = C_\sigma\,(\sigma_T/\sigma_{T,t} - 1).(\sigma_T/\sigma_{T,t})^{-1/4}.(C_\mu C_D)^{-1/4} \quad . \quad (4.2\text{-}19)$$

Jayatillaka (1966) suggested a value of 9.24 for the empirical constant C_σ after a survey of the experimental data on turbulent pipe flows.

4.2-3 The use and limitations of the Couette-flow model

a) The use: As already stated in section 4.2-1, the main function of the Couette-flow model is to provide a set of boundary conditions for the finite-difference equations a small distance away from the wall, for reasons of economy. A simple way of incorporating the Couette-flow solutions is to use the concept of 'linearizing values' * first proposed by Patankar and Spalding (1967) and subsequently modified by Spalding (1968). The essential steps in the use of this concept are as follows.

For a conserved property ϕ, the Couette-flow equation in the absence of any source terms (cf. equation (4.2-2)) is:

$$J_\phi = \Gamma_\phi . d\phi/dx = \text{constant} \quad . \qquad (4.2\text{-}20)$$

Rearrangement yields:

$$d\phi = J_\phi . \Gamma_\phi^{-1} . dx \quad . \qquad (4.2\text{-}21)$$

Formal integration, from a point 'S' on the surface of the wall to a point 'C' in the flow field, gives:

$$\phi_C = \phi_S + J_\phi . \int_{x_S}^{x_C} \Gamma_\phi^{-1} . dx \quad . \qquad (4.2\text{-}22)$$

When Γ_ϕ changes little, an appropriate algebraic analogue is:

$$\phi_C = \phi_S + 2J_\phi . (x_C - x_S)/(\Gamma_{\phi,C} + \Gamma_{\phi,S}) \quad . \qquad (4.2\text{-}23)$$

However, when the variations of Γ_ϕ are non-linear, this expression will no longer be accurate. A better expression is:

$$\phi_C = \phi_{S,L} + 2J_\phi . (x_C - x_S)/(\Gamma_{\phi,C} + \Gamma_{\phi,S}) \quad , \qquad (4.2\text{-}24)$$

where

$$\phi_{S,L} = \phi_S - 2J_\phi . (x_C - x_S)/(\Gamma_{\phi,C} + \Gamma_{\phi,S}) + J_\phi . \int_{x_S}^{x_C} \Gamma_\phi^{-1} . dx \qquad (4.2\text{-}25)$$

---

* Patankar and Spalding used the name 'slip values'.

The purpose of defining a linearizing value $\phi_{S,L}$ is to retain the homogeneity of the structure in the finite-difference relations: equation (4.2-24) is an appropriatly rearranged version of equation (3.2-18), the latter being the general finite-difference relation for the diffusional flux.

In the course of computations, the linearizing value is evaluated with the help of the equations such as (4.2-7) and (4.2-17) to calculate the value of the integral which appears in equation (4.2-25). ϕ_C can then be calculated and used as the boundary condition in the finite-difference equation for the main region of flow away from the wall.

For the predictions presented in section 5.2, the linearizing values were used only for the temperature and the kinetic energy of turbulence. The stream-function is not directly affected by diffusion and, therefore, it was not linearized. The vorticity, on the other hand, can be calculated directly from the shear-stress relation. For the present purposes, it may be written as:

$$\omega_C = du_1/dx_2 = (\tau_S + (x_{2,C}-x_{2,S}).dp/dx_1)/\mu_{eff,C} \quad (4.2\text{-}26)$$

The wall shear-stress, τ_S, can be obtained from equations (4.2-6) and (4.2-13) and dp/dx_1 from the finite-difference solutions.

b) The limitations: The major assumption behind the Couette-flow model is the absence of convection along the wall; and this also proves to be its major limitation. There are some flows in which the role of longtitudinal convection cannot be neglected even in the regions close to a wall. One such case is the heat transfer at high

Prandtl numbers when practically all the changes in the enthalpy profile occur very close to the wall; for such flows, a small amount of convection can make substantail differences. For example, we know that if the upstream section of a pipe is heated, it exerts a considerable influence on the rate of heat transfer from the downstream sections; yet, a model such as the present one, will fail to predict this effect.

Other limitations of the model lie in the assumptions about the variations in the viscosity and the kinetic energy of turbulence and, of course, in the assumption of a step-jump from the laminar to the turbulent state without any transition region. However, these limitations are not so much a part of the mathematical model and they are likely to be overcome by a better understanding of the physical processes involved in turbulent flows.

Chapter 5

Flow Prediction

We have now reached a stage where we are equipped with suitable means for the prediction of two-dimensional steady separated flows. The nucleus of the technique is the numerical procedure outlined in chapter 3, and the peripheral units are in the special flow models of chapter 4, and other relevant auxiliary information. All that now remains is to demonstrate the capabilities of the technique by solving representative practical problems.

The two problems selected for the above purpose are: the confined laminar flow in a square cavity, and the turbulent flow downstream of a sudden enlargement in a circular pipe. Both problems are of engineering interest; and the aim of the exercise is to demonstrate the width of application and generality of the technique. Wherever possible, the numerical solutions will be compared with those obtained from other sources and with the experimental data.

5.1 Laminar flow: Square cavity with a moving lid

5.1-1 Introduction

The formation of a cavity in a flow surface is a common occurrence in everyday engineering practice. Cavities may be caused by roughness elements, steps, or fins; and they lead to substantial increases in heat transfer and pressure losses compared to those for a smooth surface. A simple representation of the cavity flows is the enclosed flow in a square cavity, in which the motion is imparted to the fluid by a moving lid; in the latter respect, it differs from the usual practical problem in which the motion is caused by a stream of fluid flowing past the cavity.

The square-cavity problem is typical of steady separated flows with closed stream lines. These flows have been the subject of a long-standing theoretical and practical interest. Prandtl (1904) and, more recently, Batchelor (1956) conducted theoretical investigations of closed-stream-line flows at high Reynolds numbers. Essentially, they postulated the existence of an 'inviscid core' of fluid surrounded by thin boundary layers. They concluded that, for a two-dimensional laminar flow, the core will consist of uniform-vorticity fluid. Theoretical work of a similar nature has been reported from a number of sources and was recently reviewed by Burggraf (1966). Of late, the emphasis has shifted to numerical solutions; notable among these are the ones by Kawaguti (1961), Simuni (1964), Burggraf (1966), Runchal and Wolfshtein (1966), Runchal et al. (1967) and Greenspan (1967).

The experimental information about laminar flow in a square cavity is meagre: most of the experiments have been limited to the turbulent-flow regime (e.g. Mills 1961). Weiss and Florsheim (1965) have reported some qualitative features of the laminar flow at low Reynolds numbers. Recently Reiman (1967) has conducted a more detailed enquiry into the behaviour of laminar flows and some of his findings have been published by Reiman and Sabersky (1968).

5.1-2 Description of the problem

Fig. 5.1-1 illustrates the problem to be solved. A fluid revolves steadily in a square-shaped cavity under the influence of the sliding upper wall. This wall is held at one temperature; the opposite at another; the side-wall temperatures vary linearly between those of the top and the bottom.

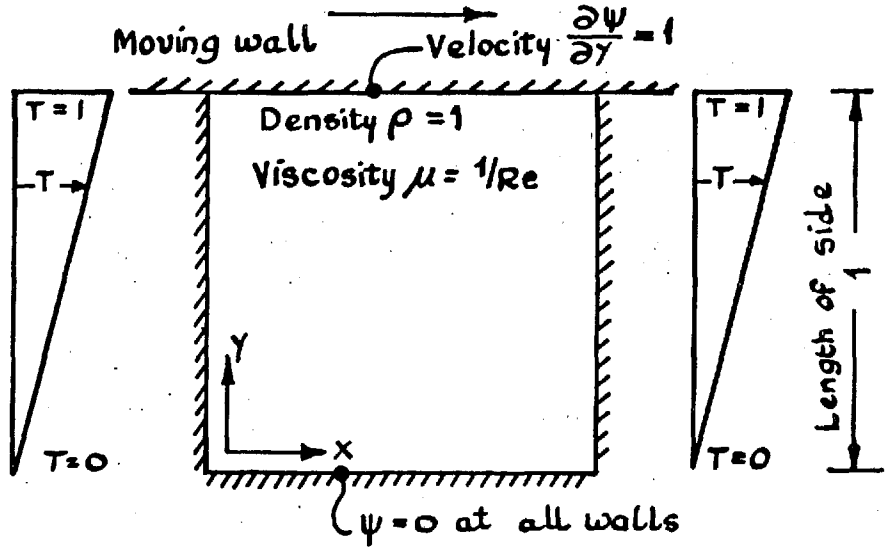

FIG. 5.1-1 GEOMETRY AND BOUNDARY CONDITIONS OF THE SQUARE-CAVITY PROBLEM.

FIG. 5·1-2 THE INFLUENCE OF REYNOLDS NUMBER ON THE SQUARE CAVITY FLOW PATTERNS ; 13×13 NON-UNIFORM GRID, P_r=1.

For convenience, the velocity of the sliding wall, the density, the length of side, and the overall temperature difference are taken as unity. Then the viscosity equals the reciprocal of the Reynolds number, which is one of the two parameters of the problem, the other being the Prandtl number,Pr, of the fluid.

The task is to determine the distributions of stream-function, vorticity and temperature within the cavity, for various values of the Reynolds and the Prandtl numbers.

5.1-3 Presentation of results

The influence of Reynolds number: Fig. 5.1-2 presents the results for Reynolds numbers of 1, 10^3, and 10^4, and a Prandtl number of unity. All the results were obtained with a 13 x 13 non-uniform grid; the grid used is indicated in just one of the diagrams.* The contours reveal the existence of a large primary eddy in the cavity; this is cushioned by small contrarotating eddies in the two lower corners for all Reynolds numbers. The temperature distribution in the field at low Re is almost the same as that in the walls; but at high Re the temperature contours are caused to bulge and sag by the convective effect of the moving fluid. The vorticity contours are similarly distorted at high Reynolds numbers from their near-symmetrical form when Re equals unity.

---

* x-coordinates: 0.,.04,.10,.20,.35,.55,.70, .85,.92,.96,.98,.99,1.0

y-coordinates: 0.0,.04,.10,.20,.32,.44,.56, .68,.80,.90,.95,.98.1.0

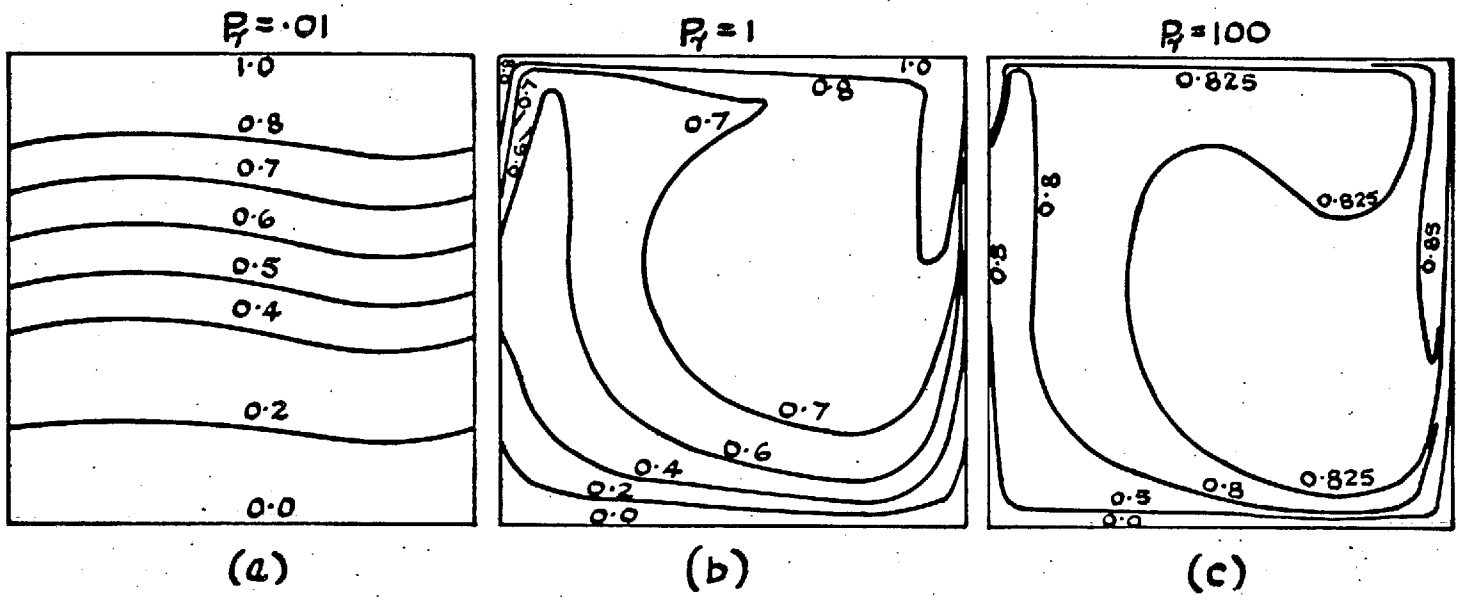

FIG. 5.1-3. THE INFLUENCE OF PRANDTL NUMBER ON THE TEMPERATURE CONTOURS; NON-UNIFORM, 13X13 GRID; Re = 1000

The influence of Prandtl number: Fig. 5.1-3 shows the temperature contours only, for a single Reynolds number of 10^3, and three different Prandtl numbers, 10^{-2}, 1 and 10^2. The central diagram has of course appeared already as Fig. 5.1-2(f) and is repeated here for ease of comparison.

Evidently the high thermal conductivity, which causes the low Prandtl number, nearly succeeds in preventing the convective processes from distorting the temperature contours from their linear, low-Reynolds-number form. When the thermal conductivity is low, on the other hand, as when Pr equals 100, the distortions are still more pronounced than for a Prandtl number of unity.

The influence of grid size and distribution: Figs. 5.1-4 and 5.1-5 show, respectively, the velocity profiles at the vertical centre-line and the vorticity (velocity-gradient) profiles at the moving wall of the cavity for four different grids. In both cases, the grid size and distribution exert a considerable influence on the profiles. This influence is especially strong for the vorticity near the corners of the cavity; this is a manifestation of the fact that the vorticity is a singular function at the two corners of the cavity; any selection of the grid is, thus, bound to reflect this aspect of the solution. It should also be noted that the effect of the grid is less pronounced on the velocity profiles than on the vorticity profiles. In both the cases, it can be concluded that the 13 x 13 non-uniform grid is a better alternative to the 21 x 21 uniform grid from the point of view of economy: the former will require calculations at 144 internal nodes

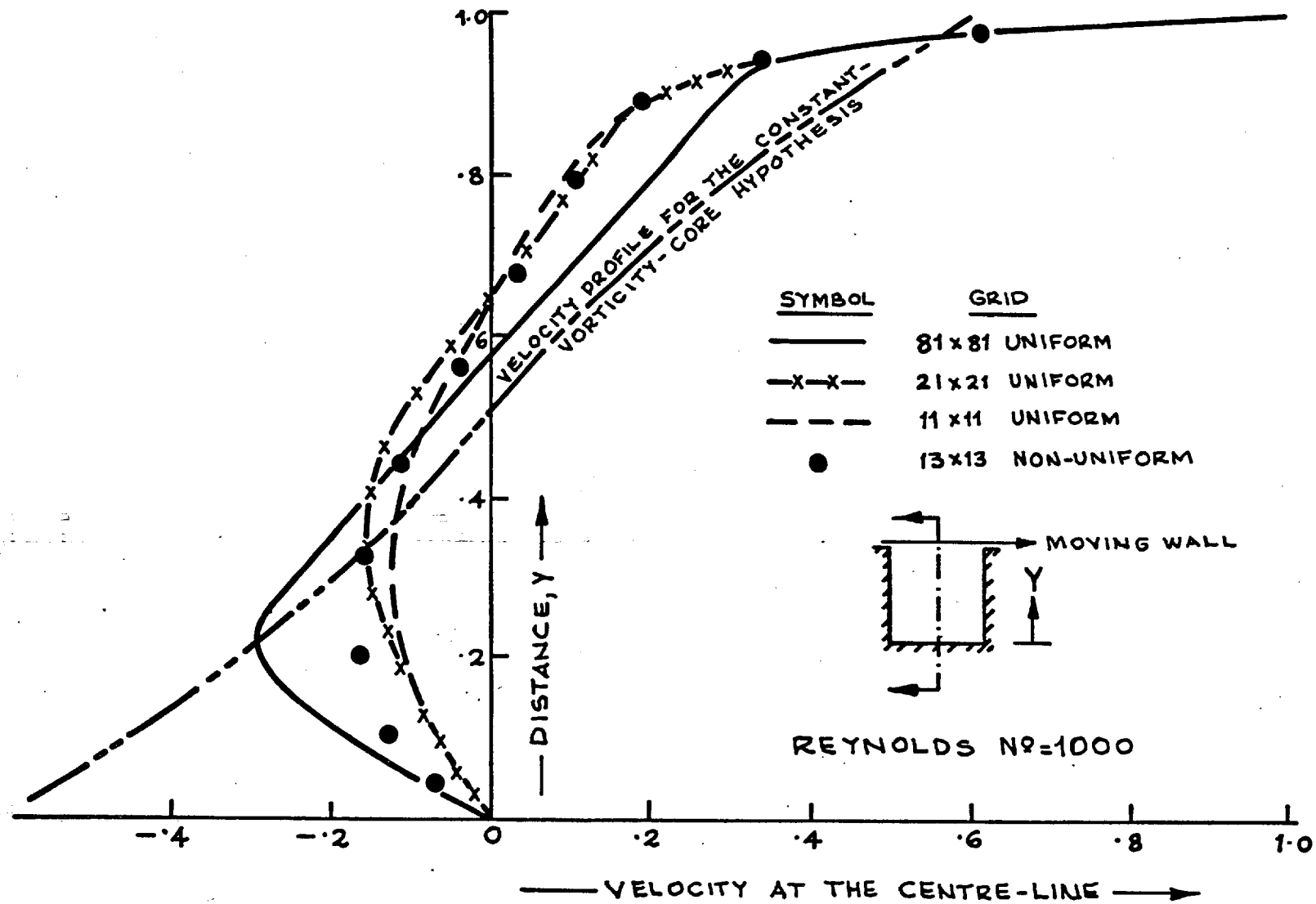

FIG. 5.1-4 EFFECT OF GRID ON THE VELOCITY PROFILE ACROSS THE VERTICAL CENTRE-LINE OF THE SQUARE CAVITY; Re=1000.

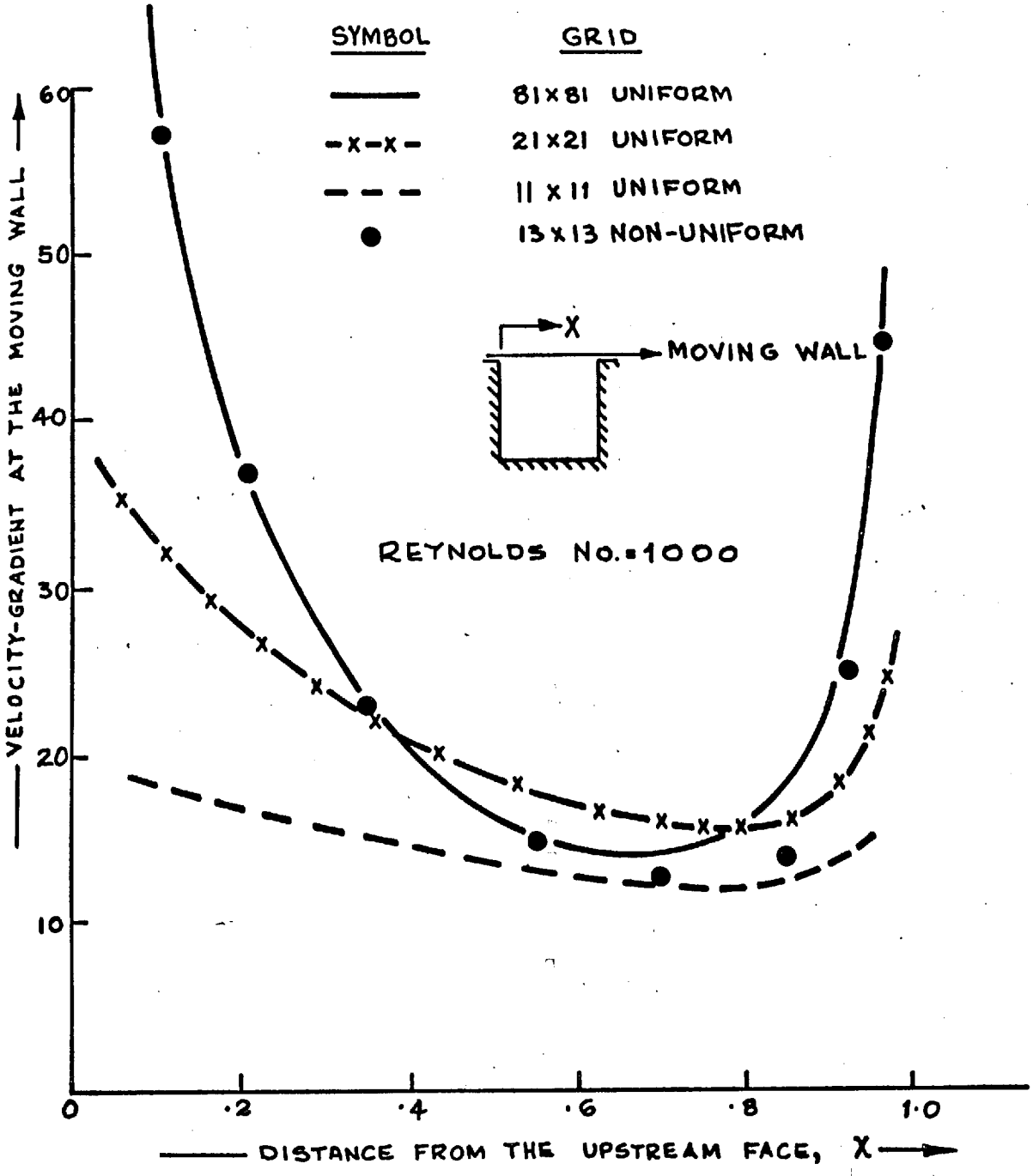

FIG. 5.1-5 EFFECT OF THE GRID ON THE VELOCITY GRADIENTS AT THE MOVING WALL

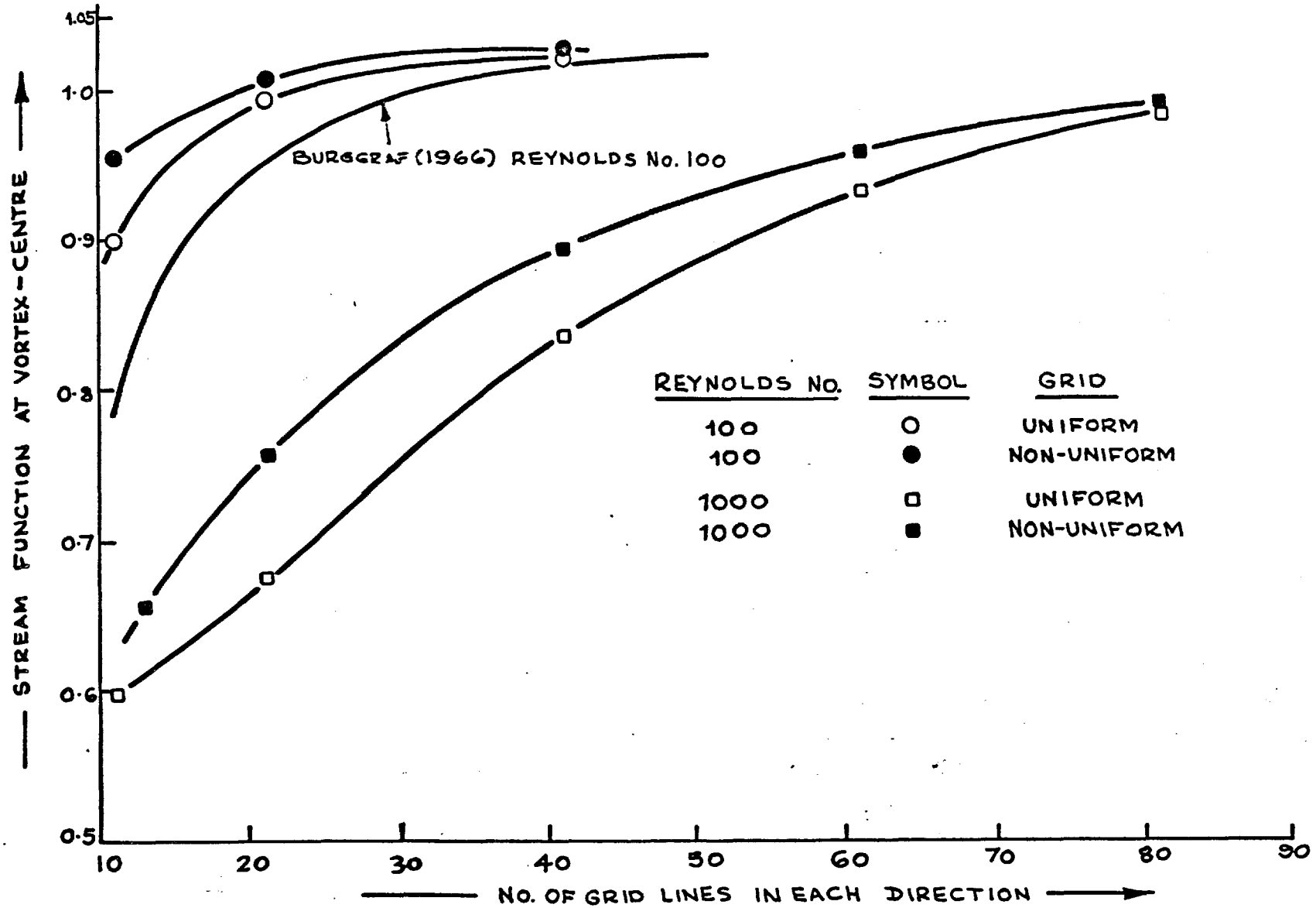

FIG. 5.16 EFFECT OF GRID SIZE AND DISTRIBUTION ON THE STRENGTH OF THE VORTEX IN THE SQUARE CAVITY.

of the grid compared to the 400 nodes of the latter.

It may be remarked here that the influence of the grid has been accentuated by the selection of a rather high Reynolds number of 1000 for the purposes of comparison. From the following discussion, and from the comparison of the present work with that of the previous investigators in the next sub-section, it will be seen that the differences between the results from various grids are much less pronounced for a Reynolds number of 100.

Another aspect of the finite-difference solutions, which is tied up with the questions of the grid size, is the extent of the discretization error as explained in section 3.3-2.

Of course, for the square cavity, the solution of the differential equations is not known; nevertheless, indirect evidence of the accuracy of the solutions may be obtained by demonstrating that the finite-difference solutions tend to a limiting solution with the refinement of the grid.

Fig. 5.1-6 shows the effect of the grid-refinement, and grid-distribution, on the strength of the main vortex, in terms of the stream-function values at the vortex centre, for Reynolds numbers of 100 and 1000. Also shown are the results obtained by Burggraf (1966), by a central-finite-difference technique, for a Reynolds number of 100. It is clearly seen that, for both the Reynolds numbers, there is a distinct convergence towards a limiting solution; though, admittedly, a sufficient flattening of the curves for a Reynolds number of 1000 has not been achieved by 81 x 81 grids, which was the limit imposed by the capacity of the computer.

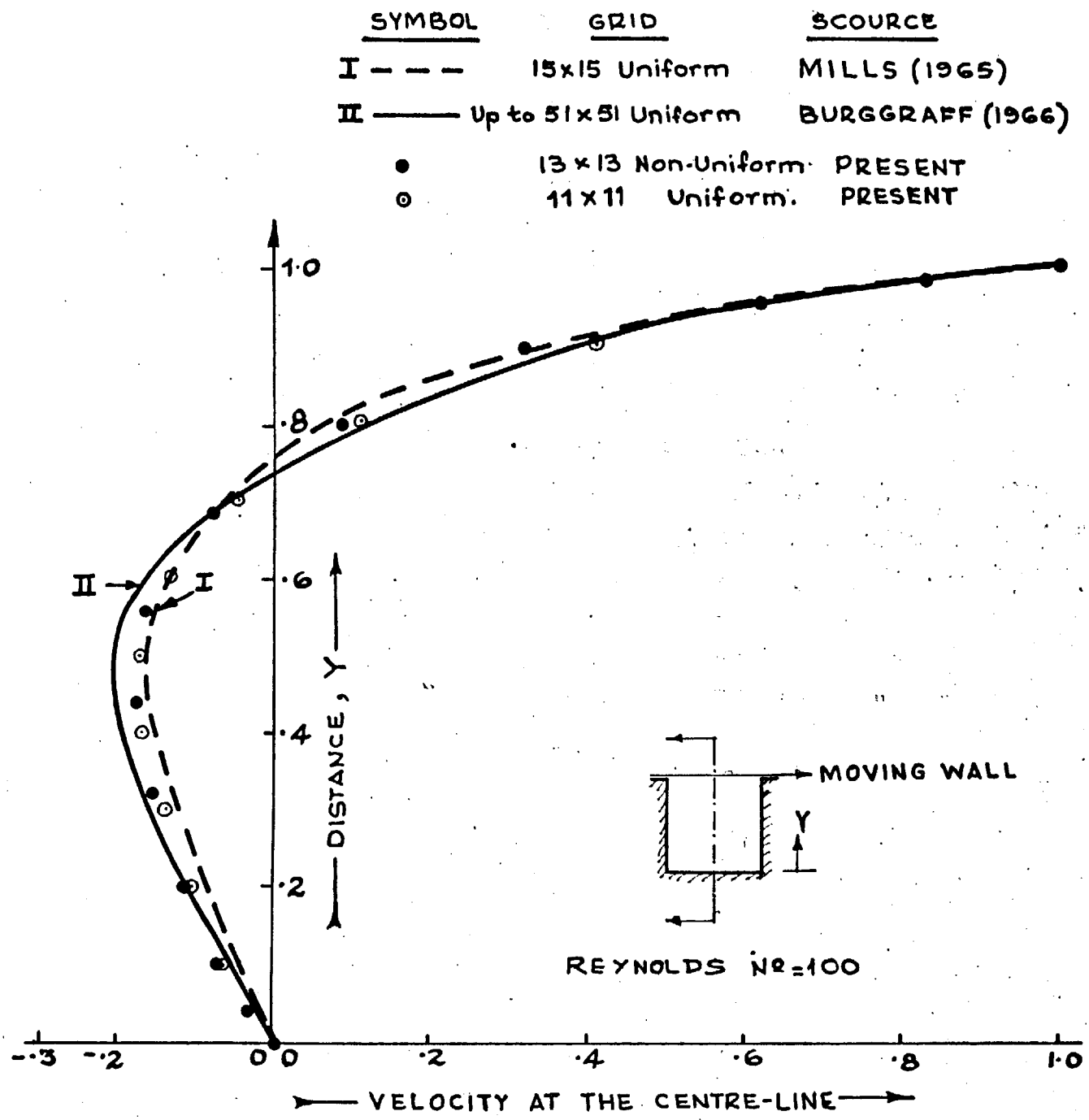

FIG. 5.1-7 COMPARISON OF SOME AVAILABLE RESULTS FOR THE VELOCITY PROFILE ACROSS THE VERTICAL CENTRE-LINE OF THE SQUARE CAVITY; Re = 100.

There are a few more conclusions yet to be drawn from this figure. Firstly, for the same number of grid nodes, non-uniform grids have proved to be consistently better than the uniform grids; thus confirming the remarks made earlier in chapters 3 and 4. Secondly, it is to be noticed that the influence of grid distribution is much less pronounced for a Reynolds number of 100 than that for a Reynolds number of 1000. And, lastly, the present method is a preferable choice to the earlier methods such as the one by Burggraf; at a Reynolds number of 100, the results from the present method are better than those obtained by Burggraf. Moreover, as already pointed out, most of the earlier methods, including Burggraf's, failed to yield convergent solutions at high Reynolds numbers.

Comparison with previous work: Fig. 5.1-7 is presented by way of comparison, and as a further comment on the accuracy of the computations. It displays the velocity profiles at the vertical centre-line of the cavity for a Reynolds number of 100. Included are the results of Mills (1965) and Burggraf (1966) along with the present computations. The agreement between the four sets of results is seen to be satisfactory. It may also be remarked that, at such a low Reynolds number, the advantage gained from finer grids is small.

So far, comparison with the previous work has been limited to the numerical solutions of other research workers; the work of Reiman & Sabersky (1968), on the other hand, enables some qualitative comparison with experimental evidence. Fig. 5.1-8 presents our computed

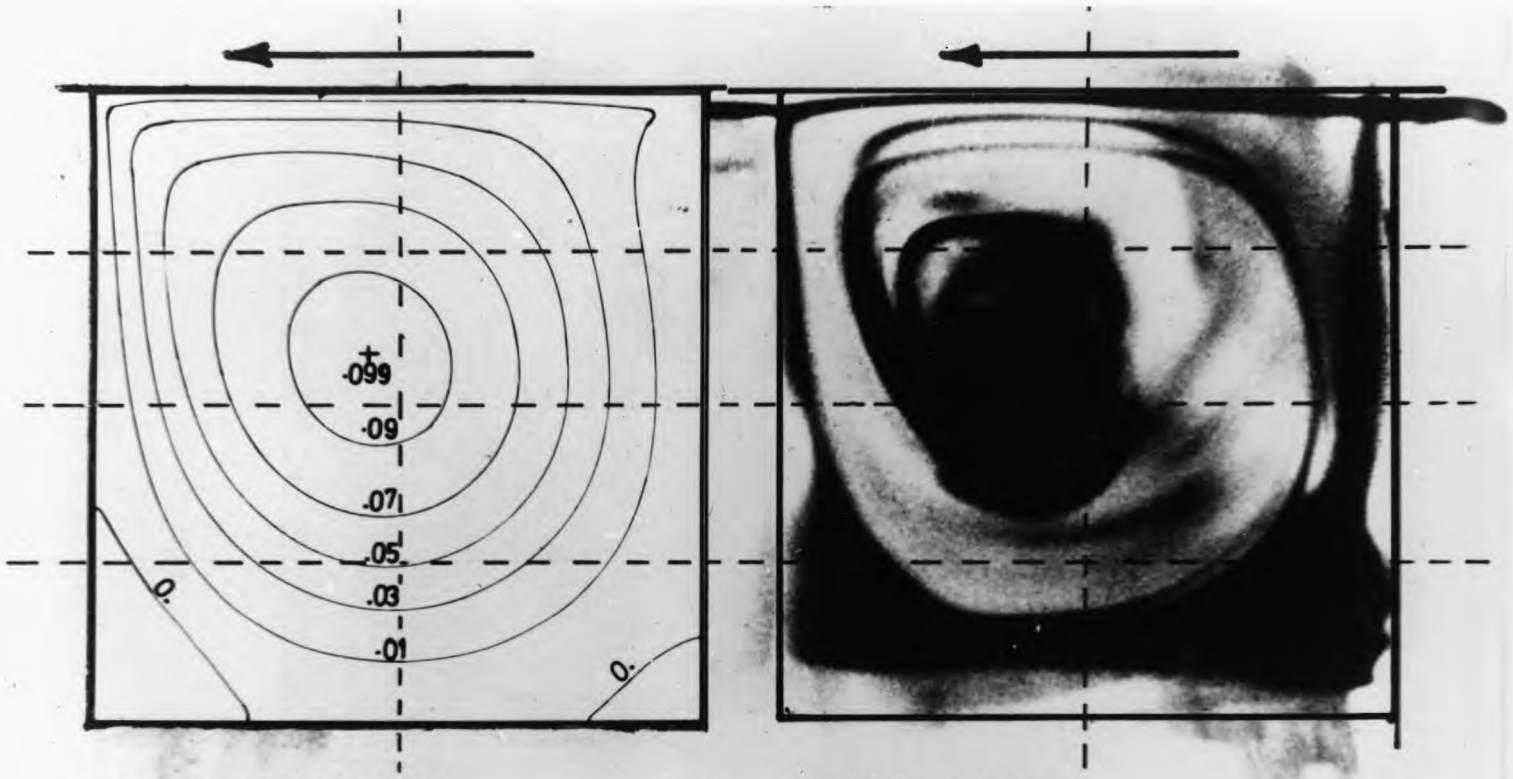

FIG. 5.1-8 Comparison Of Numerical Solution With Experiments For Laminar Incompressible Flow In A Square Cavity

flow pattern, for a Reynolds number of 1000, and a photograph obtained by Reiman & Sabersky for a Reynolds number, based on the free-stream velocity, of about 2000. It should be noted here that the Reynolds number for the latter based on the velocity at the level of the cavity-top is likely to be much less than 2000. The qualitative agreement between the two sets of results is excellent.

5.1-4 Discussion

The qualitative and quantitative features of the above results present no surprises; they are in conformity with the earlier but less extensive predictions of Squire (1956), Batchelor (1956) and Burggraf (1966). All the numerical solutions now available suggest that secondary eddies appear in the lower corners of the cavity, even for creeping flows; the work of Pan & Acrivos (1967b) and Macagno & Hung (1967) lends further credence to this observation. In fact, in confirmation of Moffatt's (1964) conclusions, a tertiary eddy was noticed in the lower corners for a Reynolds number of 1000. It was, however, too small (about .01 x cavity size) to be represented in any detail by the grid-sizes used. Finer grids were ruled out because of the limitations of the computing machine.

Some recognition should be accorded to the fact that the laminar-flow equations have been employed at Reynolds numbers in excess of those at which, in practice, laminar flow would give way to turbulence. This is being done to demonstrate that the divergence difficulties that afflicted earlier workers, the difficulties which have been solved

by the 'upstream' formulation of the convective terms, have nothing to do with the physical phenomenon of turbulence.

Of course, it should be recognised that the results presented here, especially those for coarse grids, may suffer from appreciable numerical error (see section 3.3-2). This error may be likened to a 'diffusional' effect, and the 'false-viscosity' responsible for this effect is of the order of:

$$\mu_{false} = 0.3 \cdot G_{local} \cdot \Delta x . \sin(2\,\theta) \quad , \qquad (5.1\text{-}1)$$

where G_{local} is the local velocity, Δx is the size of the grid, and θ is the angle that the local stream-line makes with the grid. More details about this effect have been given by Runchal et al. (1967). Nevertheless, the magnitude of this effect need not necessarily be large; in the cavity flows the velocity decreases very rapidly away from the moving wall; moreover, wherever the velocities are appreciable, the stream-lines more or less run parallel to the grid lines. That the effect is indeed small for a Reynolds number of 100, even for coarse grids, has already been shown in Figs. 5.1-6 and 5.1-7. However, this effect introduces serious errors at Reynolds number of 1000 (see Fig. 5.1-6) for coarser grids. It is also likely that the heat transfer results for high values of Pr are adversely affected.

And, finally, a comment about the computing time involved is probably overdue. Working with an IBM 7094 at Imperial College, it was found that the machine time to complete a given set of calculations was approximated by:

$$\text{Time} \simeq 7 \times 10^{-6}.I.N \quad \text{minutes} \quad , \qquad (5.1\text{-}2)$$

where,

I is the number of iterations, and N is the total number of grid-nodes in the field.

Typically, the time required for a 21 x 21 grid (with 400 internal grid-nodes) was 0.8 minutes for a Reynolds number of 1000.

5.2 Turbulent flow: abrupt enlargement of a pipe

5.2-1 Introduction

Flows in pipes are frequently interrupted by monitor and control devices such as orifices and valves. This interruption often leads to an abrupt change in the available cross-sectional area of the flow. In the present case, the interest lies in those situations which lead to a sudden increase in the flow-area; this increase, in turn, causes the flow to separate from the pipe walls and form a region of reversed flow immediately downstream of the enlargement. Such separation has a profound effect on the behaviour of the flow and, in general, is characterised by low shear-stresses and high heat transfer rates in the vicinity of the zone of reattachment.

The mathematical problem posed by such a flow is intractable to analytical techniques even for laminar flow; for turbulent flow, it has not even been possible to formulate it in any generally satisfactory manner. A numerical solution to the hydrodynamical problem was first obtained by Thom (1932) for a Reynolds number of 10. More recently, Macagno & Hung (1967) and Greenspan (1967) have

succeeded in obtaining numerical solutions for higher Reynolds numbers. However, as yet, no solution has been available for the problems involving heat transfer or turbulent flow.

Experimental investigation of the turbulent, sudden-enlargement problem has been mainly restricted to heat transfer. What little hydrodynamic information is available is usually of a qualitative nature, such as flow-visualization tests. Sprenger (1959) has collected some quantitative information which has not been published as yet. Boelter et al. (1948) investigated the heat-transfer augmentation caused by the location of an orifice at the entrance to a pipe. Ede and co-workers (1956, 1962) have reported a series of heat transfer and flow-visualization experiments for the sudden-enlargement of a fully-developed pipe flow. Recently, Krall & Sparrow (1966) measured the heat-transfer rates downstream of an orifice in a pipe. Some mass-transfer experiments for this problem are also presented in Part II of this thesis which, unlike the previous investigations, were conducted at very high Schmidt numbers.

5.2-2 Description of the problem

a) The control volume: Fig. 5.2-1 illustrates the problem to be considered. A jet of fluid issues into a pipe with a diameter twice that of the jet, and reattaches to the pipe wall some distance downstream of the enlargement, thus forming a region of reversed flow. The flow is assumed to be incompressible and turbulent.

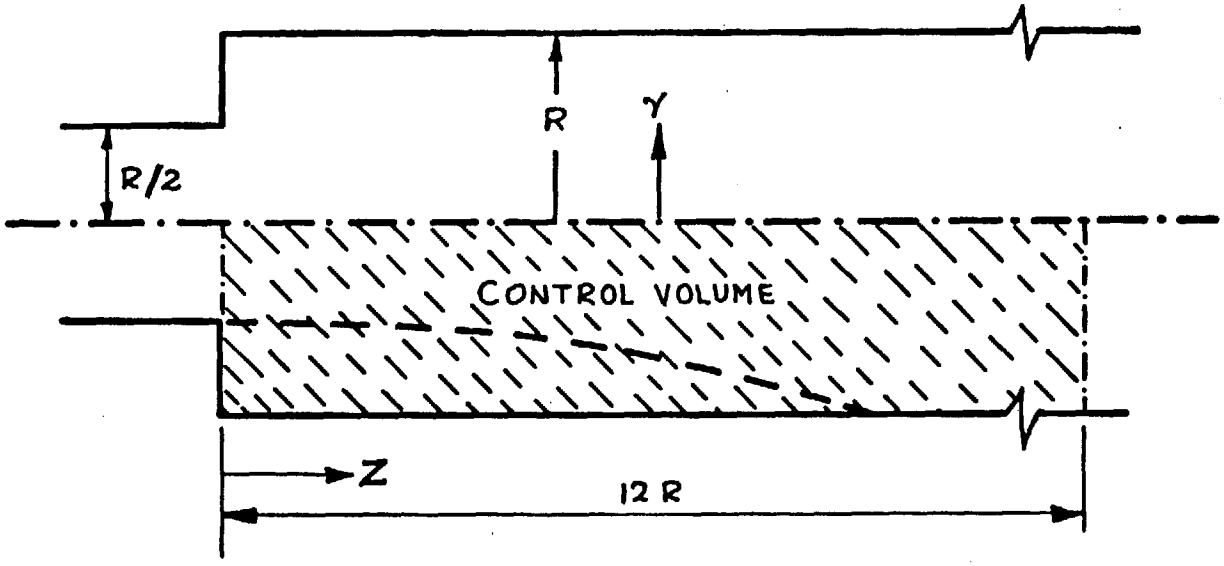

FIG. 5.2-1 THE SUDDEN ENLARGEMENT OF A CIRCULAR PIPE; ILLUSTRATION OF THE GEOMETRY OF THE PROBLEM.

The control volume is enclosed by the inlet and outlet sections, the axis of symmetry and the pipe wall. Of the four boundaries of the flow, the choice of the outlet section is arbitrary and at the discretion of the analyst; the only consideration for its selection being the availability of a set of boundary conditions. If the outlet section is chosen sufficiently far downstream, it is possible to specify the boundary conditions from the well-explored, fully-developed pipe flow data. Nevertheless, for reasons of computing economy, it is desirable to use the shortest possible axial length of the control volume. Hydrodynamic experiments by Sprenger (1959) suggest that, for the present problem, a near-uniform (plug-flow type) velocity profile exists at a distance of approximately 6 pipe-diameters downstream of the enlargement. Some test-computations were performed with control volume lengths between 6 and 15 diameters; all of these produced almost

identical results up to 5 diameters from the enlargement. As the reversed-flow region, the region of primary interest, is usually between 1.5 and 2 diameters long, the outlet section for the final set of computations was chosen at 6 diameters from the enlargement.

b) The non-dimensional parameters: For ease of interpretation of results, let us define the following non-dimensional parameters:

Non-dimensional distance: $Z \equiv 2.z/R$,

Skin-friction coefficient: $s \equiv \tau_S.\rho/G_m^2$,

Reynolds number: $Re \equiv 2.G_m.R/\mu$,

Stanton number: $St \equiv \dot{q}''_S/[c_p.G_m(T_B-T_S)]$, and

Prandtl number: $Pr \equiv \mu/(\rho.\Gamma_T)$,

(5.2-1)

where, R is the radius of the pipe,

z is the axial distance measured from the sudden enlargement,

G_m is the mean mass-velocity in the pipe, and

T_B is the bulk temperature of the fluid.

Other symbols have appeared already and are also given in the nomenclature list.

c) The boundary conditions

Inlet section: The incoming flow is assumed to be of uniform velocity and temperature, described by:

$G_z = 4.G_m$, (5.2-2)

$G_r = 0$, and (5.2-3)

$T = T_I$. (5.2-4)

G_z and G_r are respectively the axial and radial components of the mass-velocity and T_I is a prespecified constant which represents the enthalpy content of the incoming fluid.*

The vorticity and stream-function, the dependent variables of the problem, at a distance r from the axis, are then given by:

$$\omega/r = 0 \quad , \text{ and} \tag{5.2-5}$$

$$\psi = 2.G_m.r^2 + \text{constant} \quad . \tag{5.2-6}$$

The constant in the above equation is arbitrary, and it may be selected so as to make ψ zero at the pipe-wall; in that case:

$$\psi = 0.5.G_m(4.r^2 - R^2) \quad . \tag{5.2-7}$$

Unlike the square-cavity problem, the present problem involves turbulence. If the turbulence hypotheses of section 4.1 are to be used, the kinetic energy of turbulence, k, should be introduced as an additional dependent variable; the boundary conditions for k must then be supplied. Since turbulence must vanish at a wall, k is easily specified as zero at the walls bounding the flow, but no quantitative information is available about the value of k in the inlet region. Empirically, k may be related to the velocity of the inlet flow by:

$$k = C_{k,I}.(G_m/\rho)^2 \quad . \tag{5.2-8}$$

The constant $C_{k,I}$ is indicative of the level of turbulence in the incoming flow and its value was varied during the course of computations; typically, it was in the range of .01 to .05.

---

* For low-velocity incompressible flows temperature is also a conserved property and may be used instead of the enthalpy.

Outlet section: The mass-velocities at the outlet section were assumed to be given by:

$$G_z = G_0(1 - r/R)^n \quad , \text{ and} \qquad (5.2\text{-}9)$$

$$G_r = 0 \quad . \qquad (5.2\text{-}10)$$

The condition of conservation of mass and equation (5.2-5) dictate that:

$$G_0 = G_m.(1+n)(1+n/2) \quad . \qquad (5.2\text{-}11)$$

The vorticity and stream-function can now be obtained from:

$$w/r = G_z.n/[\rho r.(R-r)] \quad , \text{ and} \qquad (5.2\text{-}12)$$

$$\psi = -0.5.G_m.R(1-r/R)^{1+n}.(R+r+n.r) \quad . \qquad (5.2\text{-}13)$$

In accordance with the already mentioned experimental findings of Sprenger (1959), n was specified as a small number, typically .05, to obtain a near-uniform velocity profile.

During the course of computations it was found that the effect of variation of n was confined to two or three rows of grid-nodes immediately preceding the outlet boundary; on the rest of the upstream flow the effect was negligible. This, of course, is also to be expected from the physics of the problem; because of the strong convective effects, the changes in the downstream flow scarcely make themselves manifest in the upstream regions.

In the absence of any quantitative evidence, two types of boundary conditions are possible for the kinetic energy of turbulence and the temperature: the specification of a power law; and the specification of zero axial gradient. Both were tried during the course of computations and, as in the case of the velocity boundary condition, it was

found that the upstream region removed from the outlet boundary by two or three grid nodes was comparatively irresponsive to the boundary condition. In view of the faster rates of convergence obtainable from the specification of the variable than from the specification of its gradient, the following boundary conditions were finally used:

$$k = C_{k,0}.(G_m/\rho)^2 \quad , \text{ and} \qquad (5.2\text{-}14)$$

$$T = T_1(1-r/R)^n + T_2 \quad , \qquad (5.2\text{-}15)$$

where $C_{k,0}$ was specified in the range of .01 to .05, and T_1 and T_2 were obtained by over-all heat-balance on the incoming and outgoing fluids.

The wall boundary: The stream-function at the pipe wall and the step wall, by virtue of equation (5.2-10), is equal to zero.

The kinetic energy of turbulence is zero at a wall; and a boundary condition for T is always specified as either a heat-flux or a temperature distribution. For reasons of computing economy, it is preferable to use the concept of 'linearizing values' (see section 4.2-3) to evaluate fictitious values of k and T at the wall, with the help of the Couette-flow model as explained already in section 4.2-3. The value of ω/r at one grid-node away from the wall was obtained from equation (4.2-26).

The axis of symmetry: The boundary conditions at the axis of symmetry were specified in accordance with section 2.5.

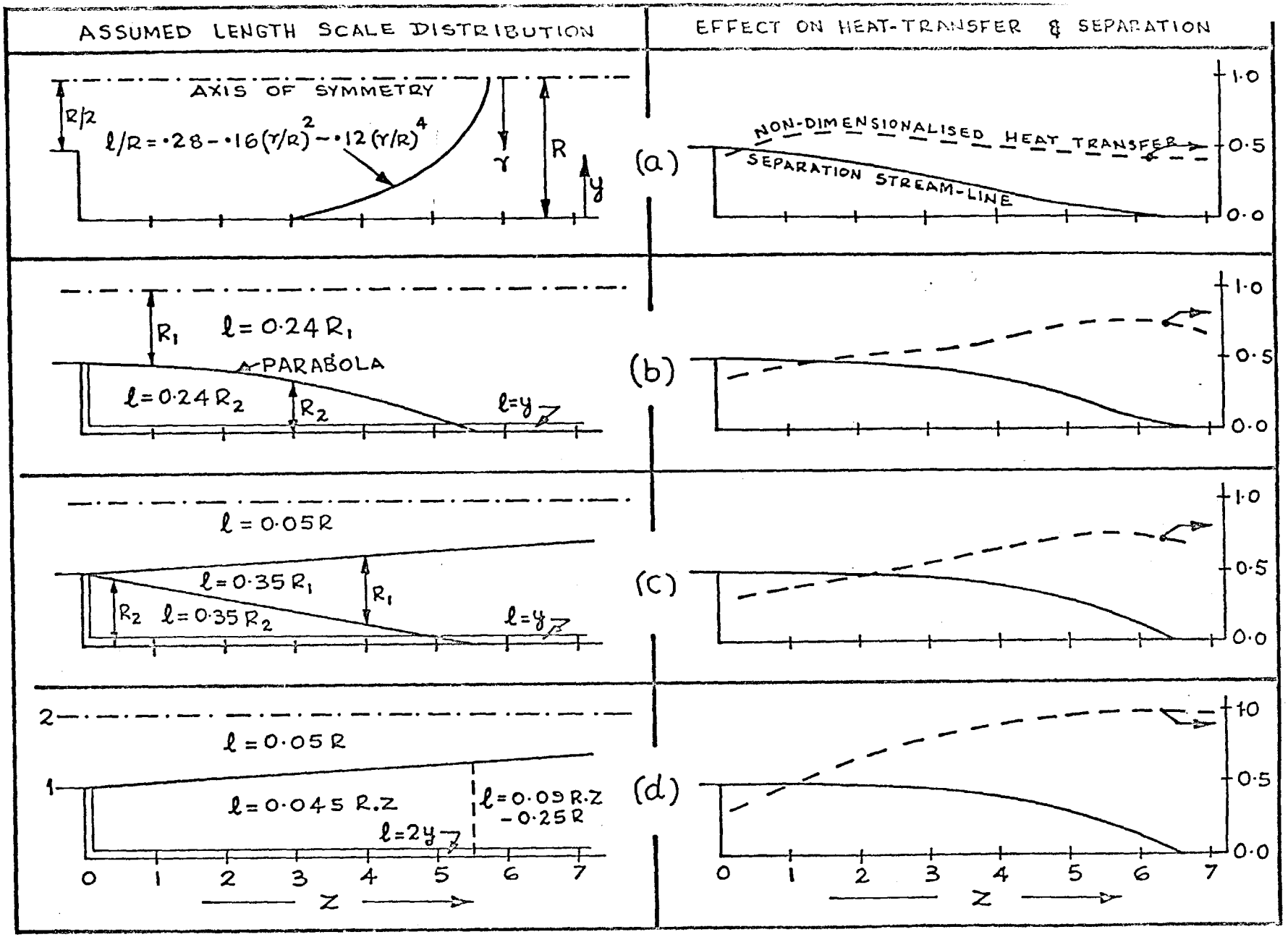

FIG. 5.2-2 EFFECT OF LENGTH SCALE ON HEAT-TRANSFER AND SEPARATION.

5.2-3 Presentation of results

a) The influence of the length scale of turbulence: It has been pointed out in section 4.1-3 that the length scale l is one of the most important inputs to the present form of the Kolmogorov-Prandtl turbulence model. For the present, l has to be obtained from extrapolations of knowledge about its distribution. Four of the distributions tried during the course of the present computations are shown in Fig. 5.2-2. Distribution (a) is based upon Nikuradse's (1932) 'Prandtl mixing-length' for a fully-developed pipe flow, whereas distribution (b) is based on the assumption of an expanding mainstream jet along with another jet-type flow in the reversed-flow region and a wall boundary layer. Case (c) assumes the growth of a linear shear-layer between the mainstream and the reversed-flow jets. Case (d) is a modification of (c) in that the diffusion is assumed to be so strong as to wipe out any radial gradients of the length scale (section 4.1-3); the length scale in the reversed-flow region is then equal to the length scale 'generated' in the shear-layer. The numerical constants in the above distributions were adjusted to yield reattachment in the vicinity of 6.5 step-heights from the enlargement (i.e., $Z = 6.5$). The resulting separation stream-lines and the heat-transfer rates, for a Reynolds number of 80000 and a Prandtl number of 3, are shown in Fig. 5.2-2. The turbulent Prandtl number for enthalpy, $\sigma_{T,t}$, was assumed to be 0.7.

The heat transfer results were non-dimensionalised with respect to the maximum value for distribution (d). On comparison, it was found that, of all the results, those from distribution (d) were in closest comparison with the

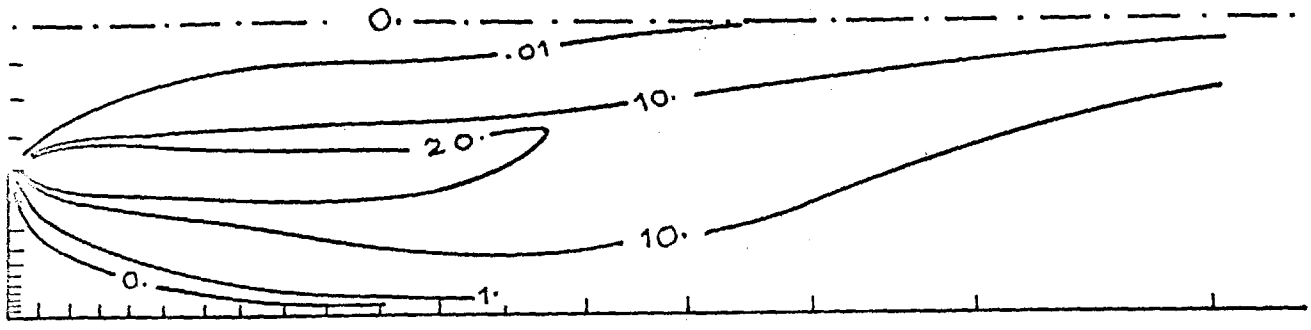

(a) VORTICITY, ω

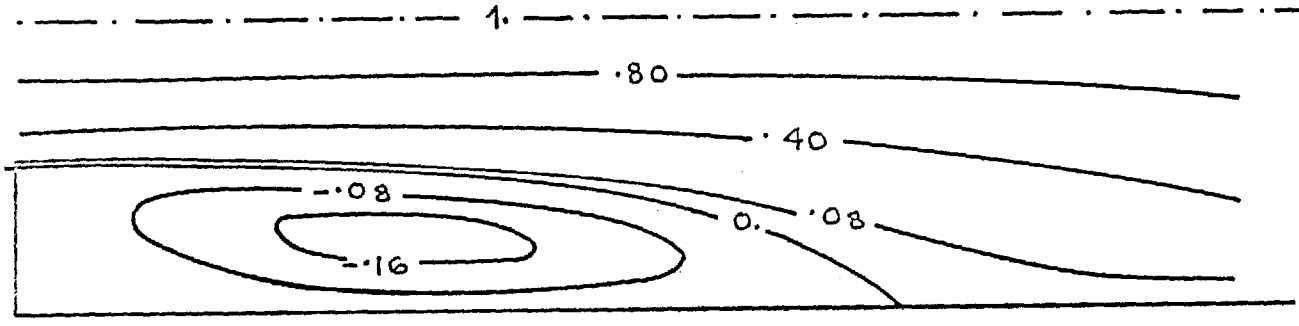

(b) STREAM-FUNCTION, ψ

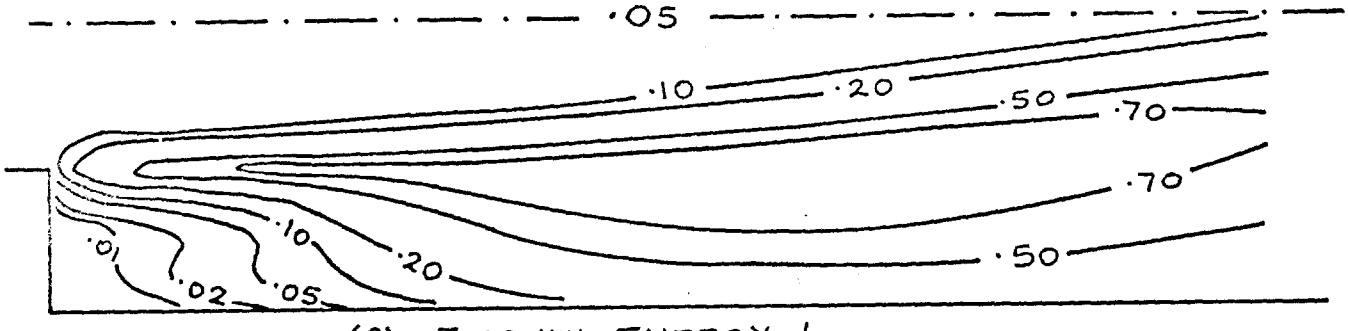

(C) TURB. KIN. ENERGY, k

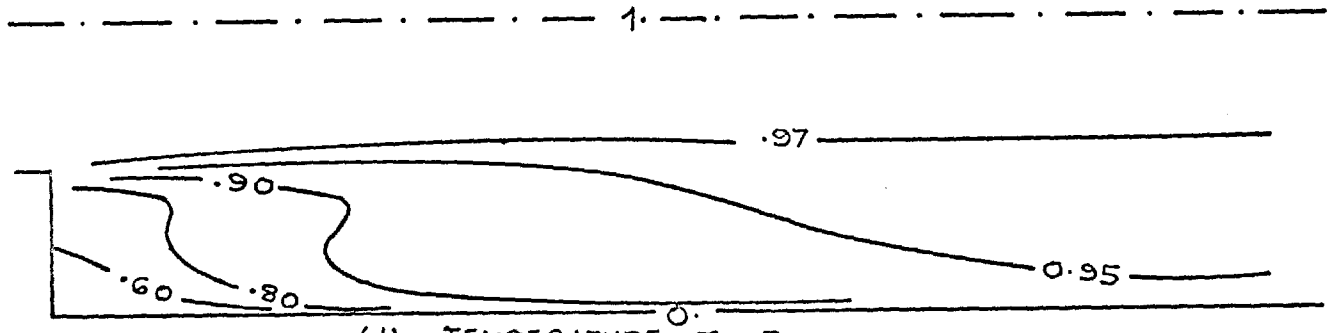

(d) TEMPERATURE, T ; $P_r = 1.$

FIG. 5.2-3 FLOW PATTERNS IN THE ABRUPT ENLARGEMENT OF A PIPE ; REYNOLDS NUMBER $= 10^4$

heat transfer data; this distribution was, therefore, adopted as the standard length scale distribution for all subsequent computations.

b) The influence of Reynolds number: Figs. 5.2-3 and 5.2-4 present the flow patterns for Reynolds numbers of 10^4 and 10^5 respectively. All the values shown in the contours have been non-dimensionalised in terms of the pipe-radius, R, and the mean mass-velocity, G_m. For temperature contours, the step-wall was assumed to be adiabatic, whereas the pipe-wall was assumed isothermal. The results were obtained for a 21 x 15 non-uniform grid and the grid used is shown in one of the diagrams; of course, it should be noted that only a part of the control volume in the axial direction is shown in the diagrams.

All the contours follow the expected pattern. The vorticity contours show the formation of a high-shear region between the incoming jet and the captive annular eddy. After this shear layer reaches the pipe-wall, it is deflected away and moves towards the centre of the pipe. The stream-line pattern also fits in with the available flow-visualization data. The gradual increase of turbulence energy in the high-shear mixing-layer and its subsequent decay as the shear-layer moves away from the wall are seen from the turbulence-energy patterns. The maximum turbulence level ($\equiv k_p^2/G_I^2$) of about 0.05 compares well with the available measurements in similar situations, such as the flow of a uniform-velocity stream past a step (e.g. Mueller & Robertson 1962). The temperature contours reveal that, apart from a thin region near the pipe wall and a part

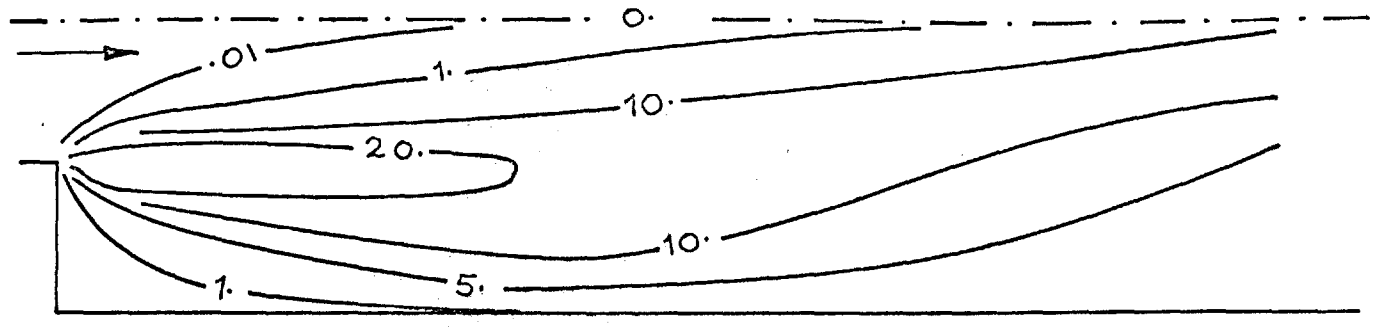

(a) VORTICITY, ω

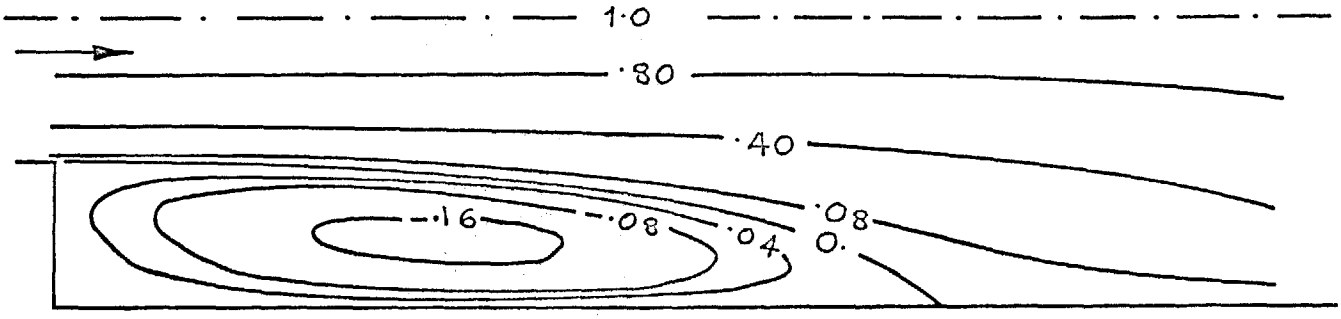

(b) STREAM-FUNCTION, ψ

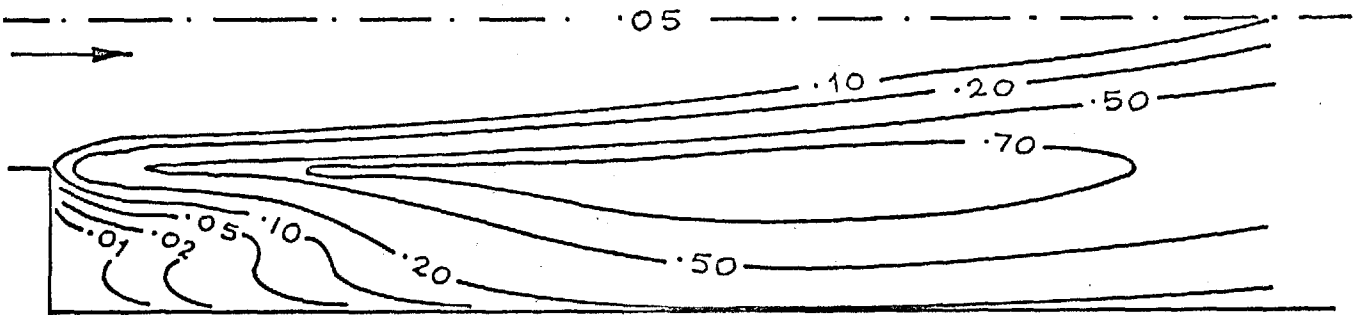

(c) TURB.KIN.ENERGY, k

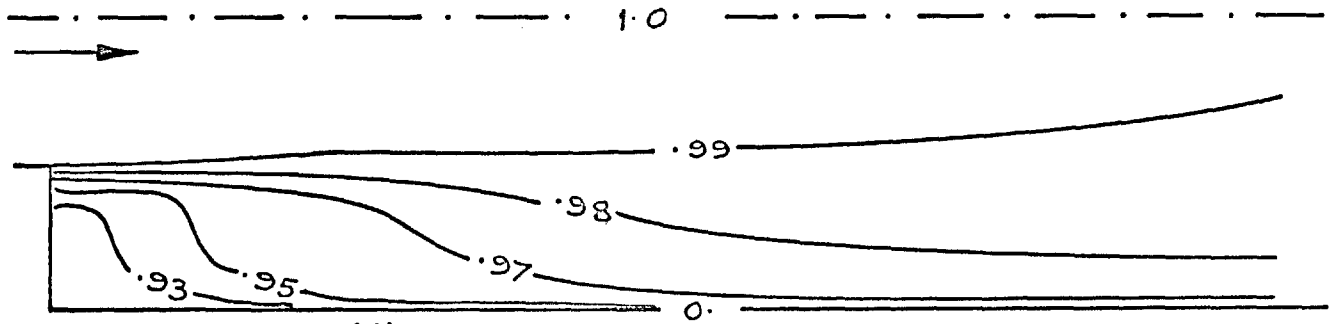

(d) TEMPERATURE, T ; $P_T = 1$

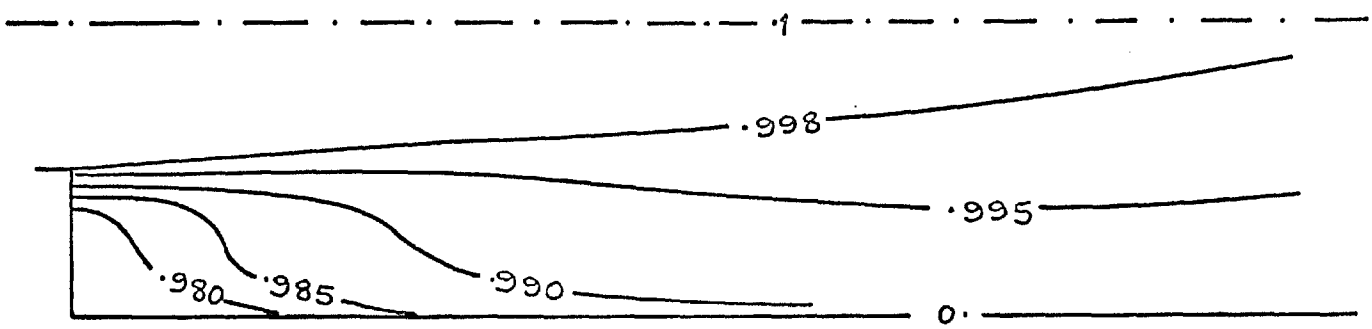

(e) TEMPERATURE T; $P_T = 10$.

FIG. 5.2-4 FLOW PATTERNS IN THE ABRUPT ENLARGEMENT OF A PIPE; REYNOLDS NUMBER = 10^5

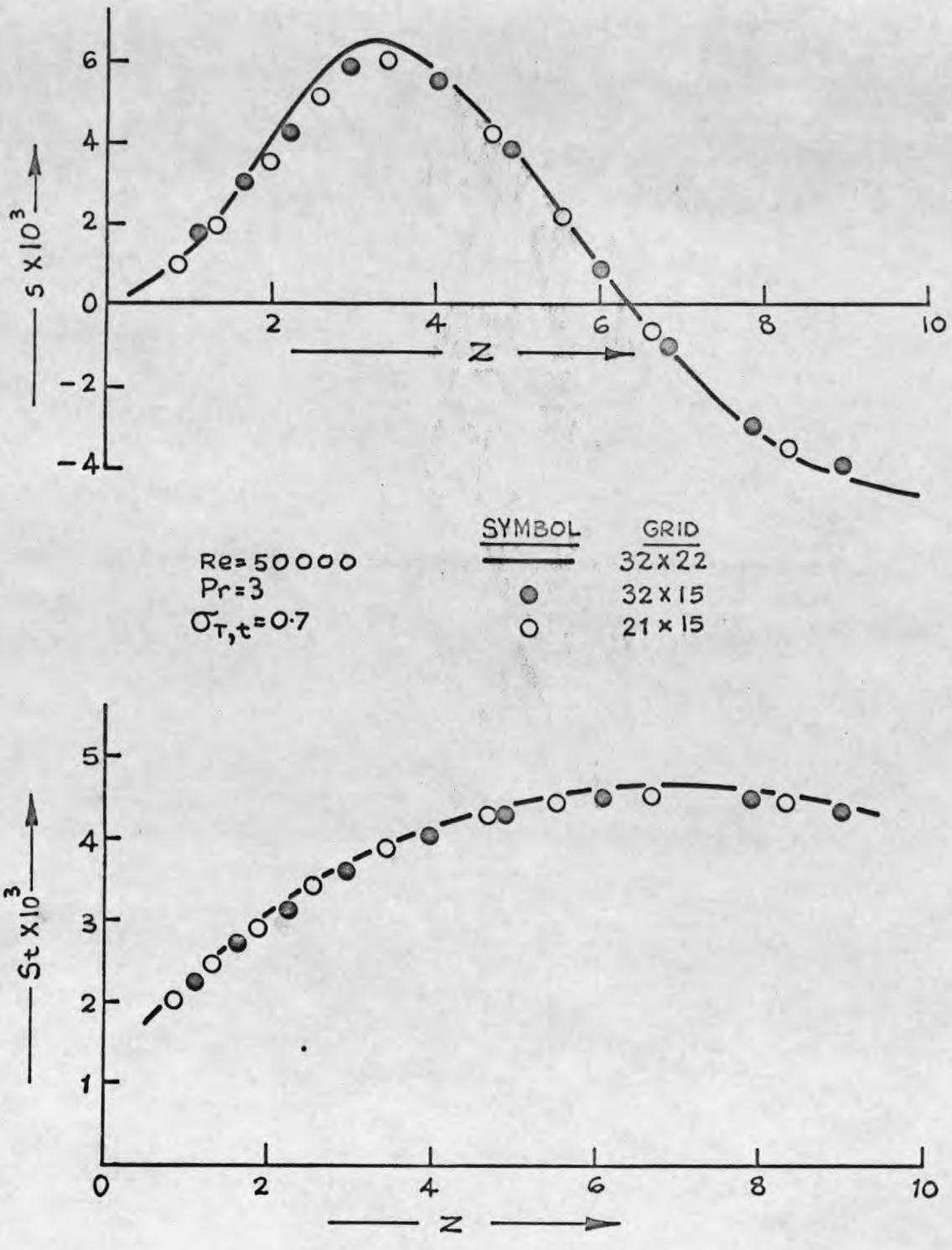

FIG. 5.2-5 THE INFLUENCE OF GRID ON THE STANTON NUMBER AND SHEAR-STRESS AT THE PIPE-WALL

of the captive eddy, the whole of the fluid is virtually at the temperature of the incoming jet. This, of course, would be expected because of the high Reynolds numbers and the intense mixing in the shear-layer.

c) The influence of the Prandtl number: Figs. 5.2-4 (d) and 5.2-4 (e) show the temperature contours for laminar Prandtl numbers of unity and ten, respectively. The higher Prandtl number has resulted in restricting the changes in temperature still closer to the wall: to this extent the influence is similar to that of an increase in the Reynolds number (cf. Figs. 5.2-3 (d) and 5.2-4 (d)). No results were obtained for Prandtl numbers less than unity because of the doubtful validity of the Couette-flow relations used near the wall (see section 4.2-2).

d) The influence of the number of grid-nodes: To investigate the effect of the number of nodes on the computed results, three different grids were used. The comparison, in terms of the Stanton number and the shear-stress at the pipe-wall, is shown in Fig. 5.2-5. The results with 21 x 15 grid (21 nodes in the axial direction) are in good comparison with those for the finer grids of 32 x 15 and 32 x 22. As a matter of economy, 21 x 15 grid was adopted as the standard grid.

This favourable conclusion about the influence of grid provides some confidence for the comparison of the computed Stanton number with the experimental data which follows in the next section.

e) Comparison with experiments: Figs. 5.2-6 and 5.2-7 compare the computed Stanton number with the corresponding experimental data of Krall & Sparrow (1966) and of the present author (see Chapter 7); it should be recalled that the computations are based on the length scale distribution (d). The computed and measured results agree qualitatively; the St vs. Re and the St vs. Z dependence is correctly predicted.

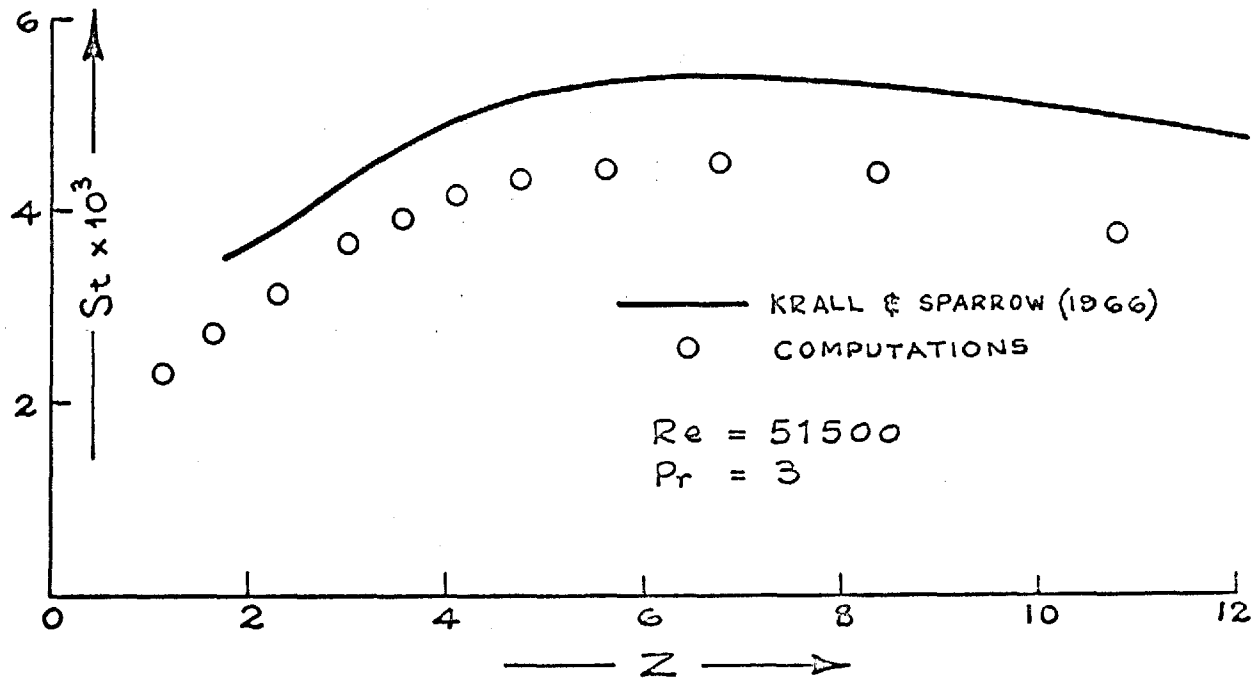

FIG. 5·2-6 COMPARISON OF COMPUTED AND EXPERIMENTAL STANTON NUMBER DOWNSTREAM OF SUDDEN ENLARGEMENT IN A CIRCULAR PIPE.

Quantitatively, however, the Stanton number, in all the cases, is under-predicted. The difference from the data of Krall & Sparrow is of the order of 15% whereas that from the data of the present author is around 30%. It should be noted that the data of the present author were obtained for a zone of active surface (a small heated zone in terms of the heat transfer analogy), whereas the computed

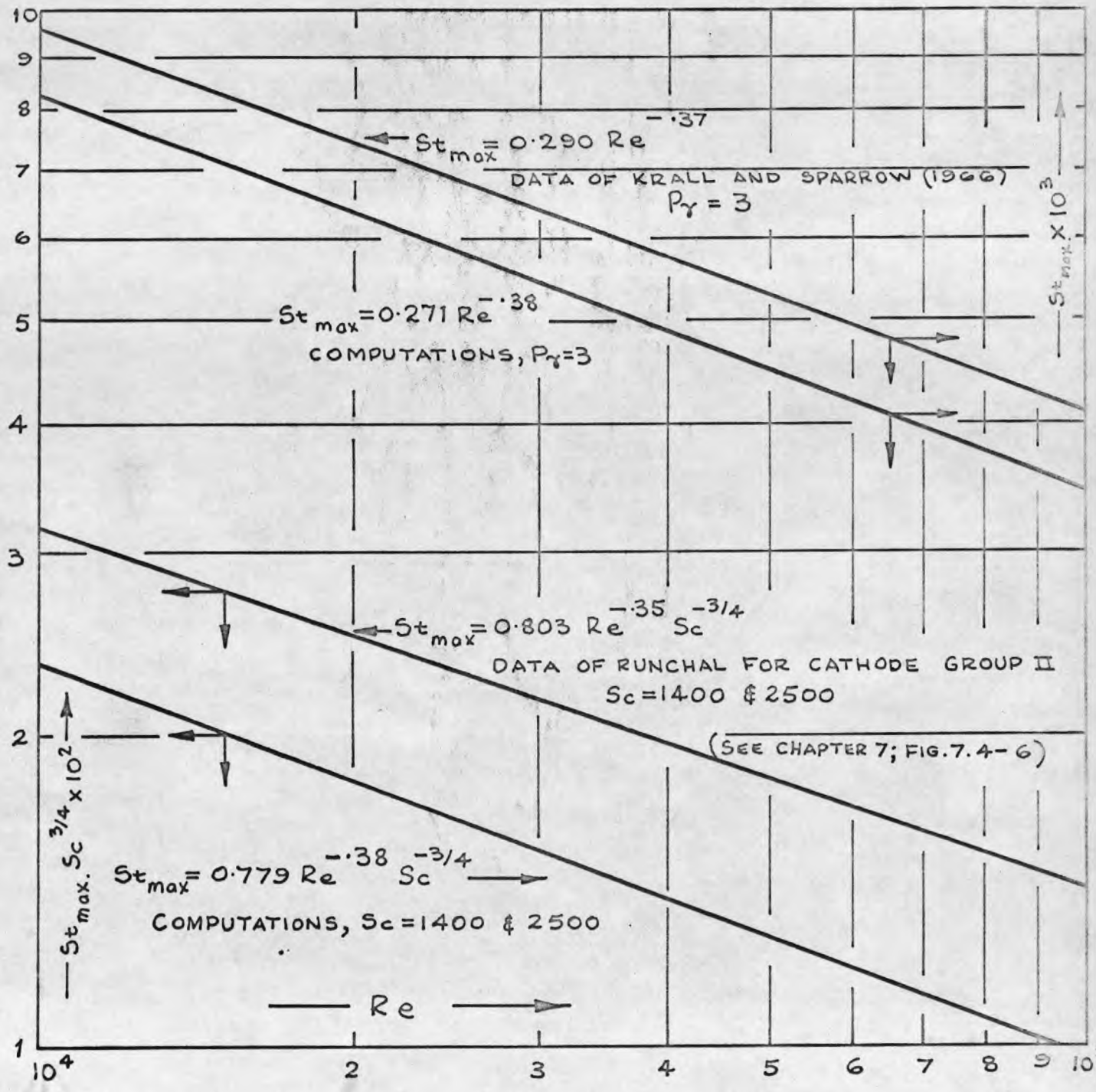

FIG. 5.2-7 COMPARISON OF THE COMPUTED AND EXPERIMENTAL STANTON NUMBER AT THE REATTACHMENT POINT FOR THE SUDDEN ENLARGEMENT IN A CIRCULAR PIPE.

results are for an iso-concentration (isothermal for heat transfer) wall. It is probably this difference in the boundary condition* which partly accounts for the large discrepancy of 30%. The choice of the boundary condition for the computations was forced by the Couette-flow assumptions near the wall (see section 4.2-3).

To some extent, the predictions can be improved by modifying the empirical input, such as the length scale, l, or the numerical constant that appears in equation (4.2-19). However, in view of the uncertainty of the empirical input, such attempts were not considered justified. It was felt that these discrepancies would act as a reminder of the lack of a satisfactory set of hypotheses for turbulence.

5.2-4 Discussion

The results obtained for the sudden-enlargement conform with the available experimental data. They are especially encouraging in view of the fact that no other prediction procedure has yet been formulated for such flows. Of course, quantitatively, the predictions reveal a large disparity with experiments. However, this is likely to be removed with the refinement of the turbulence model. For high Prandtl/Schmidt numbers, the Couette-flow model needs refinement to account for convection along the wall so that the effect of the boundary condition can be correctly incorporated. But all these represent modifications to the present solution procedure within its framework rather than any fundamental change; these modifications are likely to follow in the course of time.

---

* For the effect of boundary conditions on reattachment heat transfer see section 7.4-4.

The cost of predictions can be judged from the fact that the computing-time for a 21 x 15 grid calculation was of the order of 2 minutes on an IBM 7094 Computer. The computing-time could be approximately correlated by:

$$\text{Time} = 5.10^{-5}.I.N. \text{ minutes} \quad , \qquad (5.2\text{-}16)$$

where, I is the number of iterations, and

N is the number of grid-nodes.

Chapter 6

Discussion and conclusions

In the previous chapters, a numerical procedure has been presented for the prediction of two-dimensional, steady, separated flows. That the method is reliable and brings the prediction of such flows within the bounds of possibility has been shown by the two test cases. We are now in a position to review this procedure and to draw some conclusions about its general applicability, its economy and its accuracy. We will also reassess the physical input necessary for the prediction of turbulent flows. And finally at this stage, as a closure to Part I of the thesis, we may also venture into that space exploration of which is the privilege of every research worker: the suggestions for future research.

6.1 The capabilities of the numerical procedure

The numerical procedure presented in Chapter 3 is fairly general: it can handle almost any steady, two-dimensional, incompressible flow with or without turbulence. In fact, the condition of incompressibility may even be relaxed to include those flows in which the density is a function of temperature only (Pun and Spalding 1967). The literature demonstrating the applicability and generality of the method is growing fast; in a recent review, Gosman et al. (1968) listed eleven of its applications; the two test

cases presented here provide but a glimpse of the scope of the method.

That the predictions obtained are qualitatively and, to a large extent, also quantitatively sound, is shown in the previous chapter: wherever possible, they were compared with the available theoretical and experimental evidence; without exception, the conclusions have been favourable. Computing time required was moderate; usually of the order of a few minutes on a modern electronic computer. The cost of machine time is likely to be far less than the cost of experimentation and model-testing. And even if the possibility of numerical predictions does not eliminate the need for experiments, it will certainly diminish their extent and cost.

Of course, like any other new solution procedure, this one is also far from being perfect. But the imperfections are more physical than mathematical in nature and are likely to be dispelled by a better understanding of the involved physical processes. The numerical procedure certainly porvides a speedy and powerful means of testing any physical hypotheses which may be postulated in this context.

6.2 Physical hypotheses and their limitations

A modified Kolmogorov-Prandtl model of turbulence was presented in Chapter 4; this model is based more on experimental evidence and intuition than on any rigorous mathematical reasoning. It is naturally to be expected that not all turbulent flows can be represented by the present model.

Turbulence hypotheses are a vital auxiliary input to the numerical procedure if turbulent flows are to be analysed. The Kolmogorov-Prandtl model suffers from a lack of information about various components of its structure. The characteristic length scale of turbulence is a very important input to the hypotheses (section 4.1-3), yet, except for the simplest of the problems, there is an almost complete lack of quantitative information about it. Other important inputs to the model are the various turbulent Prandtl/Schmidt numbers. All the sources indicate that these are of the order of unity: nonetheless, specific estimates differ considerably; values ranging from 0.5 to 2.0 have been suggested and used. Indeed, these may even be functions of various flow-parameters and not constants as is generally assumed. There is also a lack of accord about the supposedly universal constants which appear in the various relations describing the hypotheses (section 4.1-2); for example, the constant associated with the diffusion of the kinetic energy of turbulence varies from the 0.08 of Glushko (1965) to the 0.152 of Wieghardt (1945). In fact, experimental evidence suggests that the presence of a wall modifies the structure of turbulence to a considerable extent (e.g. Kline et al. 1967). There is, therefore, a strong likelihood that some of these 'universal' constants may, after all, differ for flows close to a wall compared with those for flows away from a wall. Similar modifications are also likely in the presence of other factors which modify the structure of turbulence such as high pressure gradients.

It can only be concluded that our knowledge of turbulence is far from being satisfactory; nevertheless, a beginning has to be made. If the designer is unable to obtain an accurate answer,he must, at least, have a reasonable estimate. This is the reason, and the excuse, for making do with whatever information is available. It is not expected, or hoped, that this model will last in its present state; it is merely intended to provide a promising stepping-stone for future improvements.

6.3 Suggestions for further research

Undoubtedly, turbulence must form the focus of immediate attention. Extensive measurements must be made and carefully scrutinized to test and improve the various hypotheses which have been put forward to describe turbulence; in case of their inadequacy, new means of handling turbulence will have to be formulated. Experimental data of direct relevance will be those concerning the structure of turbulence and the factors which influence it. Fortunately there are signs of considerable activity in this direction (e.g. Kline et al. 1967, Hanson & Richardson 1968 etc.). It has already been pointed out in section 4.1-3 that the Kolmogorov-Prandtl model of turbulence can be put on a firmer footing by the addition of a differential equation for the characteristic length scale of turbulent eddies. It is only when more is known about turbulence that the various 'constants' associated with the model can be determined with any degree of certainty.

On the mathematical side, it has been noticed that the present finite-difference scheme may introduce considerable

numerical errors (Runchal et al. 1967). These errors stem mainly from the assumptions about the inter-nodal distribution of variables (section 3.2-1). Runchal et al. pointed out a way of reducing these errors; however, further work is necessary before any definite recommendation matures.

From the point of view of economy, the solution procedure leaves something to be desired. Because of the use of an iterative method to solve the difference equations, the computing time goes up not in direct proportion to the number of grid nodes but as a power which usually lies between 1.5 and 2. The penalty for the use of fine grids may thus be considerable. Though computing time may be cut down by economy measures such as a judicious distribution of grid nodes, the use of over-relaxation etc., unfortunately, none of these can yet be incorporated in any generally applicable way. Attention should, therefore, be turned to devising some more economical means of solving the difference equations.

PART II

EXPERIMENTAL INVESTIGATION

Chapter 7: Experimental investigation

Chapter 7

Experimental investigation

This chapter contains the results of an experimental investigation conducted into mass transfer in the turbulent separated and redeveloping regions immediately downstream of a sudden enlargement in a circular pipe. The geometry is thus similar to that of the problem discussed in section 5.2. The experimental technique used was diffusion-controlled electrolysis, and the data were obtained for Schmidt numbers of 1400 and 2500, and for Reynolds numbers between 2500 and 89000.

7.1 Introduction

The essential need for experimental data in separated flows is self-evident from the state of the approximate theories which have been put forward to predict such flows (see section 1.2-2). The need for more data is also highlighted by the inadequacies of the existing ones. Though most of the existing data agree in their qualitative trends, they are by no means consistent quantitatively. Thus, the reported rates of heat transfer in the rearward separation zone of a circular cylinder differ by a factor of two or so (Richardson 1963). Similar discrepancies have also been reported for the heat transfer downstream of a sudden enlargement in a pipe (Krall & Sparrow 1966). This conflict in results is presumably caused by the variations

in experimental conditions and an insufficient knowledge about the mechanisms that affect the behaviour of separated flows. For example, the mechanisms which cause asymmetric separation and heat transfer downstream of a double step in a flat duct are still obscure (Filetti & Kays 1967). Superimposed on all these are the other three-dimensional and unsteady effects, mentioned in section 1.1, for flows with two-dimensional and steady boundary conditions. It must therefore be concluded that, in view of the complexity of separated flows, too few data are available to serve as the basis of any general prediction procedures.

Most of the available experimental data have been reviewed by Richardson (1963), Knight (1966), Chilcott (1967) and Filetti & Kays (1967). Almost all of the existing data were obtained with air or water as the working medium and, hence, they represent a rather moderate range of Prandtl number. However, there is much to be gained from data on high Prandtl number (or Schmidt number for mass transfer data). Much of the resistance to heat and mass transfer is usually confined to a thin region close to a wall in the so-called laminar sub-layer. Significant information can be obtained from flows in which the changes in the enthalpy (or concentration) profiles are confined to this thin region. High Prandtl/Schmidt numbers provide such a flow; the present series of experiments was designed to exploit this feature.

7.2 The experimental technique

The use of diffusion-controlled electrolysis to obtain the wall-fluxes for high Schmidt numbers is now well established. Comprehensive accounts of the technique have been given by Tobias et al. (1952) and Duffield (1966). We shall therefore limit ourselves to a brief description of its essential features.

According to the concept of the ionic theory, the molecules of a binary electrolyte in solution dissociate into two types of ions: the cations possessing a negative charge and the anions possessing a positive charge. When an electromotive force (e.m.f.), above a certain critical value, is applied between two electrodes in such a solution, there is a transfer of electrons to the anions from the cathode, and a transfer of electrons to the anode from the cations. This sets up an ionic current. In the steady state, the reacting ions must be continuously supplied to the electrodes from the solution. In general three mechanisms take part in this exchange:

a) migration under the influence of the potential gradient,

b) diffusion under the influence of the concentration gradient, and

c) convection.

Migration of ions can be eliminated by reducing the potential gradients in the flow, almost to zero, by adding a high concentration of a non-reacting electrolyte with high electrical conductivity. The ionic-transfer theory states that, for such a flow, the rate of the electro-chemical reaction increases at first exponentially with the applied e.m.f. (Levich 1962); but, when the e.m.f. is

sufficiently high, the rate of reaction is independent of it and is determined only by the rate of ionic-transport to the electrodes; the reaction is then termed 'diffusion-controlled' and the current flowing through the cell is termed the 'limiting current'. If, in addition, the mass-flux of the ions at one electrode is much greater than that at the other, the limiting-current conditions are first reached at the electrode with the higher mass-flux; the ions transported to such an electrode react very rapidly and their concentration at the electrode surface falls almost to zero. The average mass-transfer coefficient, g_m, for such a system is given by:

$$g_m \equiv \dot{m}''/\emptyset = M.I/(N.F.\emptyset) \quad , \qquad (7.2\text{-}1)$$

where,

g_m is the mean mass-transfer coefficient ($g\ sec^{-1}cm^{-2}$),

$\dot{m}''$ is the mean mass-flux of the reacting ions ($g\ sec^{-1}cm^{-2}$),

$\emptyset$ is the concentration of the reacting ions in the bulk solution (g / g),

M is the molecular weight of the reacting ions ($g / g - mole$),

I is the diffusion-controlled limiting-current density (amp/cm^2),

N is the valence change during the reaction ($g\text{-}eqvt/g\text{-}mole$),

F is the Faraday's constant ($amp\ sec/g\text{-}eqvt$).

In the present series of experiments, the reaction employed was that between the ferri-cynide and the ferro-cynide ions, in the presence of an electrical field:

$$Fe(CN)_6^{3-} + e^{1-} = Fe(CN)_6^{4-} \qquad (7.2\text{-}2)$$

LEGEND

① LIQUID RESERVOIR
② CENTRIFUGAL PUMP
③ HEAT EXCHANGER
④ THERMOSTATIC DEVICE
⑤ BYPASS
⑥ LARGE ROTAMETER
⑦ SMALL ROTAMETER
⑧ FLEXIBLE TUBING 1" I.D.
⑨ FLOW STRAIGHTENER 9/8" I.D.
⑩ POSITION MONITORING DEVICE
⑪ APPROACH-NOZZLE, 9/8" - 7/8" REDUCING.
⑫ LEAKAGE CONTAINER, 7/2" I.D.
⑬ TEST-NOZZLE, 7/8" - 9/16" REDUCING.

A_U ANODE – UPSTREAM
A_M ANODE – MIDDLE
A_D ANODE – DOWNSTREAM
C_U CATHODE – UPSTREAM
C_M CATHODE – MIDDLE
C_D CATHODE – DOWNSTREAM

} 1·121" I.D. NICKEL TUBING

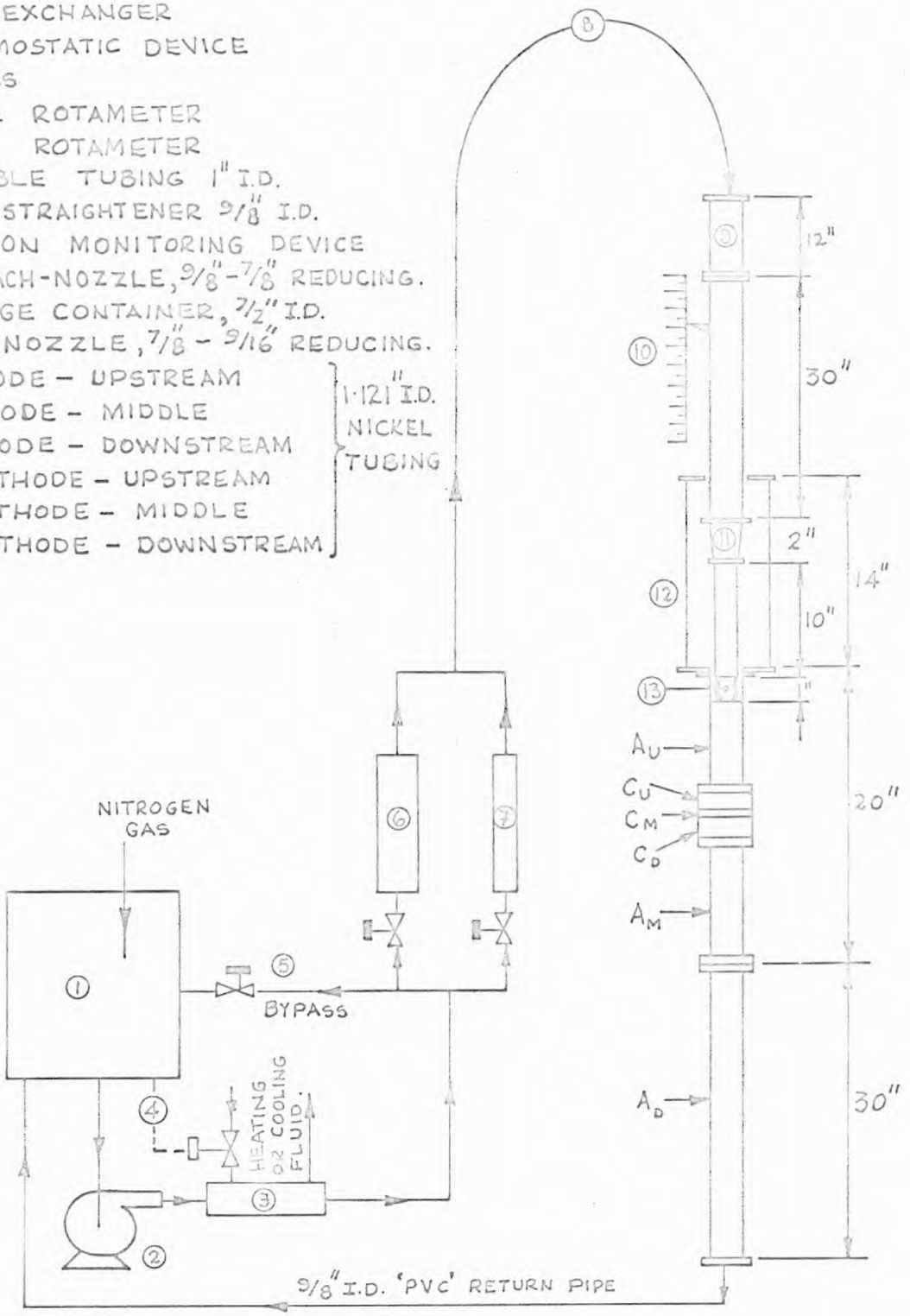

FIG. 7-3-1 SCHEMATIC DIAGRAM OF THE APPARATUS USED FOR THE DETERMINATION OF MASS TRANSFER RATES DOWNSTREAM OF A SUDDEN ENLARGEMENT IN A CIRCULAR PIPE.

Because of the small size of the cathodes (see Fig. 7.3-3), the reaction was 'cathode-controlled', i.e. limiting-current conditions were first reached at the cathodes. For the ionic current generated at the cathode, equation(7.2-1) can be written as:

$$g_m = 0.002196\ I/\emptyset \quad g\ sec^{-1}cm^{-2} \quad , \qquad (7.2\text{-}3)$$

with,

M = 211.95, N=1 and F=96 500. All the units are the same as those for equation (7.2-1).

7.3 Application of the experimental technique

7.3-1 The apparatus

a) The flow circuit: A schematic diagram of the apparatus* used is shown in Fig. 7.3-1. A centrifugal pump, 2, maintains a supply of liquid from the reservoir 1 to the Rotameters 6 and 7 via a thermostatically-controlled heat-exchanger 3. The liquid from the Rotameters is led through a flow-straightener device 9 and an approach nozzle 11 to the test nozzle 13. The jet of fluid issuing from the test nozzle expands into the test section and then returns to the reservoir. Further details and photographs of the various important parts of the apparatus are shown in Figs. 7.3-2 to 7.3-5.

The test-nozzle assembly** was designed to be movable along the upstream tube A_U of the test section, the movement

---

* Some components of the apparatus were the same as those used by Gosman (1969); he has given the details of construction and specifications of the components.

** The author gratefully acknowledges the advise given by Professor W.M. Kays for the design of the test-nozzle assembly.

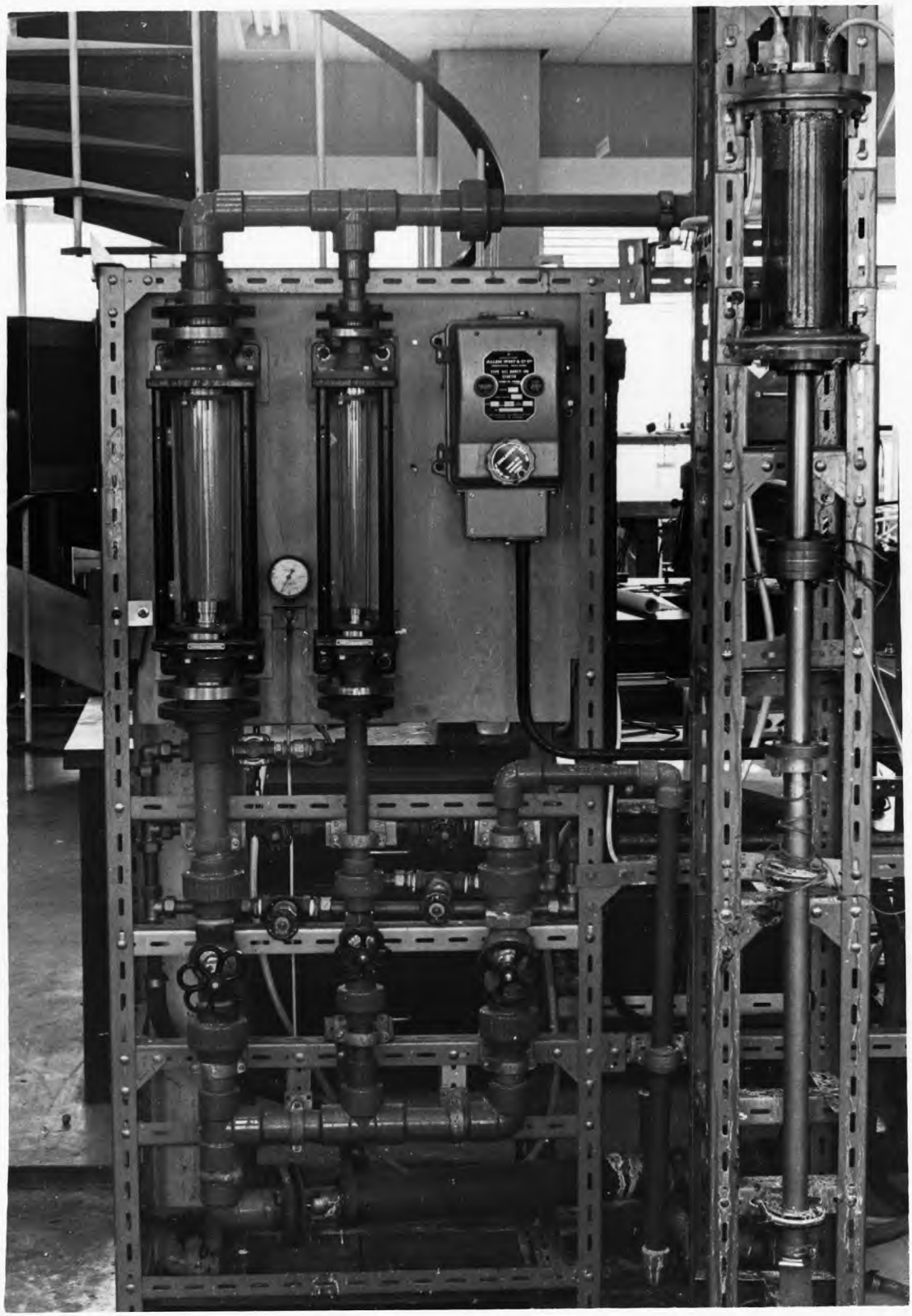

Fig. 7.3-2 The apparatus for mass-transfer experiments

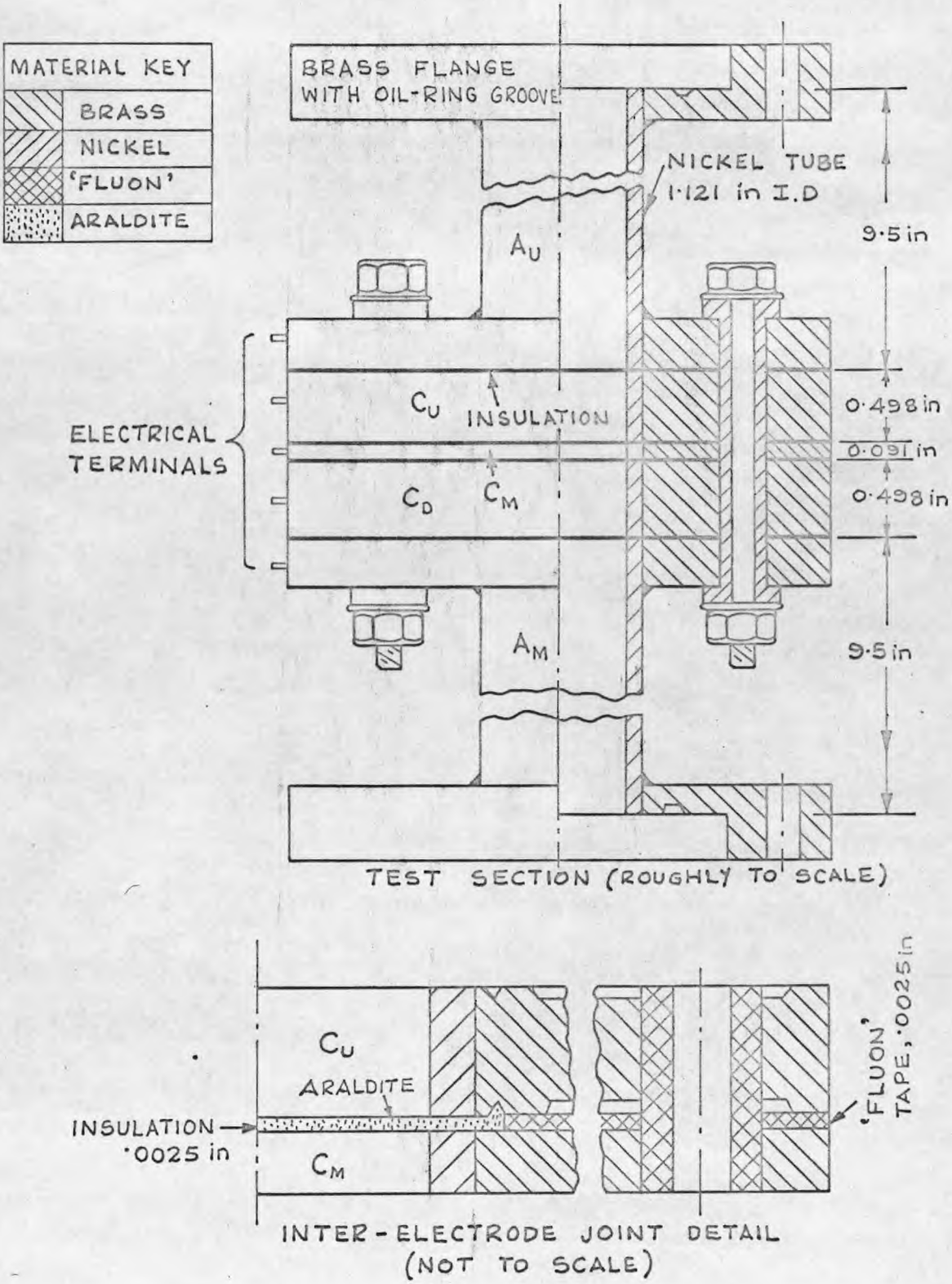

FIG. 7-3-3 ELECTRODE TEST SECTION DETAIL.

(COURTESY : A. D. GOSMAN)

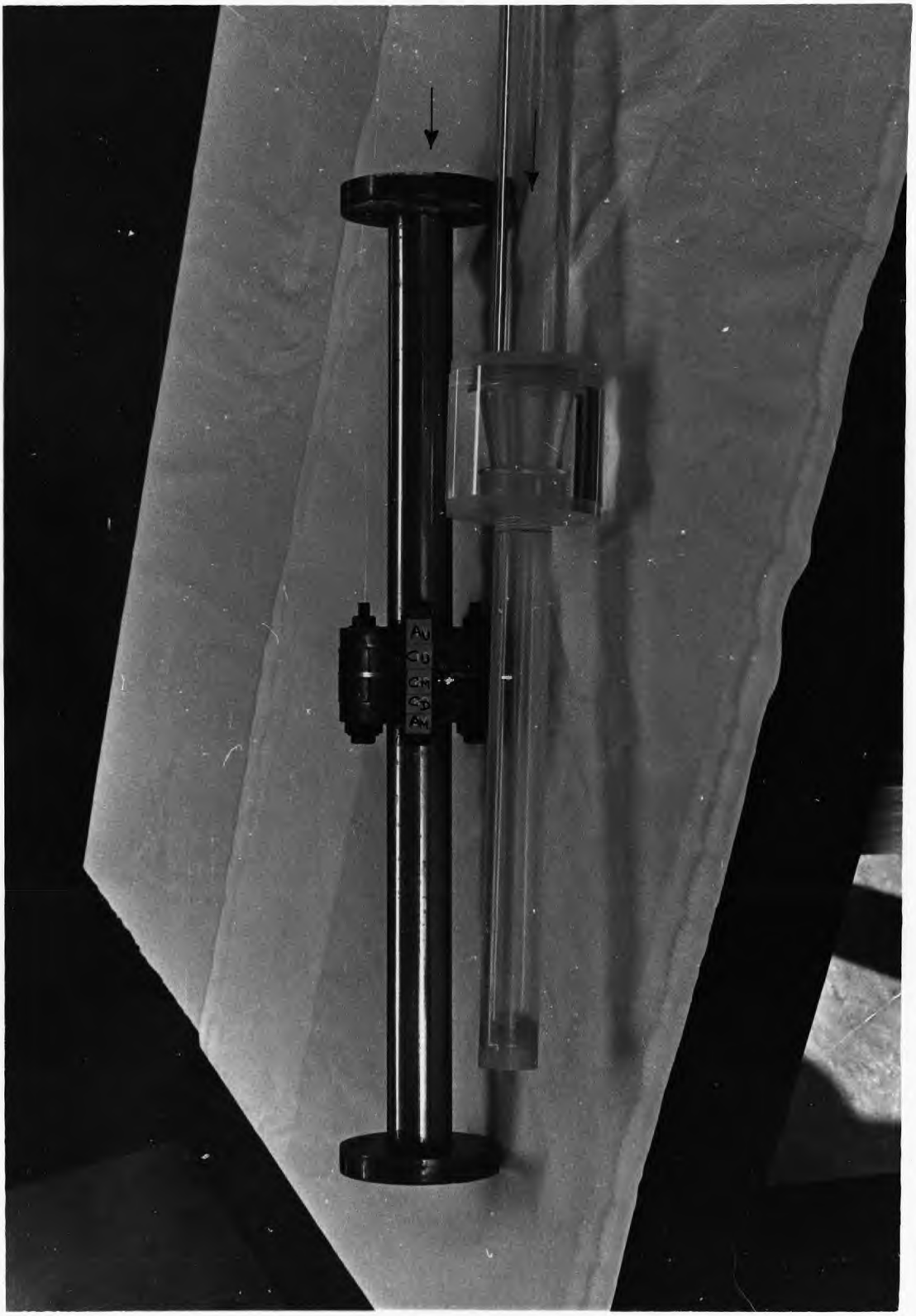

Fig. 7.3-4 The test-section and test-nozzle assembly

being absorbed by the flexible tubing, 8, at the top. The relative position of the nozzle in the test section was obtained from a scale and pointer device, 10, as shown in Fig. 7.3-1. The lower part of the nozzle-assembly was surrounded by a leakage-container, 12, which could be partially, or completely, filled with the liquid to counter-balance the leakage-pressure through the sliding joint between the nozzle and the test-section. The necessity of a movable nozzle arose from the fact that the measurements were required at a number of positions downstream of the sudden enlargement. With a fixed nozzle this can be achieved only by employing a large number of cathodes along the length of the pipe; this, however, presents an awkward design problem. With a movable nozzle the same purpose can be achieved even by a single cathode.

The flow-straightener device, made of a 12" long straight circular tube of 9/8" internal diameter, was used to eliminate any swirling of the liquid. The flow area of the tube was partitioned into four equal segments by 1/16" thick, knife-edged vanes placed along the length of the tube.

Special precautions were observed during the construction and assembly of the apparatus; these will now be described. Because of the corrosive nature of the liquid, all those components which came into direct contact with the liquid were made of corrosion-resistant materials such as 'P.V.C.', 'Perspex', stainless steel and high-purity nickel.

The test-nozzle assembly (Fig. 7.3-5) was made of 'Perspex' and all the inner surfaces and joints were carefully smoothed. The inner surface of the test nozzle

itself was first polished with a very fine emery cloth and later with a polishing liquid supplied by the manufacturers of 'Perspex'. The test section and nozzle assembly was mounted vertical within 1/16".

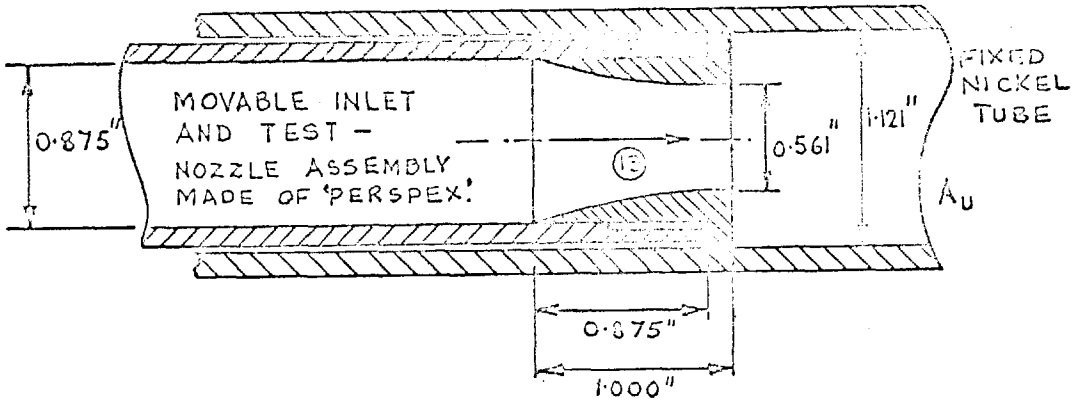

NOTE : NOZZLE INNER PROFILE : FIRST 0·375" LONG SECTION SEGMENT OF A CIRCLE 2·5" RADIUS, LAST 0·125" SECTION PART OF A STRAIGHT CIRCULAR CYLINDER.

FIG. 7-3-5 NOZZLE ASSEMBLY DETAIL.

As potassium ferri-cynide, one of the components of the liquid used, is photo-sensitive, all the transparent sections of the apparatus were covered with a deep-orange celluloid paper. To prevent degeneration of potassium ferri-cynide by oxidation, the liquid was saturated with oxygen-free nitrogen and a nitrogen atmosphere was always maintained in the reservoir.

b) The test-section: The test-section was composed of six lengths of nickel tubing, of 1.121 inch internal diameter, insulated from each other. The details of the test section (except A_D) are shown in Figs. 7.3-3 and 7.3-4. Electrical connections were taken from each segment of the test section to the external electrical circuit.

The mode of construction and assembly of the test section have been described in detail by Gosman (1969). The test section was constructed with very close tolerances because of the thinness of the concentration boundary layer at high Schmidt numbers; the mean roughness on the inner surfaces of the electrodes was less than 10^{-5} inch and the steps at the joints were less than 5×10^{-3}inch.

c) The electrical circuit: The essential features of the external electrical circuit are shown in Fig. 7.3-6. The circuit was designed to allow the operation of the electrochemical cell with any combination of the anode/cathode set-up, and also to permit measurements of current through, and potential-drop across, any of the cathodes individually or in combination with others. For this purpose, each cathode was provided with an independent sub-circuit consisting of a variable e.m.f. source (a lead accumulator across a potential divider), and terminals for calibration and for current and potential-drop measurements. Common terminals were also provided for the over-all circuit as shown in Fig. 7.3-6.

The current measurements were obtained by measuring the potential drop across a standard 1 Ohm resistance with a high-precision Digital Voltmeter*. Though the Digital Voltmeter was supplied with an in-built filter, an external resistance-cpapcitance filter with a variable time period (50 μsec to 10 sec) was used to even out the strong fluctuations in the signal. Most of the readings were taken with this filter set between 2 and 5 seconds.

* 'Fenlow' Digital Voltmeter 301-A;0.01% DC accuracy, 10 μv to 1000v range.

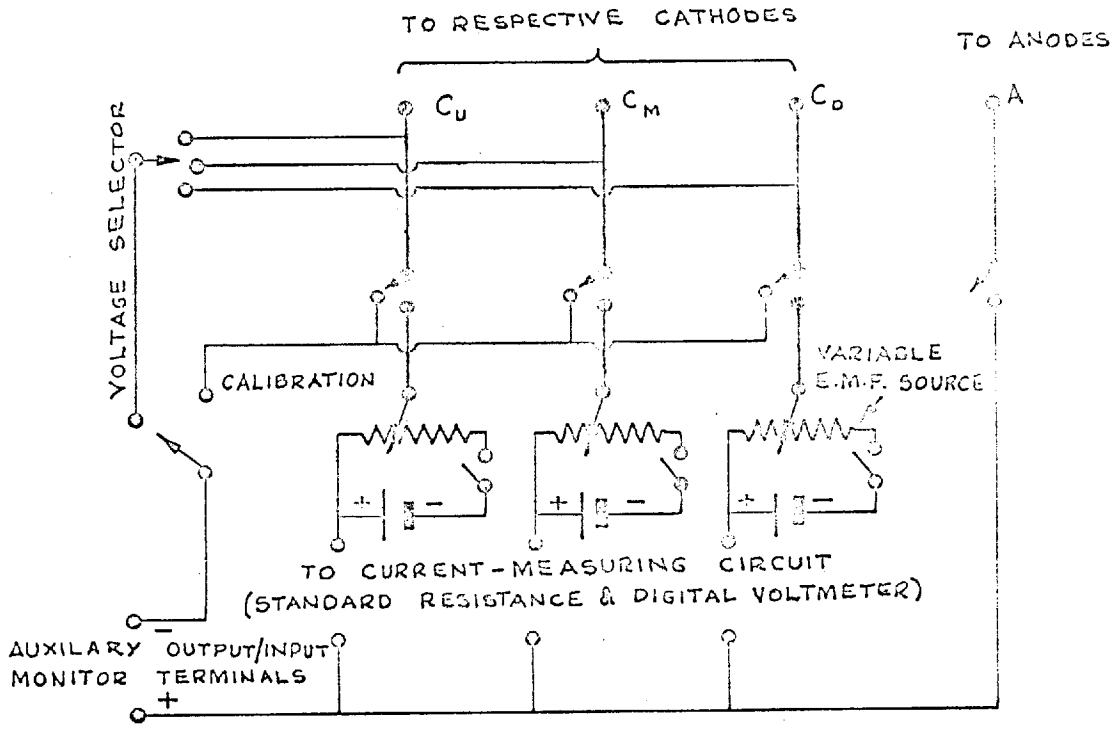

FIG.7-3-6 ESSENTIAL FEATURES OF THE ELECTRICAL CIRCUIT.

A calibration circuit was provided to enable a check on the diffusion-control characteristics of the cathodes. It could be connected to a motor-driven potential divider and the current flowing through a cathode could be recorded on a chart recorder*.

7.3-2 The electrolyte

The electrolyte employed consisted of equimolar concentrations of potassium ferri-cynide, $K_3\ Fe(CN)_6$, and potassium ferro-cynide, $K_4\ Fe(CN)_6$, in aqueous solution of sodium hydroxide, Na OH. High purity 'Analar' chemicals and distilled water were used for the above purpose. It

* 'Honeywell' 'Electronik' strip chart Recorder ¼ second series 153 x 16; ± 0.25% accuracy of scale span.. Basic chart speeds 4" and 120" per minute.

is to be noted that only ferri-cynide and ferro-cynide ions take part in the electrolysis; sodium hydroxide merely provides a supporting electrolyte of high electrical conductivity: these aspects of the technique have been discussed already in section 7.2.

The preparation of the solutions was carried out in two stages. Sodium hydroxide was dissolved in distilled water and allowed to cool to about 25°C; its strength was then determined by titration against a standard aqueous solution of oxalic acid and, if necessary, adjusted to the desired value. This solution was then saturated with oxygen-free nitrogen and the required quantities of potassium ferri- and ferro-cynides were added. The concentration of the ferri-cynide ion was determined with a Spectro-photometer* at a wavelength of 410 mμ.

About 65 litres of the solution were prepared for each series of tests and the solution was retained on the average for about 60 hours. Special precautions were taken to minimize the exposure to light and oxygen, both of which have a degenerating effect on the ferri-cynide ions; these precautions have already been described in section 7.3-1. The concentration of ferri-cynide ions was checked from time to time; any solution which degenerated by more than 2% in this respect was discarded, and the tests repeated with a new solution.

7.3-3 The experimental procedure

The procedure followed for all the mass-transfer tests consisted of the following steps:

---

* 'EEL' Spectra, range 400 to 700 mμ; band width 35 mμ.

1) The test section was removed from the apparatus and reactivated by a process suggested by Duffield (1966).

2) The test section was electrically tested to ensure that the inter-electrode insulation offered a minimum resistance of 50 000 Ohms to any short-circuit current. It was then remounted on the apparatus.

3) The electrolyte was prepared according to the procedure outlined in section 7.3-2.

4) The pump was then started.

5) The heat-exchanger controls were adjusted until the liquid reached, and maintained, the operating temperature of 25 $\pm$ 0.1^{o}C.

6) The next step was to ensure that the diffusion-control characteristics were obtained under the most adverse conditions expected during the tests: this implied obtaining the current vs. potential-drop curves for the maximum current flowing through the circuit.
For the above purpose, the flow rate was set at the maximum and the test-nozzle was positioned such that the middle cathode, C_M, was in the region of the highest mass-transfer rates; this position was about 3 nozzle-diameters downstream of the sudden enlargement.
A motor-driven e.m.f. source was connected across the selected set of electrodes, and the current-vs.-potential-drop curve was recorded on a chart-recorder.
A plateau region with less than 1% rise in current for a range of potential-drop ($\sim$0.5 volts) was accepted as the indication of diffusion-controlled electrolysis.
The tests for diffusion control were carried out for each different electrode combination (see section 7.3-4).

(In case the current-vs.-potential-drop curves failed to show a marked plateau region, the test section was reactivated and all the steps listed above were repeated).

7) The motor-driven e.m.f. source was disconnected and the electrodes were switched to their individual e.m.f. sources as shown in Fig. 7.3-5.
The applied e.m.f. was adjusted so that the potential-drop across each active cathode was in the diffusion-controlled region. The current and potential-drop measuring devices were connected according to the requirements.

8) The flow-rate was adjusted to the required value and a series of relevant readings were taken for selected nozzle positions and electrode combinations.
At the end of one set of readings, the flow-rate was adjusted to a new level and the process was repeated until readings were available for all desired rates of flow.
The diffusion-control curves, temperature readings and the concentration of ferri-cynide ions were obtained from time to time during the intermediate stages of the above series of readings.

9) The solution was drained and the apparatus was rinsed with water. This was followed by a rinse with 5% hydrochloric acid (HCl) and a final wash with water.

7.3-4 Choice of electrode combinations

a) The effect of cathode on the mass-transfer behaviour:

For a cathode-controlled system, the choice of cathode or cathodes is important for the study of the mass-transfer behaviour. It should be recalled from section 7.3-2 that the concentration of ferri-cynide ions at an active cathode falls to zero. Such a cathode, thus, implies a step-change in the boundary conditions; at an inactive surface preceding the cathode, the concentration of the ferri-cynide ions is equal to that in the bulk flow, but at the cathode this concentration falls to zero. In terms of the heat-transfer analogy, an active cathode is equivalent to a surface with a step-change in temperature, whereas an inactive surface is equivalent to an adiabatic wall.

Various types of boundary conditions can be simulated by selecting different cathode combinations from Fig. 7.3-1. The following four groupings were used for the preliminary investigations.

Group I : C_M alone acting as the cathode with C_U and C_D electrically isolated from the circuit,

Group II : C_M, C_U, and C_D all acting as cathodes,

Group III: C_M and C_D acting as cathodes with C_U electrically isolated from the circuit, and

Group IV : C_M and C_U acting as cathodes with C_D electrically isolated from the circuit.

For comparison of results, it was the current generated by the smallest electrode, C_M, which was measured for each group. The length of this cathode was small enough (1/12th of the pipe diameter) to justify the assumption that it represented the local values of the mass transfer.

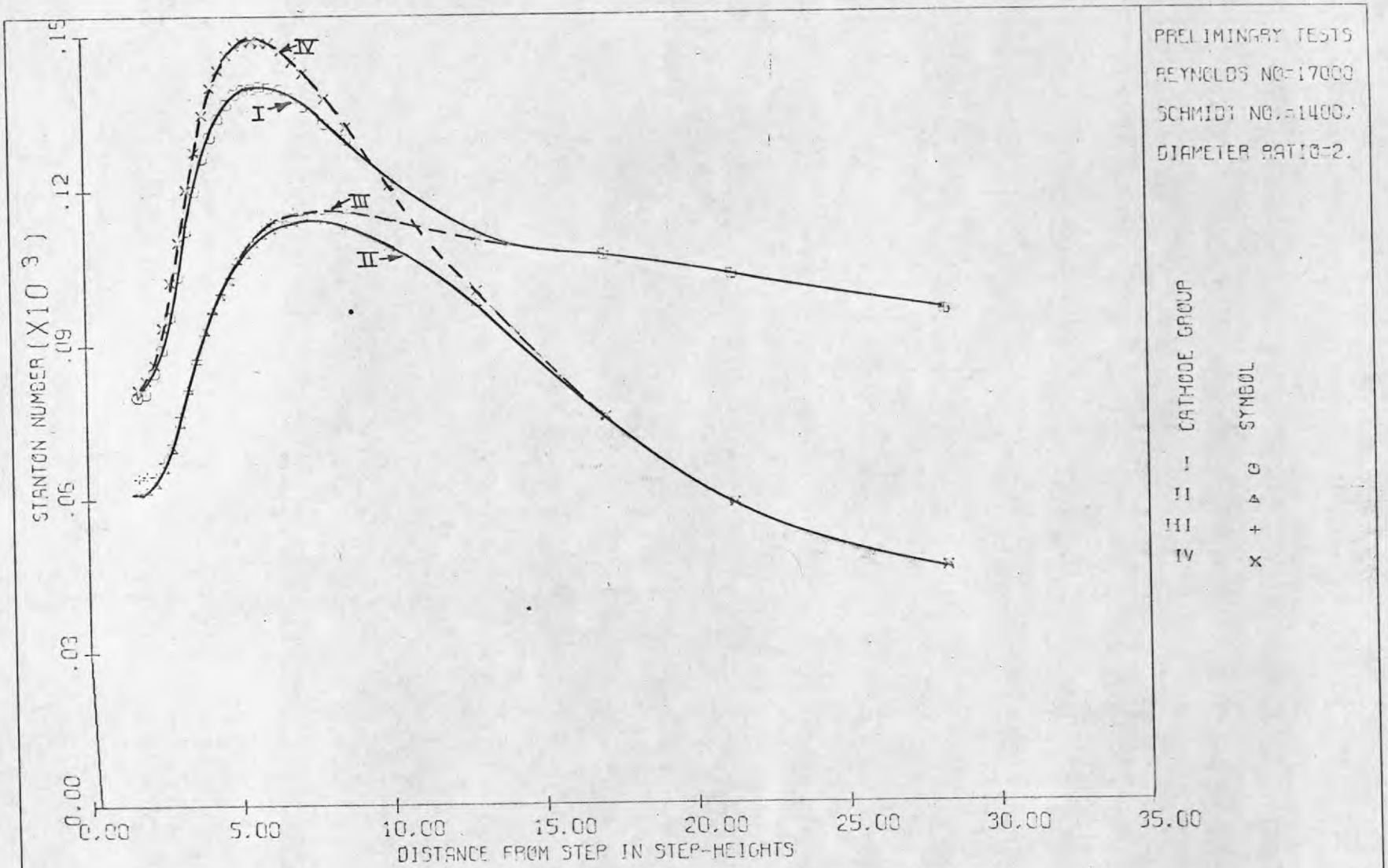

FIG. 7.3-7 MASS TRANSFER DOWNSTREAM OF A SUDDEN ENLARGEMENT IN A CIRCULAR PIPE
EFFECT OF BOUNDARY CONDITIONS (CATHODE GROUP) ON MASS TRANSFER

b) The effect of anode on the mass-transfer behaviour:

In the electrolysis process under study, ferro-cynide ions oxidise into ferri-cynide ions at the cathode. In a cathode-controlled system, the quantity measured is the current generated at the cathode; one of the parameters controlling this current is the concentration of ferri-cynide ions in the bulk flow as shown by equation (7.2-1). Because these ions are generated at an anode, the location of an anode upstream of a cathode will increase the rate of reaction at the cathode. This will produce anomalous results which cannot be interpreted properly because of lack of information about the extent of increase in the concentration of ferri-cynide ions. It was for this reason that the use of A_U, as the anode, had to be ruled out.

The first preliminary sets of results were obtained with A_M as the anode and A_U and A_D isolated from the electrical circuit. A typical set of results is displayed in Fig. 7.3-7 for the four different cathode groups. A comparison of the results for the cathode group I with those of the group IV shows a disturbing feature of the results: that for some regions of the flow, mass transfer rates are higher for group IV. As group I represents a small locally active surface, rather than a zone of active surface of group IV*, in view of the established behaviour of the convective flows, this increase is totally unexpected and points to some unconventional mechanism entering into the picture. On second thoughts it can, in fact, be concluded that there is a strong likelihood that the

---

* Group I, in heat transfer analogy, corresponds to local heating, whereas group IV represents zonal heating.

ferri-cynide ions produced at the anode A_M will be swept back onto the cathodes. This is possible because, for some of the nozzle positions, the upper part of the anode will lie in the reversed-flow region, upstream to the cathodes with respect to the direction of flow on the cathode-surface. Because the rate of generation of the ferri-cynide ions at the anode is proportional to the amount of current generated at all the cathodes, such an effect will pronounce itself at the higher current intensities of the group IV. Of course, the natural question to ask is that, 'why does such an effect not appear for groups II and III, which also have higher current intensities than those of group I?' The reason is that, for these two groups, there is an intercepting cathode C_D between the anode A_M and the cathode C_M at which the current is being measured. Thus, any increase in the concentration of ions is absorbed by this intercepting cathode before it can reach the measuring cathode C_M: the current at C_M is therefore representative only of the rate of diffusion from the bulk flow.

It is to be noted that no such anomalous increase is discernible in the measurements far downstream of the enlargement and the results of the group IV merge with those from the group II: this is to be expected on theoretical grounds as no back-flow is now possible from A_M to C_M.

From the reasoning of the previous paragraph it is to be expected that the fallacious results caused by the proximity of the anode to the cathodes can be eliminated by using A_D as the anode. Contrary to expectations, however, the use of A_D as the anode did not seem to make any substantial difference to the results. The only noticeable

difference was a slight increase in the potential drop through the cell; this increase, however, was much less than would be expected because of the ohmic drop in the extra column of electrolyte now interposed between the anode and the cathodes. Discussions of the above unexpected results with other research workers in this field, revealed that under some circumstances it is possible that the metal tube A_M, though not acting as an anode, may still act as a conductor for the passage of electrons. As the conductance of nickel is much higher than that of the electrolyte, the former provides a preferred path for the current; in such a case, the end of the tube nearer to the cathodes acts as an anode and defeats the very purpose for which A_D was used as an alternative anode for the system.

To verify the above arguments, it was decided to insulate the inner surface of the tube A_M from the solution altogether. For this purpose, a polythene tube, 9/8" O.D. and 7/8" I.D., was inserted in the test section in such a way that A_M and C_D were completely covered by it. The end of the polythene tube near the joint of C_D and C_M was formed in the shape of a nozzle and A_D was once again employed as the anode. It was noticed that now the results from the cathode group IV were the same as those from the group I for all the regions of the flow. However, the potential-drop now required to operate the cell at the diffusion-controlled level was very high (of the order of 4 volts compared to about 0.5 volts of the earlier arrangements); this high voltage level was found unsatisfactory for general work: small changes in current caused relatively large changes in the potential-drop because of the high

resistance of the electrolyte between the anode and the cathodes.

The elimination of the drawbacks of the existing electrode set-up would have required the design and construction of a new test section, and it was felt that the advantages to be gained were not justified by the effort involved; it was therefore decided to continue with the existing test section with the choice of electrodes given in the next sub-section.

c) The final choice of the electrodes: In the light of the preceding discussion, the only choice left open for the anode was that of A_M and all subsequent tests were carried out with this electrode as the anode.

Cathode group IV had to be abandoned because of the fallacious information provided by this grouping; this left the choice open between the other three groups. A glance at Fig. 7.3-7 shows that not much can be gained from the use of cathode group III either. With respect to the flow in the vicinity of the surface, C_U lies downstream of C_M for the region of reverse flow and the results of group III merge with those from group II; away from the regions of reverse flow, C_D lies downstream of C_M and the results from group III merge with those from group I: these trends are to be expected from the known behaviour of the convective flows.

Thus, the cathode groups selected for the final series of tests were the groups I and II.

7.4 Results and discussion

7.4-1 The flow parameters

For presentation of results, let us define the following non-dimensional parameters:

Diameter ratio: $D \equiv D_P/D_N$,

Distance: $Z \equiv 2.z/(D_P-D_N)$,

Reynolds number: $Re \equiv G_m.D_P/\mu$, (7.4-1)

Schmidt number: $Sc \equiv \mu/(\rho \Gamma_m)$, and

Stanton number: $St \equiv g_m/G_m$,

where,

D_P is the diameter of the pipe,

D_N is the diameter of the nozzle, and

Γ_m is the mass-diffusivity of the fluid.

All other symbols are explained in the nomenclature.. $(D_P-D_N)/2$ is, of course, the height of the step formed due to the sudden enlargement.

In general, for incompressible flows,

$$St = St\{Re, Sc, Z, D, b.c, ...\} \quad (7.4-2)$$

where b.c. denotes the effect of the boundary conditions, and the dots serve as a reminder that in a complex problem other parameters, such as the turbulence intensity, may also affect the Stanton number.

For a fixed diameter ratio (equal to 2 in the present case):

$$St = St\{Re, Sc, Z, b.c.\} \quad (7.4-3)$$

The boundary condition is governed by the selection of the cathode group in the present case (see section 7.3-4); as already mentioned, for the final tests two cathode groups, I and II, were employed.

The experiments were performed for two values of the Schmidt number: 1400 and 2500; the transport properties and concentrations of the corresponding solutions are given in table 7.4-1.

Solution No.	NaOH gm-moles per litre	$K_3Fe(CN)_6$ gm-moles per litre	ρ $gmcm^{-3}$	μ $gm.sec^{-1}.cm^{-1}$	Sc	Re Range	Data appear in
1	0.520	0.00515	1.020	0.0103	1400. ± 7%	3550. to 88500.	Figs. 7.4-1 7.4-2 Table 7.5-1 7.5-2
2	2.056	0.00504	1.080	0.0144	2500. ± 7%	2550. to 65300.	Figs. 7.4-3 7.4-4 Table 7.5-3 7.5-4

Table 7.4-1 Fluid-property data for the solutions employed for the mass-transfer experiments.

Note: Fluid-property data were taken from Duffield (1966).

The Reynolds number was varied from 2550 to 88500, and the mass transfer measurements were obtained for various locations downstream of the sudden enlargement from Z = 1.7 to Z = 34.8.

7.4-2 The experimental data

The experimental data are displayed graphically in Figs. 7.4-1 and 7.4-4 as plots of Stanton number, St, vs. the non-dimensional distance, Z, for various Reynolds numbers. The same data are later reproduced in a tabular form in section 7.5. Also shown with the above data are the asymptotic values obtained by Gosman (1969).

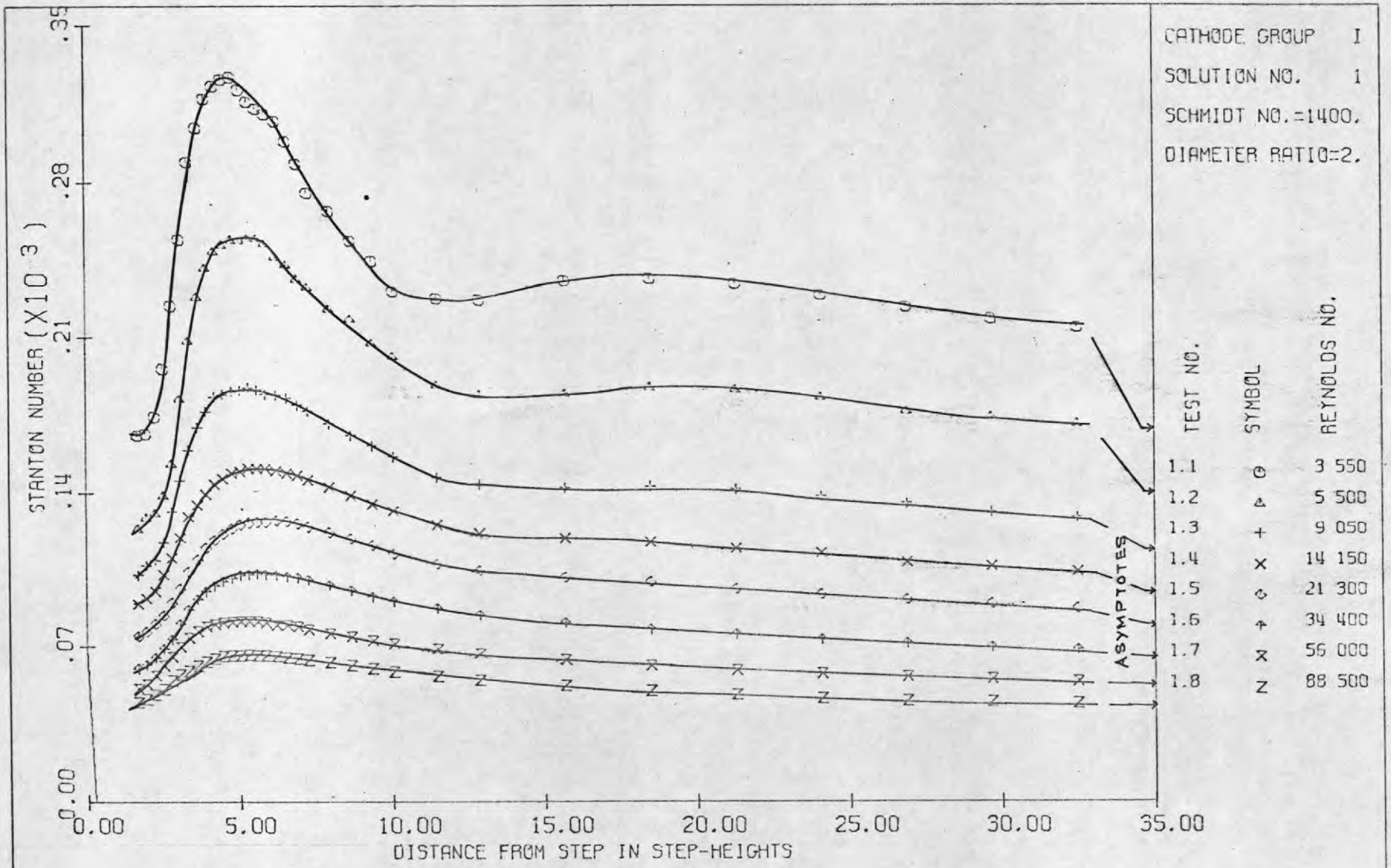

FIG. 7.4-1 MASS TRANSFER DOWNSTREAM OF A SUDDEN ENLARGEMENT IN A CIRCULAR PIPE WITH A SMALL ACTIVE ZONE AT THE POINT OF MEASUREMENT ONLY

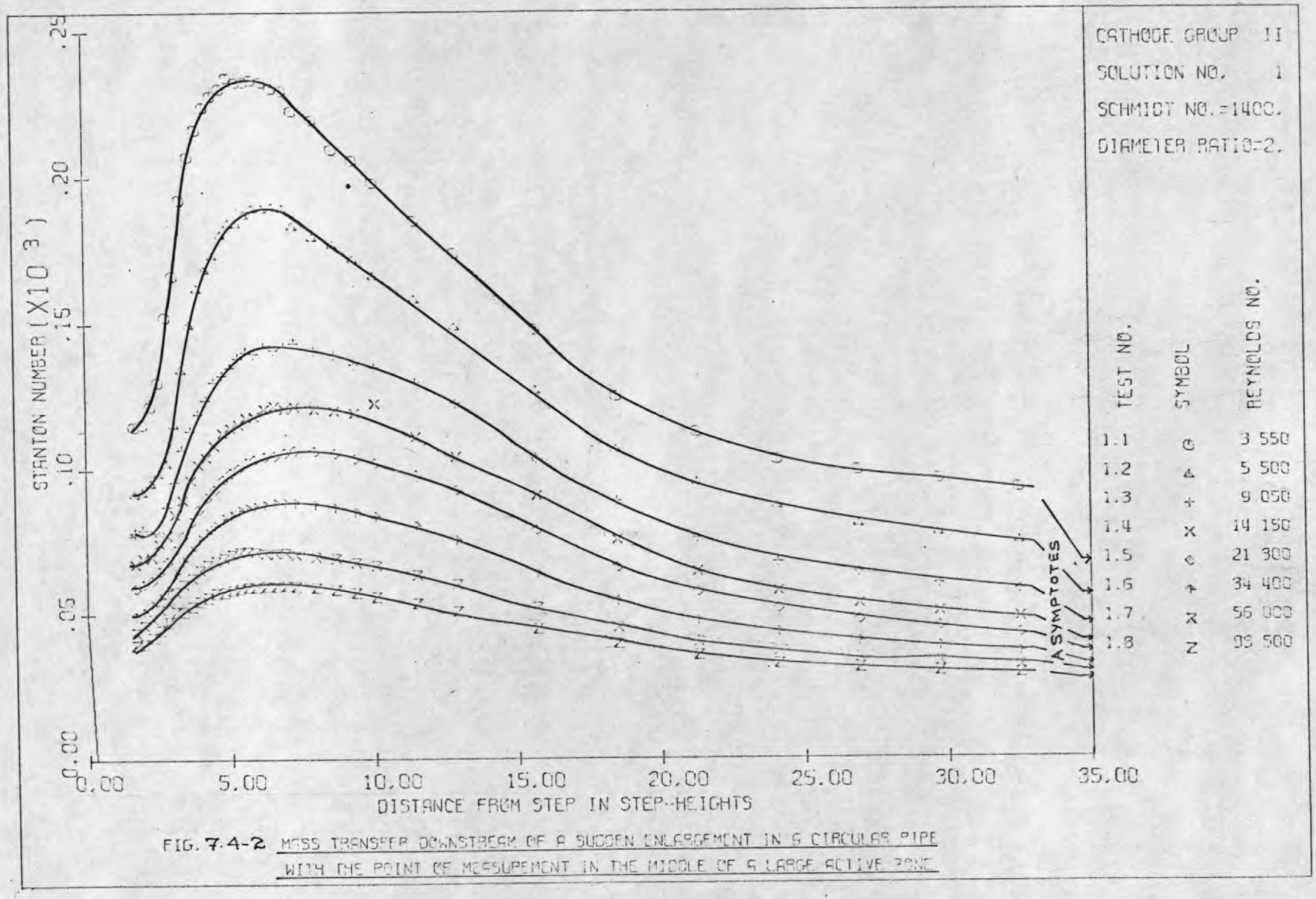

FIG. 7.4-2 MASS TRANSFER DOWNSTREAM OF A SUDDEN ENLARGEMENT IN A CIRCULAR PIPE WITH THE POINT OF MEASUREMENT IN THE MIDDLE OF A LARGE ACTIVE ZONE

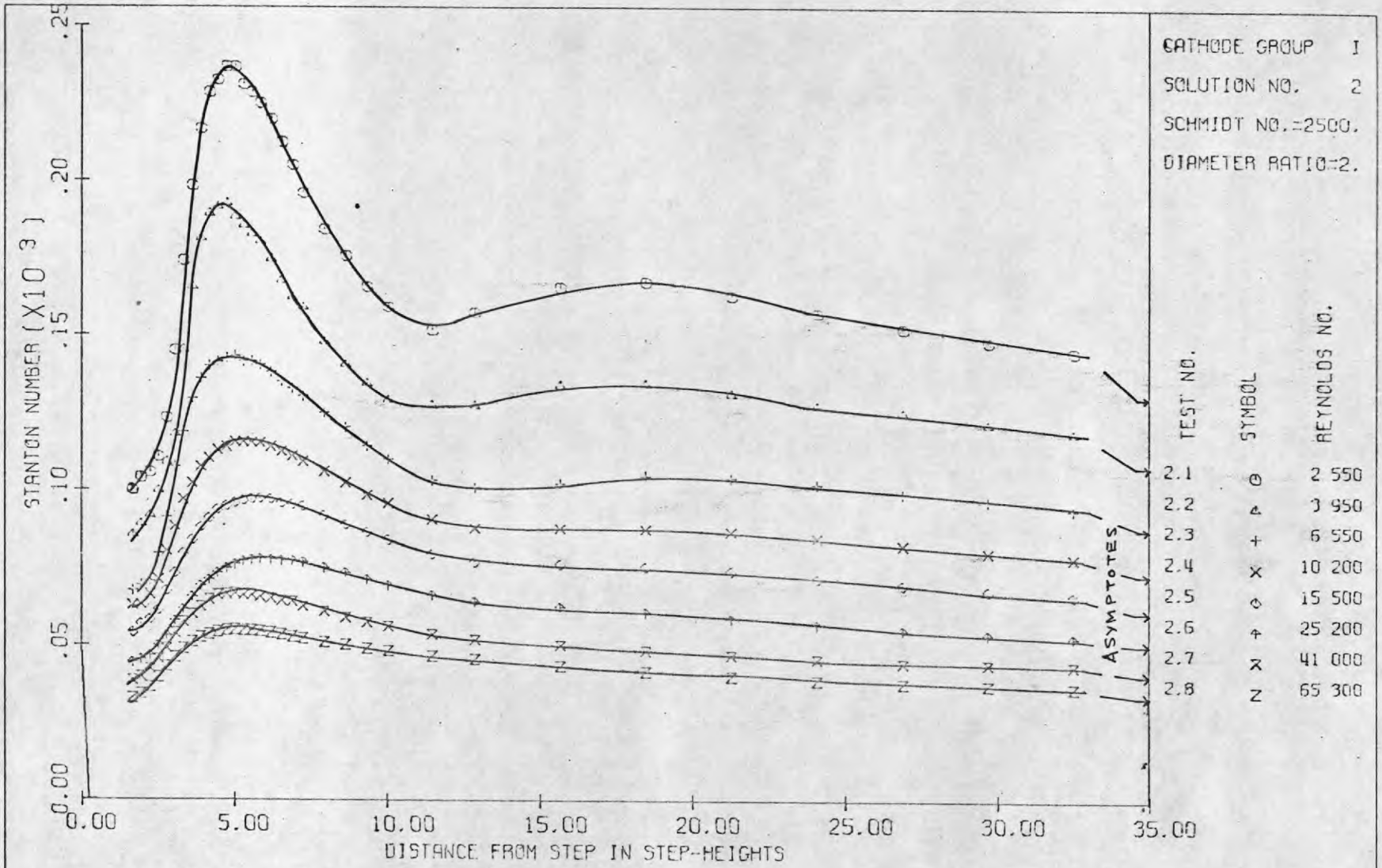

FIG. 7.4-3 MASS TRANSFER DOWNSTREAM OF A SUDDEN ENLARGEMENT IN A CIRCULAR PIPE WITH A SMALL ACTIVE ZONE AT THE POINT OF MEASUREMENT ONLY

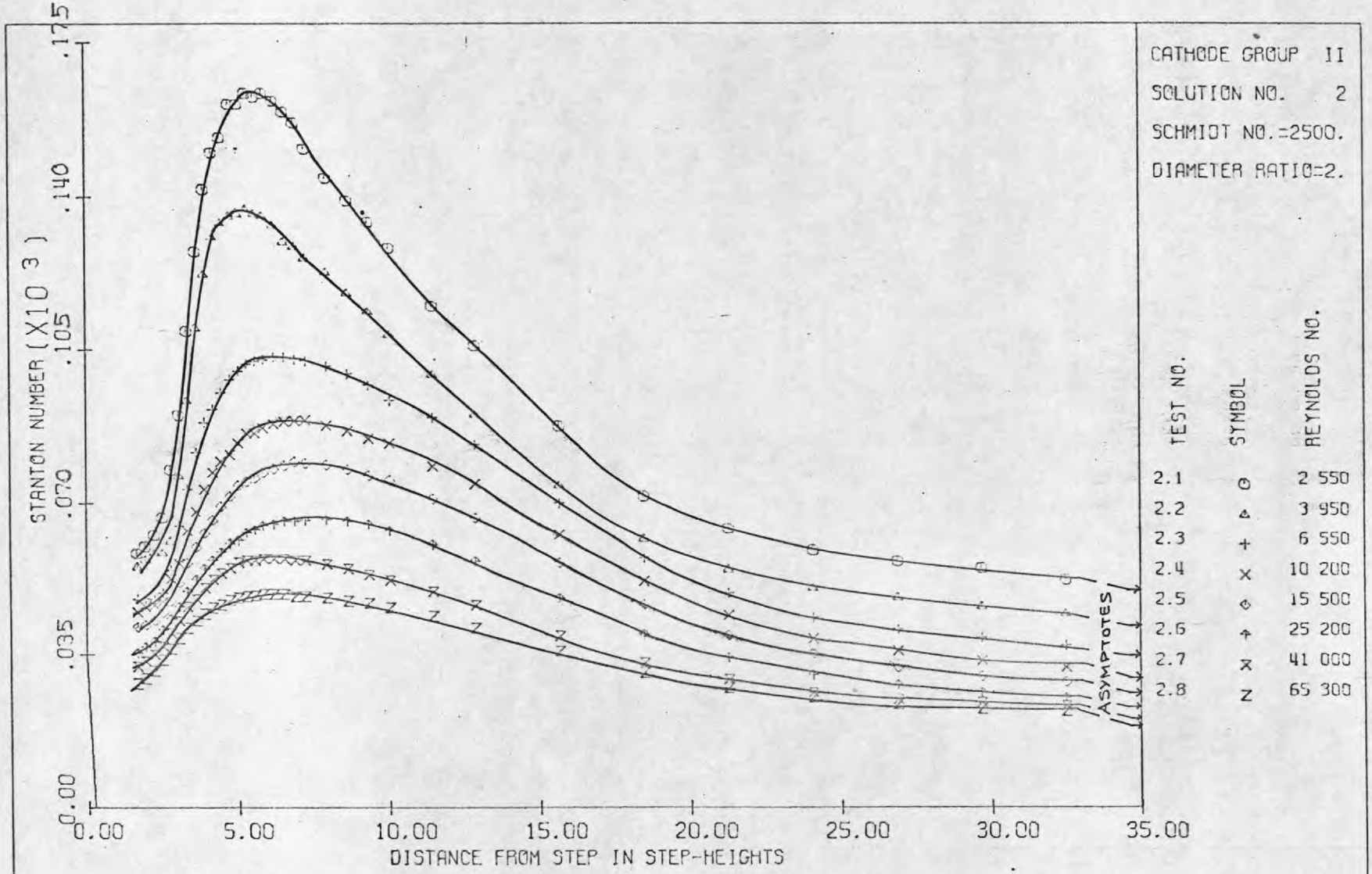

FIG. 7.4-4 MASS TRANSFER DOWNSTREAM OF A SUDDEN ENLARGEMENT IN A CIRCULAR PIPE WITH THE POINT OF MEASUREMENT IN THE MIDDLE OF A LARGE ACTIVE ZONE

The present data far downstream of the enlargement compare favourably with those obtained by Gosman (1969). The data for the separated and the redeveloping regions of the flow follow the well-established pattern of behaviour in its general trends: the mass-transfer rate rises rapidly to a maximum in the reattachment zone and then decays to its asymptotic value for the flow in a straight circular pipe.

However, there are two features of the present data which do not seem to have been reported in the existing literature. The first is a shift in the location of the Stanton number maxima with the boundary condition: the data for the cathode group I exhibit maxima, on the average, in the vicinity of $Z = 5.6$, whereas the maxima for the cathode group II are located near $Z = 7.0$. The second novel feature is the appearance of a second maximum for the data of the cathode group I at low Reynolds number.

Precisely how the boundary condition interacts with the flow to bring about these effects cannot be explained on the basis of the existing knowledge about the separated flows. It is generally agreed that the location of the time-mean maximum mass/heat transfer coincides with the mean reattachment point; however, the reattachment point itself is known to oscillate about a mean position with time(e. g. Abbot and Kline 1962). Since the instantaneous values at a certain location are a function of the boundary conditions, it is conceivable that the differences in the time-mean values are caused by the time-averaging process. Another possibility, of course, is that the inactive cathode C_D, for the cathode group I, may act as a pseudo-anode and cause a local increase in the concentration of the ferri-

cynide ions. This effect, which has been described in detail in section 7.3-4, will result in increased rates of mass transfer at C_M, especially for the reversed-flow region when C_M, relative to the local direction of flow, lies downstream of C_D.

In the existing literature, the maxima in heat/mass transfer have been reported to lie between Z = 4 and Z = 12 (see e.g. Krall and Sparrow 1966). The most frequent values quoted in this respect are between Z = 6 and Z = 8. It is interesting to note that almost identical values have been noted for external flows such as the flow past a step (e.g. Mueller and Robertson 1962). The present data, especially those for cathode group II, are thus consistent with the data obtained by earlier workers. It should be noted that almost all of the earlier data were obtained with uniform (temperature or heat-flux) boundary conditions for a considerable length downstream of separation: the boundary conditions of the cathode group II are nearer to this situation than those of the cathode group I.

7.4-3 Correlation of the data

a) A small locally active surface: cathode group I: For very high Schmidt numbers and small mass-transfer surfaces the concentration gradients are likely to lie entirely within the laminar sub-layer. It can be shown that (e.g. Spalding 1964) away from the reattachment point

$$St \propto Sc^{-2/3} \quad , \qquad (7.4-7)$$

and therefore, for purposes of correlation:

$$St = \text{const.}\ Re^{-q}.\ Sc^{-2/3} \quad . \qquad (7.4-8)$$

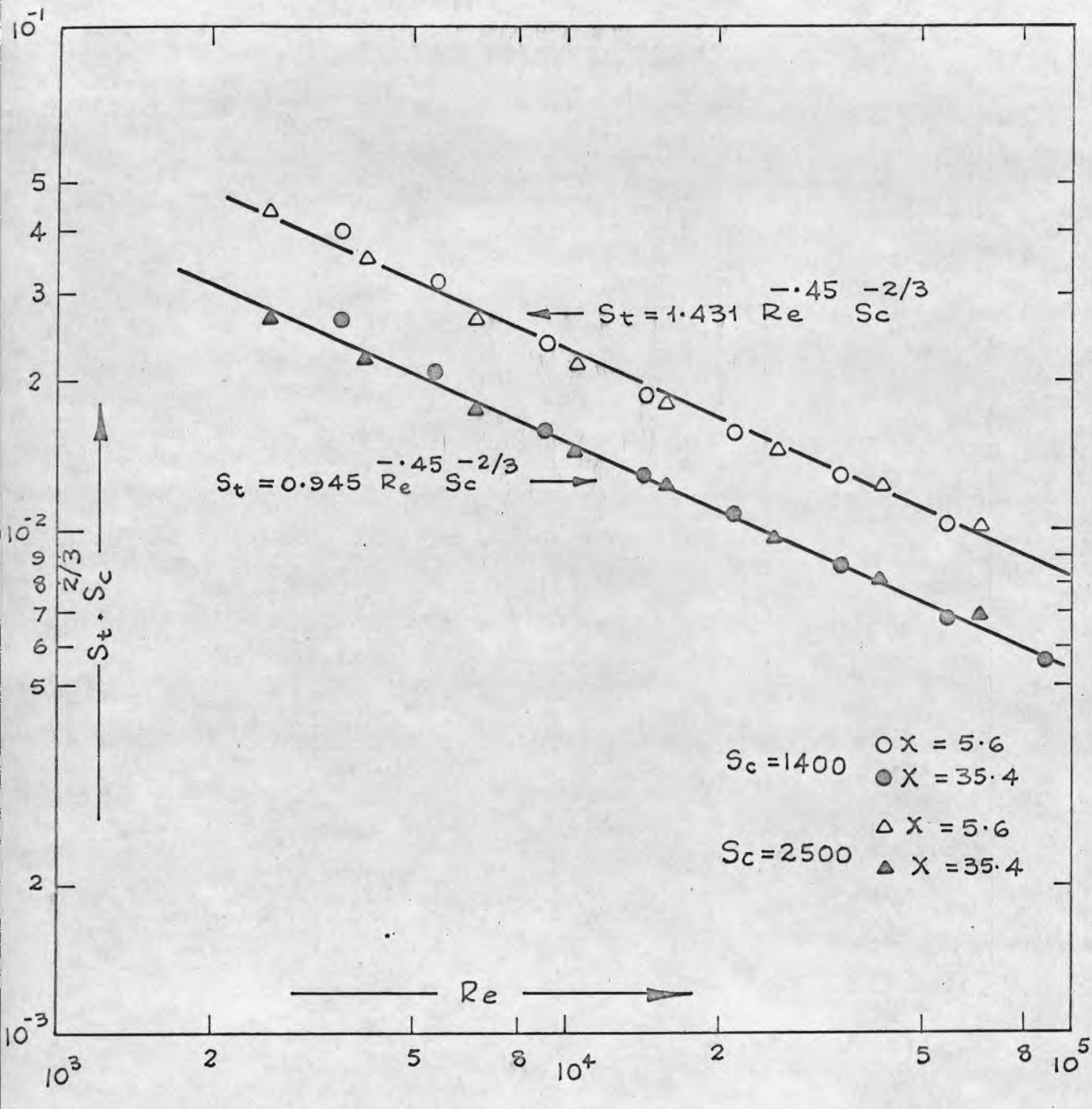

FIG. 7-4-5 CORRELATION OF EXPERIMENTAL DATA FOR SMALL LOCALLY ACTIVE SURFACE : CATHODE GROUP I.

Fig. 7.4-5 presents Re vs. $St.Sc^{2/3}$ in a graphical form for two locations downstream of the sudden enlargement: the location of the mass-transfer maxima and a location far downstream of the enlargement. In both cases, the data can be well correlated with $q = 0.45$.

According to Spalding (1964), the value of q for a fully developed pipe flow at high Schmidt and Reynolds numbers is 0.417. In the vicinity of the reattachment point in a turbulent separated flow, Spalding (1967b) deduced that the value of q should be 0.40.

b) A zone of active surface: cathode group II: For fully developed turbulent flow at high Schmidt and Reynolds numbers, it can be shown that (e.g. Diessler 1955, Spalding 1964):

$$St = \text{const.}\ Re^{-.125}.\ Sc^{-3/4} \quad . \qquad (7.4\text{-}9)$$

Though the boundary conditions of the cathode group II are not likely to yield a fully developed flow, it is convenient to employ the following generalisation of the above relation:

$$St = \text{const.}\ Re^{-q}.\ Sc^{-3/4} \quad . \qquad (7.4\text{-}10)$$

Fig. 7.4-6 displays Re vs. $St.Sc^{3/4}$ for two locations similar to the ones for the cathode group I. In this case, however, the data can be correlated as a simple power law only for the location of the maximum mass transfer; the index of the power law, q, is equal to 0.35. The values far downstream cannot be represented by a simple power law: in fact, even the dependence on Schmidt number does not appear to be a simple power of 3/4. However, for Re greater than 2.5×10^4, q in the above equation may be chosen as 0.20.

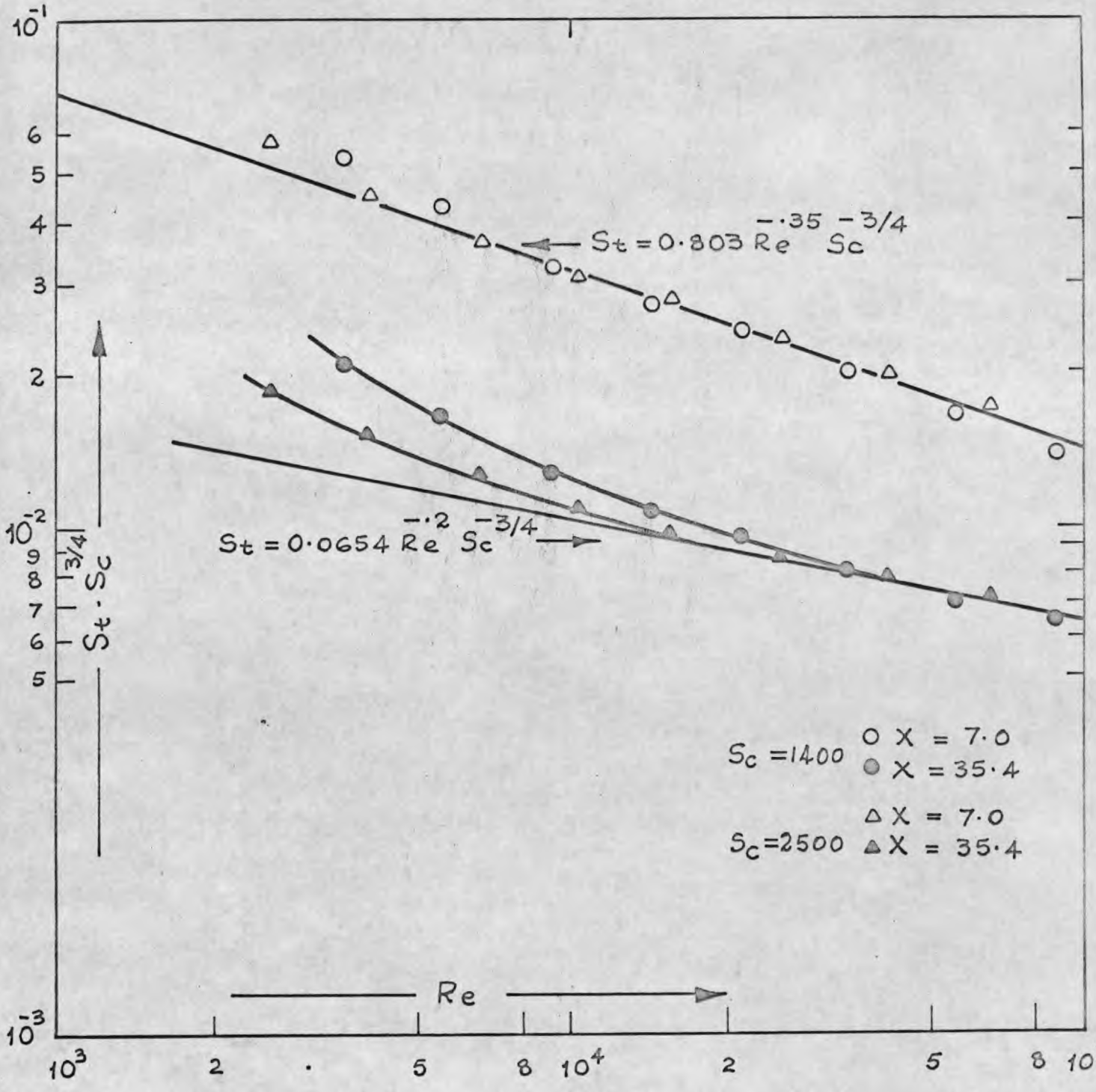

FIG. 7-4-6 CORRELATION OF EXPERIMENTAL DATA: A LARGE ZONE OF ACTIVE SURFACE: CATHODE GROUP II.

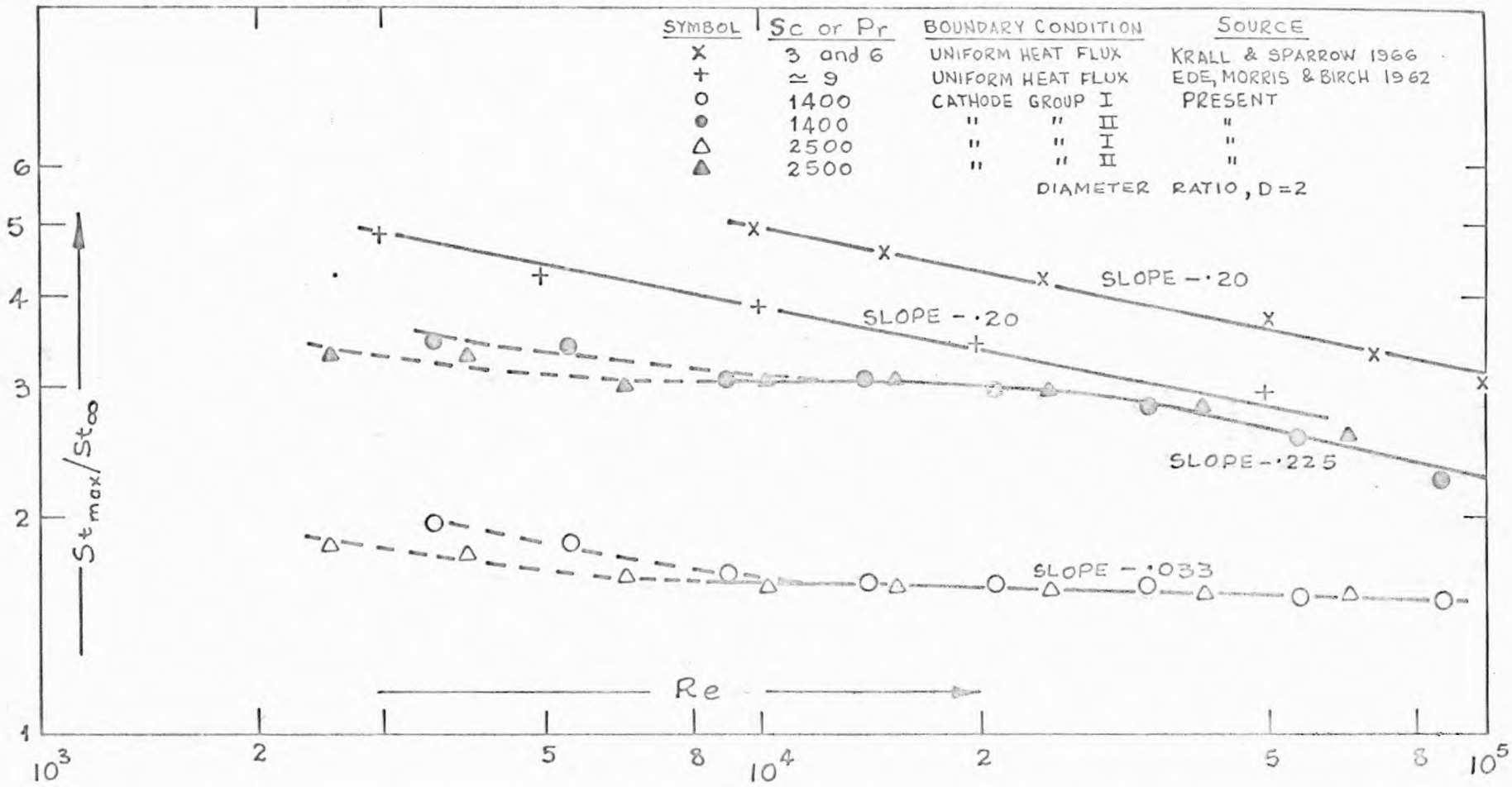

FIG. 7-4-7 COMPARISON OF EXPERIMENTAL DATA FOR MAX. HEAT/MASS TRANSFER DOWNSTREAM OF SUDDEN ENLARGEMENT IN A CIRCULAR PIPE.

It is to be noted that the values reported by earlier research workers, for uniform heat-flux at the wall, are approximated by q = o.33 in the reattachment region. The value of q predicted by Spalding (1966) for the reattachment region is 0.40.

7.4-4 Comparison with previous investigations and concluding remarks

A number of investigations have now been conducted into the behaviour of the separated flows, and some of these have already been referred to in the previous sections; however, none is directly comparable with the present one in both the geometrical arrangement and the experimental conditions.

Fig. 7.4-7 presents the data of Krall and Sparrow (1966) and Ede et al. (1962) along with some data from the present experiments. All the data collected here were obtained for sudden enlargement in a circular pipe for a diameter ratio of two; however, the experimental conditions varied considerably. Krall and Sparrow induced separation by inserting an orifice into a pipe with fully-developed upstream flow; the pipe was heated electrically and the tests were conducted at Prandtl number of 3 and 6. The data of Ede and co-workers were obtained for the sudden expansion of a fully-developed pipe flow into a bigger pipe; electrical heating and a Prandtl number of about 9 were employed. St_∞ for the data of Ede et al. was obtained from a correlation recommended by Knight (1966) for similar data:

$$St_\infty = .0109\ Re^{-.116}.Pr^{-.6} \qquad (7.4\text{-}11)$$

It should be noted that the slopes of -.033 and -.225 in Fig. 7.4-7 were arrived at from the correlations of the maxima and the asymptotic solutions recommended by Spalding: both of these have been discussed in detail in the preceding section.

Fig. 7.4-7 shows that the effect of the Prandtl/Schmidt number of St_{max}/St_{∞}, especially at high Reynolds numbers, is small. The differences between the results of Krall and Sparrow and those of Ede et al. can, then, only be ascribed to the differences in the experimental conditions, such as the increased turbulence in the incoming flow in the case of Krall and Sparrow because of the presence of an orifice in the pipe.

The Reynolds number dependence of St_{max}/St_{∞} is considerably influenced by the boundary conditions as can be seen from the comparison of the data for cathode group I with those of cathode group II. Also the data show a large variation in the magnitude of St_{max}/St_{∞} at any fixed Reynolds number.

More experimental data are clearly needed to understand and explain the mechanisms which bring about these changes of heat/mass-transfer behaviour.

7.5 Experimental data in tabular form

CATHODE GROUP I

SOLUTION NO. 1

SCHMIDT NO. 1400

DIAMETER RATIO 2

Z \ Re	3550	5500	9050	14150	21300	34400	56000	88500
1.7	1.659	1.235	1.026	0.897	0.750	0.603	0.512	0.452
2.0	1.666	1.284	1.072	0.922	0.770	0.621	0.531	0.466
2.2	1.743	1.304	1.096	0.953	0.804	0.651	0.570	0.488
2.5	1.959	1.389	1.177	1.028	0.843	0.693	0.616	0.510
2.8	2.245	1.532	1.316	1.107	0.902	0.736	0.654	0.551
3.1	2.546	1.820	1.458	1.196	0.968	0.805	0.701	0.577
3.4	2.893	2.083	1.597	1.290	1.043	0.870	0.743	0.592
3.7	3.047	2.281	1.697	1.346	1.101	0.916	0.769	0.617
3.9	3.178	2.415	1.769	1.398	1.152	0.951	0.790	0.634
4.2	3.232	2.490	1.832	1.443	1.186	0.975	0.801	0.648
4.5	3.263	2.519	1.844	1.466	1.216	0.999	0.810	0.657
4.8	3.271	2.544	1.860	1.493	1.239	1.012	0.813	0.660
5.1	3.217	2.539	1.863	1.499	1.257	1.024	0.817	0.661
5.3	3.163	2.549	1.875	1.512	1.264	1.030	0.817	0.663
5.6	3.132	2.549	1.866	1.512	1.268	1.032	0.817	0.663
5.9	3.109	2.524	1.844	1.512	1.267	1.030	0.808	0.662
6.3	3.078	2.465	1.841	1.502	1.273	1.025	0.799	0.657
6.6	2.985	2.430	1.826	1.493	1.270	1.020	0.797	0.652
7.0	2.885	2.366	1.796	1.481	1.261	1.013	0.789	0.649
7.3	2.754	2.326	1.769	1.460	1.247	1.004	0.776	0.642
8.0	2.669	2.227	1.712	1.427	1.221	0.978	0.758	0.630
8.7	2.538	2.182	1.660	1.391	1.193	0.955	0.744	0.616
9.4	2.445	2.073	1.612	1.350	1.162	0.928	0.727	0.603
10.1	2.307	2.013	1.564	1.321	1.125	0.906	0.712	0.589
11.5	2.276	1.885	1.470	1.252	1.079	0.874	0.688	0.566
12.9	2.268	1.840	1.440	1.215	1.048	0.842	0.668	0.548
15.7	2.361	1.845	1.425	1.192	1.015	0.809	0.639	0.523
18.5	2.368	1.875	1.431	1.176	0.994	0.778	0.614	0.500
21.4	2.345	1.865	1.416	1.148	0.964	0.756	0.592	0.484
24.2	2.291	1.830	1.386	1.126	0.937	0.732	0.577	0.465
27.0	2.237	1.766	1.355	1.084	0.914	0.716	0.562	0.455
29.8	2.183	1.741	1.316	1.067	0.895	0.697	0.552	0.450
32.6	2.145	1.711	1.292	1.043	0.877	0.686	0.544	0.443
34.8	2.098	1.671	1.268	1.028	0.864	0.677	0.539	0.439
∞*	1.682	1.399	1.138	0.944	0.796	0.652	0.532	0.440

Table 7.5-1. Stanton Number (X 10^4) downstream of a sudden enlargement in a circular pipe with a small active zone at the point of measurement only.

* Values at $Z \rightarrow \infty$, in Tables 7.5-1 to 7.5-4, are those of Gosman (1969).

CATHODE GROUP II

SOLUTION NO. 1

SCHMIDT NO. 1400

DIAMETER RATIO 2

Z \ Re	3550	5500	9050	14150	21300	34400	56000	88500
1.7	1.149	0.913	0.785	0.675	0.591	0.497	0.441	0.397
2.0	1.157	0.922	0.794	0.694	0.607	0.512	0.464	0.403
2.2	1.219	0.952	0.782	0.700	0.619	0.538	0.486	0.425
2.5	1.304	0.987	0.776	0.748	0.651	0.559	0.519	0.451
2.8	1.527	1.022	0.875	0.775	0.685	0.588	0.545	0.478
3.1	1.666	1.156	0.960	0.849	0.724	0.645	0.579	0.512
3.4	1.929	1.344	1.072	0.899	0.772	0.687	0.604	0.512
3.7	2.075	1.498	1.138	0.964	0.822	0.726	0.629	0.531
3.9	2.168	1.622	1.195	1.020	0.865	0.762	0.656	0.548
4.2	2.245	1.686	1.244	1.045	0.906	0.782	0.672	0.560
4.5	2.283	1.736	1.304	1.084	0.933	0.807	0.686	0.574
4.8	2.307	1.809	1.328	1.126	0.966	0.833	0.694	0.578
5.1	2.345	1.845	1.355	1.146	0.993	0.843	0.706	0.584
5.3	2.330	1.845	1.389	1.157	1.007	0.859	0.714	0.589
5.6	2.330	1.875	1.407	1.180	1.028	0.868	0.717	0.595
5.9	2.337	1.894	1.401	1.186	1.037	0.873	0.716	0.596
6.3	2.330	1.894	1.425	1.211	1.047	0.877	0.710	0.597
6.6	2.307	1.899	1.413	1.219	1.051	0.884	0.710	0.597
7.0	2.299	1.894	1.425	1.211	1.060	0.884	0.712	0.601
7.3	2.229	1.835	1.437	1.217	1.069	0.885	0.705	0.599
8.0	2.199	1.795	1.410	1.207	1.065	0.878	0.698	0.592
8.7	2.098	1.770	1.395	1.202	1.057	0.867	0.692	0.585
9.4	2.060	1.721	1.361	1.194	1.039	0.852	0.677	0.575
10.1	1.983	1.661	1.352	1.227	1.024	0.837	0.668	0.560
11.5	1.851	1.582	1.301	1.113	0.983	0.805	0.634	0.537
12.9	1.743	1.488	1.229	1.045	0.927	0.754	0.602	0.510
15.7	1.481	1.270	1.038	0.908	0.791	0.640	0.521	0.451
18.5	1.250	1.066	0.887	0.756	0.660	0.542	0.453	0.397
21.4	1.126	0.952	0.761	0.644	0.576	0.476	0.401	0.356
24.2	1.034	0.868	0.676	0.577	0.518	0.434	0.371	0.328
27.0	0.995	0.803	0.640	0.532	0.477	0.402	0.346	0.314
29.8	0.964	0.774	0.601	0.505	0.454	0.384	0.331	0.300
32.6	0.933	0.744	0.580	0.486	0.430	0.366	0.319	0.292
34.8	0.918	0.724	0.561	0.471	0.418	0.355	0.314	0.286
∞	0.676	0.560	0.471	0.401	0.366	0.318	0.295	0.274

Table 7.5-2. Stanton number (X 10^4) downstream of a sudden enlargement in a circular pipe with the point of measurement in the middle of large active zone.

CATHODE GROUP I

SOLUTION NO. 2

SCHMIDT NO. 2500

DIAMETER RATIO 2

Z \ Re	2550	3950	6550	10200	15500	25200	41000	65300
1.7	1.002	0.853	0.675	0.630	0.544	0.445	0.387	0.331
2.0	1.043	0.891	0.694	0.633	0.571	0.454	0.399	0.344
2.2	1.060	0.918	0.707	0.664	0.585	0.468	0.426	0.368
2.5	1.110	0.998	0.798	0.712	0.615	0.499	0.458	0.399
2.8	1.235	1.180	0.915	0.805	0.677	0.532	0.492	0.434
3.1	1.452	1.454	1.077	0.884	0.735	0.580	0.542	0.466
3.4	1.744	1.658	1.191	0.972	0.796	0.617	0.577	0.493
3.7	1.986	1.814	1.298	1.026	0.840	0.659	0.602	0.514
3.9	2.170	1.894	1.363	1.078	0.882	0.691	0.628	0.530
4.2	2.287	1.916	1.402	1.105	0.914	0.713	0.651	0.540
4.5	2.329	1.926	1.415	1.132	0.940	0.736	0.664	0.548
4.8	2.370	1.910	1.428	1.142	0.953	0.750	0.668	0.553
5.1	2.370	1.883	1.434	1.157	0.962	0.761	0.670	0.554
5.3	2.312	1.857	1.415	1.157	0.971	0.773	0.664	0.554
5.6	2.287	1.830	1.418	1.155	0.975	0.778	0.665	0.553
5.9	2.254	1.803	1.405	1.155	0.977	0.781	0.659	0.550
6.3	2.203	1.749	1.382	1.142	0.975	0.776	0.655	0.545
6.6	2.128	1.679	1.353	1.128	0.962	0.775	0.648	0.540
7.0	2.053	1.626	1.330	1.113	0.957	0.774	0.645	0.533
7.3	1.961	1.594	1.304	1.095	0.952	0.769	0.631	0.528
8.0	1.845	1.481	1.253	1.063	0.922	0.753	0.613	0.514
8.7	1.761	1.406	1.204	1.028	0.893	0.739	0.592	0.507
9.4	1.661	1.347	1.145	0.988	0.867	0.715	0.577	0.495
10.1	1.594	1.293	1.103	0.963	0.841	0.696	0.564	0.488
11.5	1.519	1.277	1.035	0.909	0.796	0.665	0.540	0.469
12.9	1.577	1.277	1.012	0.880	0.773	0.646	0.523	0.460
15.7	1.661	1.341	1.029	0.880	0.765	0.627	0.505	0.438
18.5	1.678	1.347	1.051	0.878	0.757	0.609	0.487	0.420
21.4	1.636	1.315	1.045	0.870	0.744	0.591	0.472	0.405
24.2	1.577	1.277	1.025	0.849	0.721	0.573	0.459	0.394
27.0	1.527	1.256	0.996	0.828	0.701	0.555	0.448	0.383
29.8	1.486	1.218	0.973	0.805	0.682	0.543	0.444	0.376
32.6	1.452	1.191	0.944	0.787	0.667	0.532	0.440	0.371
34.8	1.427	1.180	0.935	0.774	0.656	0.526	0.437	0.370
∞	1.312	1.092	0.885	0.736	0.617	0.504	0.412	0.339

Table 7.5-3. Stanton number (X 10^4) downstream of a sudden enlargement in a circular pipe with a small active zone at the point of measurement only.

CATHODE GROUP II

SOLUTION NO. 2

SCHMIDT NO. 2500

DIAMETER RATIO 2

Z \ Re →	2550	3950	6550	10200	15500	25200	41000	65300
1.7	0.584	0.553	0.480	0.449	0.415	0.352	0.324	0.285
2.0	0.601	0.585	0.480	0.462	0.421	0.356	0.336	0.298
2.2	0.626	0.585	0.477	0.466	0.430	0.369	0.352	0.315
2.5	0.668	0.612	0.493	0.474	0.449	0.381	0.372	0.339
2.8	0.776	0.762	0.545	0.526	0.475	0.407	0.400	0.366
3.1	0.901	0.934	0.649	0.562	0.518	0.433	0.429	0.389
3.4	1.093	1.100	0.733	0.637	0.563	0.463	0.463	0.412
3.7	1.277	1.223	0.818	0.683	0.600	0.496	0.480	0.430
3.9	1.419	1.309	0.886	0.732	0.632	0.525	0.506	0.446
4.2	1.502	1.341	0.915	0.772	0.664	0.549	0.525	0.459
4.5	1.536	1.358	0.954	0.797	0.695	0.569	0.540	0.468
4.8	1.611	1.363	0.983	0.812	0.717	0.587	0.551	0.477
5.1	1.611	1.374	1.003	0.839	0.742	0.607	0.563	0.483
5.3	1.636	1.368	1.019	0.861	0.751	0.615	0.568	0.486
5.6	1.628	1.363	1.025	0.861	0.759	0.631	0.569	0.489
5.9	1.636	1.358	1.029	0.874	0.772	0.638	0.573	0.492
6.3	1.619	1.336	1.035	0.882	0.780	0.649	0.573	0.492
6.6	1.594	1.298	1.035	0.886	0.787	0.653	0.573	0.491
7.0	1.569	1.288	1.029	0.889	0.796	0.660	0.569	0.487
7.3	1.511	1.261	1.025	0.891	0.794	0.661	0.568	0.486
8.0	1.444	1.229	1.012	0.878	0.789	0.663	0.560	0.483
8.7	1.394	1.180	0.996	0.866	0.779	0.659	0.550	0.476
9.4	1.344	1.138	0.970	0.849	0.765	0.652	0.535	0.471
10.1	1.285	1.084	0.935	0.839	0.754	0.637	0.524	0.460
11.5	1.152	0.993	0.896	0.787	0.713	0.606	0.497	0.440
12.9	1.060	0.901	0.834	0.745	0.669	0.567	0.465	0.414
15.7	0.876	0.740	0.701	0.628	0.564	0.482	0.394	0.361
18.5	0.718	0.617	0.574	0.522	0.467	0.397	0.333	0.309
21.4	0.643	0.547	0.493	0.443	0.396	0.344	0.293	0.2 7
24.2	0.593	0.504	0.438	0.389	0.354	0.305	0.265	0.254
27.0	0.568	0.483	0.409	0.360	0.322	0.281	0.249	0.239
29.8	0.551	0.461	0.389	0.337	0.302	0.264	0.239	0.228
32.6	0.526	0.445	0.373	0.323	0.290	0.252	0.233	0.222
34.8	0.526	0.429	0.360	0.310	0.276	0.245	0.226	0.219
∞	0.502	0.415	0.348	0.296	0.260	0.226	0.205	0.190

Table 7.5-4. Stanton number (X 10^4) downstream of a sudden enlargement in a circular pipe with the point of measurement in the middle of a large active zone.

PART III

COMPUTATIONAL ASPECTS

Chapter 8: Computational aspects

Chapter 8

Computational aspects

This chapter, to a large extent, is an appendix to chapter 3: it presents in a computer language what chapter 3 presented in a mathematical language - namely, a numerical procedure for general, steady, two-dimensional flows. But this chapter also has something more to present. It is exclusively devoted to the description of a particular Computer Programme. Because this Computer Programme deals with a particular problem, it incorporates some additional relevant information. The problem described is that of the turbulent flow in the sudden enlargement of a circular pipe. Thus, in the context of this problem, the boundary conditions of section 2.5, the turbulence model of section 4.1, and the Couette flow model of section 4.2, are also described in this chapter.

8.1 Introduction

The main purpose of this chapter is to provide a prepared foundation upon which the prospective users may assemble their super-structure to programme problems similar to the one described here. The problem described is the same as the one described in section 5.2-2: that of the turbulent flow downstream of a sudden enlargement in a circular pipe.

The notation of the Computer Programme is derived from the notations of chapter 3, which describes the numerical procedure, of chapter 4, which describes a model of turbulence and a model of the Couette-flow, and of chapter 5 which describes the problem of sudden enlargement. The important FORTRAN symbols are listed and explained in section 8.3; adequate comment-cards have been inserted in the Programme-Listing to make it self-explanatory. Similar programmes have been described in detail by Runchal and Wolfshtein (1967) and Gosman et al. (1968).

The Computer Programme is written in FORTRAN IV and has been run on the Imperial College IBM 7090, IBM 7094 II, and the University College IBM 360 computers.

8.2 A listing of the Computer Programme: 'ANSWER'

This section presents a listing of a Computer programme which, with minor changes, was used for all computations concerning the sudden-enlargement problem of section 5.2. Computer-control statements have been removed from the listing. The subroutines appear in the order of the calling statements in the main subroutine named 'ANSWER', which is the coordinating subroutine for the Programme. The listing of each individual subroutine is preceded by a brief statement about its function.

```
C*************************************************************************
C****     BLOCK DATA
C****1      SUBROUTINE FOR THE FEED-IN OF NUMERICAL DATA AND INDICES FOR
C****2      CONTROL AND EXECUTION OF THE PROGRAMME
C*************************************************************************
      BLOCK DATA
      COMMON/CNUMBR/NW,NF,NH,NK,NMU,NL,NG1,NG2,IE,IV
     2/CGRID / IN,JN,IN1,JN1,X1(41),X2(41),R(41)
     2/CPROP / ROREF,ZMUREF,CMU,CD,CDE,RKJ,PRH,SL,PR(9)
     2/CGEN  / NMAX,NPRINT,IP,CC,RSDU(9)
     2/CFLOW / RE,GM,PLEN,PRAD,JNOZ,DRATIO
     2/CWALLB/ TI,QS,TS(41),ST(41)
C****1   INDICES FOR THE DEPENDENT VARIABLES
      DATA NW,NF,NH,NK,IE/1,2,4,3,4/
C****1   DATA FOR CONTROL OF ITERATION-CYCLE
     2   ,NMAX,CC/120,.0050/     ,RSDU/9*0.0/
C****1   DATA FOR CONTROL OF PRINT-OUT ... RESULTS FROM IP SUCCESSIVE
C****2     ITERATIONS SHALL BE PRINTED OUT AFTER EVERY NPRINT ITERATIONS
     3   ,IP,NPRINT/1,100/
C****1   SPECIFICATION OF TURBULENCE-CONSTANTS
     4   ,CMU,CD,CDE,RKJ/.200,.313,.131,23.3/
C****1   DATA FOR GRID DISTRIBUTION
     5   ,IN,JN/21,15/ ,DRATIO/2.0/, PLEN/12.0/
C****1   DATA FOR FLOW PROPERTIES AND PARAMETERS
     6   ,GM,ROREF,ZMUREF/1.0,1.0,0.01/ ,RE/100000./
     7   ,PR/9*1.0/,PR(4)/0.7/,PRH/1.0/ ,TI/1.0/
      END
```

```
C*************************************************************************
C****     ANSWER
C****1      COORDINATING SUBROUTINE FOR CONTROL OF INPUT, ITERATION
C****2      PROCEDURE AND PRINT-OUT
C*************************************************************************
      DOUBLE PRECISION ANAME(6, 8),ASYMBL( 6),ASIMBL(12),ATITLE(18)
      DIMENSION A(41,41, 8)
      COMMON/CNUMBR/NW,NF,NH,NK,NMU,NL,NG1,NG2,IE,IV
     2/CGRID / IN,JN,IN1,JN1,X1(41),X2(41),R(41)
     2/CCOEFF/ CWF(41),CEF(41),CSF(41),CNF(41)
     2/CCOEFK/ BW1(41),BE1(41),BS1(41),BN1(41)
     2/CPROP / ROREF,ZMUREF,CMU,CD,CDE,RKJ,PRH,SL,PR(9)
     2/CGEN  / NMAX,NPRINT,IP,CC,RSDU(9)
     2/CFLOW / RE,GM,PLEN,PRAD,JNOZ,DRATIO
     2/CWALLA/ DP(41),TAU(41),RC(41),RK(41),QK(41),TAU2(41)
     2/CWALLB/ TI,QS,TS(41),ST(41)
C****1   ENSURE THAT THE DIMENSIONS OF THE ARRAYS A(N1,N2,N3) AND
C****2   ANAME(6,N3) CORRESPOND WITH THE FOLLOWING DATA CARD
      DATA N1,N2,N3/41,41, 8/
C****1   INDICES FOR THE STORAGE OF VARIABLES AND PROGRAMME CONTROL
      IN1=IN-1
      JN1=JN-1
```

Why should ANAME be double precision

```
      NG1=IE+1
      NG2=NG1+1
      NMU=NG2+1
      NL=NMU+1
      IV=NL
C****1   READ-IN THE TITLE OF THE PROBLEM BEING SOLVED
      READ(5,200) ATITLE
C****1   READ-IN THE ALPHAMERIC NAMES AND SYMBOLS FOR VARIABLES
      READ(5,200)ANAME,ASYMBL,ASIMBL
      WRITE (6,301) ATITLE
      WRITE(6,310) (K,(ANAME(L,K),L=1,6),K=1,IE)
      CALL        GRID
      CALL        INIT   (N1,N2,N3,A)
      WRITE(6,103) (ASYMBL(K),K=1,6 )
      NITER=0
C ***1   ITERATION LOOP BEGINS
    1 CONTINUE
      NITER=NITER+1
      CALL        EQN    (N1,N2,N3,A)
      IF((NITER+NPRINT-IP)/NPRINT.EQ.NITER/NPRINT)
     2CALL        PRINT  (N1,N2,N3,A,ANAME,IN ,JN ,1      ,IE     )
      WRITE(6,104)NITER,RE,(RSDU(K),K=1,5 )
      IF(NITER.EQ.NMAX) GO TO 8
      RES=0.
      DO 7  K=1,IE
      IF(ABS(RES).LT.ABS(RSDU(K))) RES=RSDU(K)
    7 RSDU(K)=0.
      IF(ABS(RES).GT.CC.OR.NITER.LE.5) GO TO 1
C ***1   ITERATION LOOP ENDS
      GO TO 9
    8 WRITE(6,106) NITER
    9 CONTINUE
C****    FINAL PRINT OUT OF VARIABLES IN THE FIELD
      CALL        PRINT  (N1,N2,N3,A,ANAME,IN ,JN ,I      ,IV     )
C****    CALCULATION AND PRINT-OUT OF SHEAR STRESS,STANTON NUMBER ETC.
      WRITE(6,116) (ASIMBL(I),I=1,12)
      DO 77 I=2,IN1
      TRATIO=(A(I,JN1,NH)-TS(I))/(TI-TS(I))
      ST(I)=ST(I)*RK(I)*A(I,JN1,NG1)*TRATIO/RC(I)/GM
      Z=2.*X1(I)/PRAD
      WRITE(6,117) QK(I),DP(I),TAU(I),RC(I),RK(I),ST(I),TS(I),Z,I
   77 CONTINUE
      STOP
  103 FORMAT(6H1NITER,5X,9(3X,A6,1X)//)
  104 FORMAT(1H ,I4,5X,9(1PE12.3))
  106 FORMAT (32H0THE PROCESS DID NOT CONVERGE IN,I5,13H  ITERATIONS)
  116 FORMAT(1H1,11(3X,A6,2X))
  117 FORMAT(1H0,1P 8E11.3,I5)
  200 FORMAT( 6A6)
  301 FORMAT(1H1 24X,75HFINITE-DIFFERENCE ITERATIVE SOLUTION IS UNDER CON
     2SIDERATION FOR THE CASE OF/ 25X,75H--------
     2-------                                        // 1X,19A6////
     3              46H THE DEPENDENT VARIABLES BEING CONSIDERED ARE,)
  310 FORMAT(1H0 9X,I1,3H.  ,6A6)
      END
```

```
C*****************************************************************************
C****    GRID
C****1   SUBROUTINE FOR THE CALCULATIONS REGARDING THE GRID-SYSTEM
C*****************************************************************************
      SUBROUTINE GRID
      COMMON/CNUMBR/NW,NF,NH,NK,NMU,NL,NG1,NG2,IE,IV
     2/CGRID / IN,JN,IN1,JN1,X1(41),X2(41),R(41)
     2/CCOEFF/ CWF(41),CEF(41),CSF(41),CNF(41)
     2/CCOEFK/ BW1(41),BE1(41),BS1(41),BN1(41)
     2/CPROP / ROREF,ZMUREF,CMU,CD,CDE,RKJ,PRH,SL,PR(9)
     2/CFLOW / RE,GM,PLEN,PRAD,JNOZ,DRATIO
C****1   SPECIFY THE CONSTANTS FOR GRID SPACING IN DIRECTION-1
      DATA C1,C2/0.0,1.45/
C****1   CALCULATE THE RADIUS OF THE PIPE
      PRAD=0.5*RE*ZMUREF/GM
C****1   COORDINATES FOR DIRECTION-1
      DO 10 I=1,IN
   10 X1(I)=FLOAT(I-1)/FLOAT(IN1)
      DO 12 I=1,IN
      Z=C1+C2*X1(I)
   12 X1(I)=TAN(Z)
      Z=X1(1)
      DO 13 I=1,IN
   13 X1(I)=(X1(I)-Z)/(X1(IN)-Z) *PLEN*PRAD
C****1   COORDINATES FOR DIRECTION-2
      R(1)=0.
      READ(5,107) (X2(J),J=1,JN )
      DO 15 J=2,JN
      IF(ABS(X2(J)-X2(JN)/DRATIO).LT.1.E-5) JNOZ=J
      X2(J)=X2(J)/X2(JN ) *PRAD
   15 R(J)=X2(J)
C ***1   CALCULATIONS OF GEOMETRICAL COEFFICIENTS IN LAPLACIAN TERMS
      DO 21 I=2,IN1
      DX1=2./(X1(I+1)-X1(I-1))
      CWF(I)=DX1/(X1(I)-X1(I-1))/ROREF
      CEF(I)=DX1/(X1(I+1)-X1(I))/ROREF
      BW1(I)=DX1/(X1(I)-X1(I-1))
   21 BE1(I)=DX1/(X1(I+1)-X1(I))
      DO 22 J=2,JN1
      DX2=1./(X2(J+1)-X2(J-1))
      Z2F=DX2*4.*R(J)/ROREF
      CSF(J)=Z2F/(X2(J)-X2(J-1))/(R(J-1)+R(J))
      CNF(J)=Z2F/(X2(J+1)-X2(J))/(R(J+1)+R(J))
      BS1(J)=(1.+R(J-1)/R(J))/(X2(J+1)-X2(J-1))/(X2(J)-X2(J-1))
   22 BN1(J)=(1.+R(J+1)/R(J))/(X2(J+1)-X2(J-1))/(X2(J+1)-X2(J))
      WRITE(6,101) (X1(I),I=1,IN )
      DO 33 I=1,IN
      X=X1(I)/X1(IN)
   33 WRITE(6,111)X
      WRITE(6,102) (X2(J),J=1,JN )
      DO 34 J=1,JN
      X=X2(J)/X2(JN)
   34 WRITE(6,111)X
      RETURN
  101 FORMAT(25H1DISTANCES IN DIRECTION-1/(1H 4E25.8))
  102 FORMAT(25H1DISTANCES IN DIRECTION-2/(1H 4E25.8))
  107 FORMAT(6F10.0)
  111 FORMAT(1H ,E12.4)
      END
```

```
C*************************************************************************
C****     INIT
C****1      SUBROUTINE FOR THE INITIALISATION OF THE PROGRAMME AND
C****2      SPECIFICATION OF THE FIXED BOUNDARY CONDITIONS
C*************************************************************************
      SUBROUTINE INIT   (N1,N2,N3,A)
      DIMENSION A(N1,N2,N3)
      COMMON/CNUMBR/NW,NF,NH,NK,NMU,NL,NG1,NG2,IE,IV
     2/CGRID / IN,JN,IN1,JN1,X1(41),X2(41),R(41)
     2/CPROP / ROREF,ZMUREF,CMU,CD,CDE,RKJ,PRH,SL,PR(9)
     2/CFLOW / RE,GM,PLEN,PRAD,JNOZ,DRATIO
     2/CWALLA/ DP(41),TAU(41),RC(41),RK(41),QK(41),TAU2(41)
     2/CWALLB/ TI,QS,TS(41),ST(41)
C****1   CALCULATION OF SOME TURBULENCE PARAMETERS
      PR(NK)=CMU/CDE
      PRR=PRH/PR(NH)
      SL=9.24*(PRR-1.)*(CD*CMU*PRR)**(-.25)
C****1   SET VALUES IN STORE TO ZERO
      DO 30 K=1,N3
      DO 30 J=1,JN
      DO 30 I=1,IN
30    A(I,J,K)=0.0
C****1   SET TEMPERATURE IN THE FIELD EQUAL TO INLET TEMPERATURE
      DO 10 J=1,JN
      DO 10 I=1,IN
10    A(I,J,NH)=TI
      CALL      LENGTH (N1,N2,N3,A)
C****1   BOUNDARY CONDITIONS AT INLET
      GZ=4.*GM
      I=1
      DO 20 J=1,JNOZ
      A(I,J,NG1)=GZ
      A(I,J,NF)=0.5*GZ*(R(J)*R(J) -R(JNOZ)*R(JNOZ))
      A(I,J,NK)=0.004*GZ*GZ/ROREF/ROREF
      A(I,J,NMU)=CMU*A(I,J,NL)*SQRT(A(I,J,NK))*ROREF
20    CONTINUE
C****1   BOUNDARY CONDITIONS AT THE AXIS OF SYMMETRY
      DO 40 I=1,IN
40    A(I,1,NF)=A(I,1,NF)
C****1   INITIAL CONDITIONS IN THE FIELD
      DO 60 J=1,JN1
      DO 60 I=2,IN1
      A(I,J,NW)=A(1,J,NW)
      A(I,J,NF)=A(1,J,NF)
      A(I,J,NK)=A(1,J,NK)
      A(I,J,NG1)=A(1,J,NG1)
      A(I,J,NMU)=CMU*A(I,J,NL)*SQRT(A(I,J,NK))*ROREF
60    CONTINUE
C****1   BOUNDARY CONDITIONS AT OUTLET
      Q=0.03
      RO=R(JN)
      GO=0.5*GM*(1.+Q)*(2.+Q)/RO**Q
      I=IN
      A(I,1,NG1)=GO*RO**Q
      A(I,1,NW)=A(I,1,NG1)*Q*(1.-Q)/RO/RO/ROREF
      A(I,1,NK)=0.010*GM*GM/ROREF/ROREF
      DO 70 J=2,JN1
      Y=X2(JN)-X2(J)
```

```
      A(I,J,NG1)=GO*Y**Q
      A(I,J,NW)=A(I,J,NG1)*Q/Y/ROREF/R(J)
      A(I,J,NF)=A(I,J,NG1)*Y/(1.+Q) *(Y*(1.+Q)/(2.+Q) -RO)
      A(I,J,NK)=A(I,1,NK)
70    CONTINUE
      A(I,JN,NW)=A(I,JN1,NW)
      DO 80 J=1,JN1
80    A(I,J,NMU)=CMU*A(I,J,NL)*SQRT(A(I,J,NK))*ROREF
C****1   INITIAL CONDITIONS FOR WALL SHEAR STRESSES AND TEMPERATURE
      DO 798 I=1,41
      TAU(I)=0.
      TAU2(I)=0.
798   TS(I)=0.
      RETURN
      END
```

```
C*************************************************************************
C****    LENGTH
C****1      SUBROUTINE FOR CALCULATION OF THE LENGTH SCALE OF TURBULENCE
C*************************************************************************
      SUBROUTINE LENGTH (N1,N2,N3,A)
      DIMENSION A(N1,N2,N3)
      COMMON/CNUMBR/NW,NF,NH,NK,NMU,NL,NG1,NG2,IE,IV
     2/CGRID / IN,JN,IN1,JN1,X1(41),X2(41),R(41)
     2/CFLOW / RE,GM,PLEN,PRAD,JNOZ,DRATIO
C****1   CALCULATE THE TYPICAL TURBULENCE LENGTH SCALE
      RN=PRAD/DRATIO
      XL1=5.50*RN
      XL2=16.0*RN
      ZLMAX=RN
      DO 10 J=1,JN
      DO 10 I=1,IN
      A(I,J,NL)=(X2(JN)-X2(J))
      IF(X1(I).LT.A(I,J,NL).AND.J.GE.JNOZ) A(I,J,NL)=X1(I)
      IF(X2(J).GT.RN*1.9) GO TO 9
      XI=0.
      IF(X1(I).LT.XL2) XI=RN*(1.-X1(I)/XL2)
      IF(X2(J)-XI) 1,2,2
1     A(I,J,NL)=0.10*RN
      GO TO 11
2     ZL=0.090*X1(I)
      IF(X1(I).GT.XL1) ZL=.090*XL1 + .180*(X1(I)-XL1)
      IF(ZL.GT.ZLMAX) ZL=ZLMAX
      A(I,J,NL)=2.*A(I,J,NL)
      IF(A(I,J,NL).GT.ZL) A(I,J,NL)=ZL
      IF(X1(I).LE.8.*RN) A(I,J,NL)=ZL
      IF(A(I,J,NL).LT.A(I+1,NL)) A(I,J,NL)=A(I+1,NL)
      GO TO 11
9     CONTINUE
      A(I,J,NL)=2.*A(I,J,NL)
11    CONTINUE
10    CONTINUE
      RETURN
      END
```

```
C*****************************************************************************
C****    EQN
C****1   SUBROUTINE FOR SOLUTION OF THE DIFFERENCE EQUATIONS
C*****************************************************************************
      SUBROUTINE EQN      (N1,N2,N3,A)
      DIMENSION A(N1,N2,N3)
      COMMON/CNUMBR/NW,NF,NH,NK,NMU,NL,NG1,NG2,IE,IV
     2/CGRID / IN,JN,IN1,JN1,X1(41),X2(41),R(41)
     2/CCOEFF/ CWF(41),CEF(41),CSF(41),CNF(41)
     2/CPROP / ROREF,ZMUREF,CMU,CD,CDE,RKJ,PRH,SL,PR(9)
     2/CGEN  / NMAX,NPRINT,IP,CC,RSDU(9)
C****
C****1   CALCULATION OF STREAM-FUNCTION
C****
      DO 52 J=2,JN1
      DO 52 I=3,IN1
      Z=A(I,J,NF)
      SIGMA=CWF(I)+CEF(I)+CSF(J)+CNF(J)
      IF(SIGMA.EQ.0.) SIGMA=.00001
      A(I,J,NF)=(A(I-1,J,NF)*CWF(I)+A(I+1,J,NF)*CEF(I)
     2          +A(I,J-1,NF)*CSF(J)+A(I,J+1,NF)*CNF(J)
     3          +A(I,J,NW)*R(J)*R(J))/SIGMA
      IF(A(I,J,NF).EQ.0.) A(I,J,NF)=.00001
      RS=1.-Z/A(I,J,NF)
52    IF(ABS(RS).GT.ABS(RSDU(NF)))RSDU(NF)=RS
C****
C****1   CALCULATION OF MASS-VELOCITIES
C****
      DO 50 J=2,JN1
      H2=(X2(J)-X2(J-1))/(X2(J+1)-X2(J))
      RX2=R(J)*(X2(J+1)-X2(J-1))
      DO 50 I=2,IN1
      H1=(X1(I-1)-X1(I))/(X1(I+1)-X1(I))
      RX1=R(J)*(X1(I+1)-X1(I-1))
      A(I,J,NG1)=(A(I,J+1,NF)-A(I,J,NF))*H2+(A(I,J,NF)-A(I,J-1,NF))/H2
      A(I,J,NG1)=A(I,J,NG1)/RX2
      A(I,J,NG2)=(A(I+1,J,NF)-A(I,J,NF))*H1+(A(I,J,NF)-A(I-1,J,NF))/H1
50    A(I,J,NG2)=A(I,J,NG2)/RX1
      DELR=R(2)-R(1)
      DO 20 I=2,IN
20    A(I,1,NG1)=2.*(A(I,2,NF)-A(I,1,NF))/DELR/DELR
C****
C****1   CALCULATION OF VORTICITY
C****
      JN2=JN-2
      DO 51 J=2,JN2
      DO 51 I=3,IN1
      Z=A(I,J,NW)
      CALL        EQVORT (N1,N2,N3,A,I,J)
      IF(A(I,J,NW).EQ.0.) A(I,J,NW)=.00001
      RS=1.-Z/A(I,J,NW)
51    IF(ABS(RS).GT.ABS(RSDU(NW)))RSDU(NW)=RS
C****
C****1   CALCULATION OF OTHER VARIABLES
C****
      IF(IE.LE.2) GO TO 72
      DO 71 K=3,IE
      DO 53 J=2,JN1
```

```
      DO 53 I=2,IN1
      Z=A(I,J,K )
      CALL        EQPHI  (N1,N2,N3,A,I,J, K)
      IF(A(I,J, K).EQ.0.) A(I,J, K)=.00001
      RS=1.-Z/A(I,J,K )
53    IF(ABS(RS).GT.ABS(RSDU(K ) ))RSDU(K )=RS
71    CONTINUE
72    CONTINUE
C****
C****1    CALCULATION OF EFFECTIVE VISCOSITY
C****
      DO 60 J=1,JN1
      DO 60 I=2,IN1
60    A(I,J,NMU)=CMU*A(I,J,NL)*SQRT(A(I,J,NK))*ROREF
      CALL        BOUND    (N1,N2,N3,A)
      RETURN
      END
```

```
C*************************************************************************
C****     EQVORT
C****1       SUBROUTINE FOR THE SOLUTION OF THE VORTICITY EQUATION
C*************************************************************************
      SUBROUTINE EQVORT (N1,N2,N3,A,I,J)
      DIMENSION A(N1,N2,N3)
      COMMON/CNUMBR/NW,NF,NH,NK,NMU,NL,NG1,NG2,IE,IV
     2/CGRID / IN,JN,IN1,JN1,X1(41),X2(41),R(41)
     2/CCOEFK/ BW1(41),BE1(41),BS1(41),BN1(41)
      DV=R(J)*(X1(I+1)-X1(I-1))*(X2(J+1)-X2(J-1))*2.
      G1PW= A(I,J+1,NF)-A(I,J-1,NF)+A(I-1,J+1,NF)-A(I-1,J-1,NF)
      G1PE= A(I,J+1,NF)-A(I,J-1,NF)+A(I+1,J+1,NF)-A(I+1,J-1,NF)
      G2PS= A(I-1,J,NF)-A(I+I,J,NF)+A(I-1,J-1,NF)-A(I+1,J-1,NF)
      G2PN= A(I-1,J,NF)-A(I+1,J,NF)+A(I-1,J+1,NF)-A(I+1,J+1,NF)
      AW=(ABS(G1PW)+G1PW)/DV
      AE=(ABS(G1PE)-G1PE)/DV
      AS=(ABS(G2PS)+G2PS)/DV
      AN=(ABS(G2PN)-G2PN)/DV
      RSQ=R(J)*R(J)
      BS=BS1(J)*R(J-1)*R(J-1)/RSQ
      BN=BN1(J)*R(J+1)*R(J+1)/RSQ
      CW=AW +BW1(I)*A(I-1,J,NMU)
      CE=AE +BE1(I)*A(I+1,J,NMU)
      CS=AS +BS    *A(I,J-1,NMU)
      CN=AN +BN    *A(I,J+1,NMU)
      SIGMA=AW+AE+AS+AN +(BW1(I)+BE1(I)+BS+BN)*A(I,J,NMU)
      IF(SIGMA.EQ.0.) RETURN
      A(I,J,NW)=(A(I-1,J,NW)*CW +A(I+1,J,NW)*CE
     2          +A(I,J-1,NW)*CS +A(I,J+1,NW)*CN)/SIGMA
      RETURN
      END
```

```
C*****************************************************************************
C****    EQPHI
C****1     SUBROUTINE FOR SOLUTION OF 'OTHER VARIABLES(PHI)' EQUATION
C*****************************************************************************
      SUBROUTINE EQPHI  (N1,N2,N3,A,I,J, K)
      DIMENSION A(N1,N2,N3)
      COMMON/CNUMBR/NW,NF,NH,NK,NMU,NL,NG1,NG2,IE,IV
     2/CGRID / IN,JN,IN1,JN1,X1(41),X2(41),R(41)
     2/CCOEFK/ BW1(41),BE1(41),BS1(41),BN1(41)
     2/CPROP / ROREF,ZMUREF,CMU,CD,CDE,RKJ,PRH,SL,PR(9)
      IF(K.NE.NK) GO TO 2
C****1    SOURCE TERMS FOR KINETIC ENERGY OF TURBULENCE
      DX1=X1(I+1)-X1(I-1)
      DX2=X2(J+1)-X2(J-1)
      ROR=ROREF*R(J)
      DF=A(I+1,J+1,NF)-A(I+1,J-1,NF)-A(I-1,J+1,NF)+A(I-1,J-1,NF)
      DG1X=DF/DX1/DX2
      Z=(A(I,J+1,NF)-A(I,J,NF))/(X2(J+1)-X2(J))
      DG1R=2.*(Z-(A(I,J,NF)-A(I,J-1,NF))/(X2(J)-X2(J-1)))/DX2-A(I,J,NG1)
      Z=(A(I,J,NF)-A(I-1,J,NF))/(X1(I)-X1(I-1))
      DG2X=2.*(Z-(A(I+1,J,NF)-A(I,J,NF))/(X1(I+1)-X1(I)))/DX1
      DG2R=-DG1X-A(I,J,NG2)
      DG=DG1R+DG2X
      SOURCE=(2.*(DG1X*DG1X+DG2R*DG2R)+DG*DG)*A(I,J,NMU)/ROR/ROR
      ZQ=CD*SQRT(A(I,J,NK))/A(I,J,NL)*ROREF
C****
C****1    THE DIFFERENCE EQUATION FOR 'PHI'
C****
1     CONTINUE
      DV=R(J)*(X1(I+1)-X1(I-1))*(X2(J+1)-X2(J-1))*2.
      G1PW= A(I,J+1,NF)-A(I,J-1,NF)+A(I-1,J+1,NF)-A(I-1,J-1,NF)
      G1PE= A(I,J+1,NF)-A(I,J-1,NF)+A(I+1,J+1,NF)-A(I+1,J-1,NF)
      G2PS= A(I-1,J,NF)-A(I+1,J,NF)+A(I-1,J-1,NF)-A(I+1,J-1,NF)
      G2PN= A(I-1,J,NF)-A(I+1,J,NF)+A(I-1,J+1,NF)-A(I+1,J+1,NF)
      AW=(ABS(G1PW)+G1PW)/DV
      AE=(ABS(G1PE)-G1PE)/DV
      AS=(ABS(G2PS)+G2PS)/DV
      AN=(ABS(G2PN)-G2PN)/DV
      CW=AW +BW1(I)*(A(I-1,J,NMU)+A(I,J,NMU))*.5/PR(K)
      CE=AE +BE1(I)*(A(I+1,J,NMU)+A(I,J,NMU))*.5/PR(K)
      CS=AS +BS1(J)*(A(I,J-1,NMU)+A(I,J,NMU))*.5/PR(K)
      CN=AN +BN1(J)*(A(I,J+1,NMU)+A(I,J,NMU))*.5/PR(K)
      SIGMA=CW+CE+CN+CS+ZQ
      IF(SIGMA.EQ.0.) RETURN
      A(I,J, K)=(A(I-1,J, K)*CW +A(I+1,J, K)*CE
     2          +A(I,J-1, K)*CS +A(I,J+1, K)*CN +SOURCE)/SIGMA
      IF(A(I,J,K).LT.0.) A(I,J,K)=0.
      RETURN
2     SOURCE=0.
      ZQ=0.
      GO TO 1
      END
```

```
C*****************************************************************************
C****    BOUND
C****1     SUBROUTINE FOR CALCULATION OF VARIABLE BOUNDARY CONDITIONS
C*****************************************************************************
      SUBROUTINE BOUND   (N1,N2,N3,A)
      DIMENSION A(N1,N2,N3)
      COMMON/CNUMBR/NW,NF,NH,NK,NMU,NL,NG1,NG2,IE,IV
     2/CGRID / IN,JN,IN1,JN1,X1(41),X2(41),R(41)
     2/CCOEFF/ CWF(41),CEF(41),CSF(41),CNF(41)
     2/CPROP / ROREF,ZMUREF,CMU,CD,CDE,RKJ,PRH,SL,PR(9)
     2/CFLOW / RE,GM,PLEN,PRAD,JNOZ,DRATIO
     2/CWALLA/ DP(41),TAU(41),RC(41),RK(41),QK(41),TAU2(41)
     2/CWALLB/ TI,QS,TS(41),ST(41)
C****
C****1   INLET BOUNDARY
C****
      I=2
C****    NOZZLE REGION ONLY
      JNOZM1=JNOZ-1
      DO 1  J=2,JNOZM1
      CALL        EQVORT (N1,N2,N3,A,I,J)
1     CALL        EQSTRM (N1,N2,N3,A,I,J)
C****    FOR THE NODE AGAINST THE NOZZLE
      J=JNOZ
      A1   =(CWF(I)+CEF(I)+CSF(J)+CNF(J))*A(I,J,NF)
      A2         =(A(I-1,J,NF)*CWF(I)+A(I+1,J,NF)*CEF(I)
     2          +A(I,J-1,NF)*CSF(J)+A(I,J+1,NF)*CNF(J))
      A(I,J,NW)=(A1-A2)/R(J)/R(J)
C****    STEP-WALL REGION
      JNOZP1=JNOZ+1
      YC=X1(I)
      DX1=X1(I+1)-X1(I-1)
      DO 11 J=JNOZP1,JN1
      DTAU=A(I+1,J,NMU)*A(I+1,J,NW)*R(J)-TAU2(J)
      DPDX=DTAU/DX1
      SQRTK=SQRT(A(I,J,NK))
      RKZ=ROREF*YC*SQRTK/ZMUREF
      PST=DPDX*YC/SQRTK/A(I,J,NG2)
      Z=A(I,J,NW)*YC*R(J)
      ZST=CMU*Z*Z/A(I,J,NK)
      CALL        WALL    (NH,ZST,PST,RKZ,QKZ,SSRK,SHRK)
      TAU2(J)=SSRK*A(I,J,NG2)*SQRTK
      A(I,J,NW)=(DPDX*YC+TAU2(J))/A(I,J,NMU)/R(J)
      A(1,J ,NK)=(1.-QKZ)*A(I,J,NK)
      A(1,J ,NMU)=-.5*QKZ*A(I,J,NMU)
      A(1,J,NH)=A(2,J,NH)
11    CALL        EQSTRM (N1,N2,N3,A,I,J)
C****
C****1   AXIS OF SYMMETRY
C****
      DO 51 I=1,IN
      A(I,1,NW)=2.*(A(I,1,NG1)-A(I,2,NG1))/R(2)/R(2)
      IF(A(I,1,NW).LT.0.) A(I,1,NW)=0.
      A(I,1,NK)=A(I,2,NK)
      A(I,1,NH)=A(I,2,NH)
51    CONTINUE
```

```
C****
C****1    OUTLET BOUNDARY
C****
      DO 71 J=2,JN1
71    A(IN,J,NH)=A(IN1,J,NH)
C****
C****1    WALL OF THE PIPE
C****
      J=JN1
      YC=X2(JN)-X2(JN1)
      DX2=X2(J+1)-X2(J-1)
      DO 31 I=2,IN1
      DTAU=(R(J+1)*TAU(I)+R(J-1)*A(I,J-1,NMU)*A(I,J-1,NW)*R(J-1))/R(J)
      DP(I)=DTAU/DX2
      SQRTK=SQRT(A(I,J,NK))
      RK(I)=ROREF*YC*SQRTK/ZMUREF
      PST=DP(I)*YC/SQRTK/A(I,J,NG1)
      Z=A(I,J,NW)*YC*R(J)
      ZST=CMU*Z*Z/A(I,J,NK)
      CALL          WALL    (NH,ZST,PST,RK(I),QK(I),SSRK,SHRK)
      TAU(I)=-SSRK*A(I,J,NG1)*SQRTK
      A(I,J,NW)=(DP(I)*YC-TAU(I))/A(I,J,NMU)/R(J)
      A(I,JN,NK)=(1.-QK(I))*A(I,J,NK)
      A(I,JN,NMU)=-.5*QK(I)*A(I,J,NMU)
      A(I,JN,NH)=(1.-PR(NH)*SHRK/CMU)*(A(I,J,NH)-TS(I)) +TS(I)
      RC(I)=A(I,J,NG1)*YC/ZMUREF
      ST(I)=SHRK
31    CONTINUE
      RETURN
      END
```

```
C*************************************************************************
C****     EQSTRM
C****1      SUBROUTINE FOR STREAM-FUNCTION EQUATION
C*************************************************************************
      SUBROUTINE EQSTRM (N1,N2,N3,A,I,J)
      DIMENSION A(N1,N2,N3)
      COMMON/CNUMBR/NW,NF,NH,NK,NMU,NL,NG1,NG2,IE,IV
     2/CGRID / IN,JN,IN1,JN1,X1(41),X2(41),R(41)
     2/CCOEFF/ CWF(41),CEF(41),CSF(41),CNF(41)
      SIGMA=CWF(I)+CEF(I)+CSF(J)+CNF(J)
      IF(SIGMA.EQ.0.) SIGMA=.00001
      A(I,J,NF)=(A(I-1,J,NF)*CWF(I)+A(I+1,J,NF)*CEF(I)
     2          +A(I,J-1,NF)*CSF(J)+A(I,J+1,NF)*CNF(J)
     3          +A(I,J,NW)*R(J)*R(J))/SIGMA
      RETURN
      END
```

```
C*************************************************************************
C****    WALL
C****1      SUBROUTINE FOR COUETTE-FLOW CALCULATIONS NEAR A WALL
C*************************************************************************
      SUBROUTINE WALL    (NH,ZST,PST,RK,QK,SSRK,SHRK)
      COMMON
     2/CPROP / ROREF,ZMUREF,CMU,CD,CDE,RKJ,PRH,SL,PR(9)
C****1   EXAMINE IF FLOW IS FULLY TURBULENT
      IF(RK.LT.RKJ) GO TO 17
C****
C****1    FOR FULLY TURBULENT FLOW
C****
      RKJST=RKJ/RK
      ZCD=CD-ZST
      IF(ZCD)11,12,12
11    QK=0.
      GO TO 13
12    QK=SQRT (2.*ZCD/3./CDE)
13    Z=RKJST**(-QK/(2.+QK))
      IF(QK) 1,1,2
1     ZI1=RKJ-ALOG(RKJST)/CMU
      GO TO 3
2     Z1=2./CMU/QK
      Z2=RKJ+Z1
      ZI1=Z*Z2-Z1
3     CONTINUE
5     Z1=2./CMU/(2.-QK)
      ZI2=(RKJ/2.-Z1)*RKJST**((2.-QK)/(2.+QK)) +Z1
6     SSRK=(1.-PST*ZI2)/ZI1
      IF(SSRK.LT.0.) SSRK=0.
      ZI3=PR(NH)*(ZI1 +SL*Z)
      SHRK =1./ZI3
      RETURN
C****
C****1    FOR LAMINAR FLOW
C****
17    CONTINUE
      QK=1.000
      SSRK=1./RK -PST
      IF(SSRK.LT.0.) SSRK=0.
      SHRK=1./RK/PRH
      RETURN
      END
```

```
C*************************************************************************
C****    PRINT
C****1      SUBROUTINE FOR PRINT-OUT OF VARIABLES IN THE FIELD
C*************************************************************************
      SUBROUTINE PRINT  (N1,N2,N3,A,ANAME,IN,JN,NBEGIN,NTOTAL)
      DOUBLE PRECISION ANAME(6,N3)
      DIMENSION A(N1,N2,N3)
C****1   PRINT-OUT SHALL BE PRODUCED FOR A(I,J,K),WHERE
C****2   I VARIES FROM 1 TO IN, J VARIES FROM 1 TO JN, AND
C****3   K VARIES FROM NBEGIN TO NTOTAL
```

```
      K=NBEGIN
      DO 10 M=1,NTOTAL
      WRITE(6,100) (ANAME(L,K),L=1,6)
      IA=IN/11
      DO 12 IB=1,IA
      IC=(IB-1)*11 +1
      ID=IB*11
      WRITE(6,101) (J,(A(I,J,K),I=IC,ID),J=1,JN)
      WRITE(6,103) (I,I=IC,ID)
      IF(ID.EQ.IN) GO TO 11
12    WRITE(6,104)
      IE=ID+1
      WRITE(6,111) (J,(A(I,J,K),I=IE,IN),J=1,JN)
      WRITE(6,113)(I,I=IE,IN)
11    CONTINUE
      K=K+1
10    CONTINUE
100   FORMAT(1H130X,21HTHE DISTRIBUTION OF ,6A6/
     231X,57H---------                                                //
     33HO J/4H ---//)
101   FORMAT(1H I2,5X,1P11E11.3)
103   FORMAT(1HO,3X,11(9X,I2))
104   FORMAT(1H155X,17HC O N T I N U E D//)
111   FORMAT(1H I2,5X,1P10E11.3)
113   FORMAT(1HO,3X,10(9X,I2))
      RETURN
      END
```

```
C*****************************************************************
C****1      DATA FOR THE PROGRAMME
C****2      FIRST 3 CARDS FOR ARRAY ATITLE, NEXT 8 CARDS FOR ARRAY ANAME,
C****3      NEXT CARD FOR ARRAY ASYMBL, NEXT 2 CARDS FOR ARRAY ASIMBL,
C****4      AND LAST 3 CARDS FOR ARRAY X2
C*****************************************************************
SUDDEN ENLARGEMENT IN A PIPE  ***
RUN NO. 999 - TEST CASE FOR LISTING
****   A.K.RUNCHAL  **** DATE 690128
VORTICITY COMPONENT
STREAM FUNCTION
TURBULENT KINETIC ENERGY
MASS CONCENTRATION
DIR.-1 MASS VELOCITY
DIR.-2 MASS VELOCITY
EFFECTIVE VISCOSITY
TYPICAL LENGTH SCALE
 RE  RSVORTRSSTRMRSKINE
  QK    DPDX  TAUS    RC      RK      ST
  TS      Z       I
 .000      0.125      0.250      0.375      0.500      0.625
 .750      0.825      0.870      0.910      0.940      0.962
 .978      0.990      1.000
C*****************************************************************
C****1      END
C*****************************************************************
```

8.3 FORTRAN IV symbols

FORTRAN symbol	Meaning	Subroutine/s of mention
A(I,J,K)	an array containing all the variables (Ø's, G_1, G_2, 1 and μ_{eff}) which require storage over the field of computations. I and J refer to the locations in directions 1 and 2 respectively, and K refers to the name of the variable.	All Subroutines except BLOCK DATA and WALL
AW,AE, AS,AN	A_W/V_P, etc. of equation (3.2-26)	EQPHI, EQVORT
BW1(I),BE1(I), BS1(J),BN1(J)	$2.B_W/(\beta_P.V_P.(\Gamma_W+\Gamma_P))$ etc. of equation (3.2-27)	GRID,EQPHI, EQVORT
CC	λ_{ref} of equation (3.3-7)	ANSWER, BLOCK DATA
CD	C_D of equation (4.1-7)	BLOCK DATA, EQPHI,INIT WALL
CDE	$C_{\mathcal{D}}$ of equation (4.1-5)	BLOCK DATA, INIT,WALL
CMU	C_μ of equation (4.1-6)	BLOCK DATA, BOUND,EQN, INIT,WALL
CW,CE, CS,CN	$C_W.\Sigma_{AB}$, etc. of equation (3.2-25)	EQPHI,EQVORT
CWF(I),CEF(I), CSF(J),CNF(J)	$C_W.\Sigma_{AB}$, etc. of equation (3.2-25) for the stream-function	BOUND,EQN, EQSTRM,GRID
DP(I)	dp/dx_1 of equation (4.2-4)	ANSWER,BOUND
DRATIO	the diameter ratio in the sudden-enlargement problem	BLOCK DATA, GRID,INIT

FORTRAN symbol	Meaning	Subroutine/s of mention
DV	V_p of equation (3.2-25)	EQPHI,EQVORT
GM	G_m of equation (5.2-2)	ANSWER,BLOCK DATA GRID, INIT
GZ	G_z of equation (5.2-2)	INIT
GO	G_O of equation (5.2-9)	INIT
I	the subscript referring to the location of the corresponding variable in direction-1	All subroutines except BLOCK DATA and WALL
IE	the total number of elliptic differential equations, of the type of equation (2.4-2), to be solved	ANSWER, BLOCK DATA EQN
IN	the total number of grid lines in direction-1	ANSWER,BLOCK DATA BOUND, EQN, GRID,INIT, LENGTH,PRINT
IN1	IN-1	same as IN
IP	an index for control of print-out	ANSWER, BLOCK DATA
IV	an index for control of print-out	ANSWER
J	the subscript referring to the location of the corresponding variable in direction-2	same as for I
JN	the total number of grid lines in direction-2	same as for IN
JN1	JN-1	same as for IN
JNOZ	the value of J at the point of enlargement of the pipe	BOUND,GRID,INIT

FORTRAN symbol	Meaning	Subroutine/s of mention
K	the subscript referring to any of the variables in A(I,J,K)	ANSWER,EQN, EQPHI
NF	the index number for the stream-function, ψ	BLOCK DATA,BOUND, EQN,EQPHI,EQSTRM, EQVORT,INIT
NG1	the index number for the mass-velocity in direction-1, G_1	ANSWER,BOUND,EQN, EQPHI,INIT
NG2	the index number for the mass-velocity in direction-2, G_2	ANSWER,BOUND, EQN,EQPHI
NH	the index number for the temperature, T	ANSWER, BLOCK DATA BOUND, INIT, WALL
NITER	the running number of iterations	ANSWER
NK	the index number for the kinetic energy of turbulence	BLOCK DATA,BOUND, EQN,EQPHI,INIT
NL	the index number for the length scale of turbulence	ANSWER,EQN, INIT,LENGTH
NMAX	the maximum permissible number of iterations	ANSWER, BLOCK DATA
NMU	the index number for the effective viscosity, μ_{eff}	ANSWER,BOUND,EQN, EQPHI,EQVORT,INIT
NPRINT	an index number for control of print-out	ANSWER,BLOCK DATA
NW	the index number for the vorticity, ω/r	BLOCK DATA,BOUND, EQN,EQSTRM, EQVORT,INIT
P	P_* of equation (4.2-3)	BOUND,WALL

NA, NZ NB

FORTRAN symbol	Meaning	Subroutine/s of mention
PLEN	the control-volume length of the pipe in terms of R	BLOCK DATA,GRID
PR(K)	$\sigma_{\phi,eff}$ of equation (2.2-3)	BLOCK DATA,EQPHI, INIT,WALL
PRAD	R of equation (5.2-1)	ANSWER,GRID, LENGTH
PRH	σ_T of equation (5.2-1)	BLOCK DATA, INIT,WALL
PST	p_* of equation (4.2-4)	BOUND,WALL
Q	q of equation (5.2-9)	INIT
QK(I)	q of equation (5.2-1)	ANSWER,BOUND, WALL
QS	$\dot{q}''_S$ of equation (5.2-1)	INIT
R(J)	r of equation (2.1-1)	BOUND,EQN,EQPHI, EQSTRM,EQVORT, GRID,INIT
RC(I)	Re of equation (4.2-5)	ANSWER,BOUND
RE	Re of equation (5.2-1)	ANSWER,BLOCK DATA GRID
RK(I)	R_t of equation (4.2-5)	ANSWER,BOUND, WALL
RKJ	$R_{t,J}$ of equation (4.2-8)	BLOCK DATA,WALL
RKJST	R_{t*} of equation (4.2-8)	WALL
ROREF	ρ, the reference mass-density	BLOCK DATA,BOUND, EQN,EQPHI,INIT
RSDU(K)	λ of equation (3.3-7)	ANSWER, BLOCK DATA EQN
SIGMA	Σ_{AB} of equation (3.2-25)	EQN,EQPHI, EQSTRM,EQVORT
SL	I_1 of equation(4.2-19)	INIT,WALL
SHRK	St.Re/R_t of equation (4.2-5)	BOUND,WALL

FORTRAN symbol	Meaning	Subroutine/s of mention
SOURCE	$S_{\emptyset,P}$ of equation (3.2-23)	EQPHI
SSRK	$s.Re/R_t$ of equation (4.2-5)	BOUND,WALL
ST(I)	St of equation (5.2-1)	ANSWER
TAU(I)	τ_S of equation (4.2-5) for direction-1	ANSWER, BOUND, INIT
TAU2(J)	τ_S of equation (4.2-5) for direction-2	ANSWER, BOUND, INIT
TI	T_I of equation (5.2-4)	INIT
TS(I)	T_S of equation (5.2-1)	ANSWER, BOUND, INIT
X1(I)	x_1 of equation (2.1-1);the direction-1 coordinate	ANSWER,BOUND,EQN, EQPHI,EQVORT, GRID,LENGTH
X2(J)	x_2 of equation(2.1-1);the direction-2 coordinate	BOUND,EQN,EQPHI, EQVORT,GRID, INIT,LENGTH
Z	Z of equation (5.2-1)	ANSWER
ZI1	I_1 of equation (4.2-12)	WALL
ZI2	I_2 of equation (4.2-12)	WALL
ZI3	I_3 of equation (4.2-17)	WALL
ZMUREF	μ, the reference molecular viscosity	BLOCK DATA, BOUND,GRID

References

1. ABBOTT, D.E. and KLINE, S.J. (1962) "Experimental investigation of subsonic turbulent flow over single and double backward facing steps". ASME, J. Basic Engg. 84, 3, 317-325.

2. ABRAMOVICH, G.N. (1963) The Theory of Turbulent Jets. M.I.T. Press, Cambridge, Mass.

3. ALLEN, D.N. De G. and SOUTHWELL, R.V. (1955) "Relaxation methods applied to determine the motion, in two-dimensions, of a viscous fluid past a fixed cylinder". Quart. J. Mech. Appl. Math., 8, 2, 129-145.

4. AMES, W.F. (1967) Nonlinear Partial Differential Equations. Academic Press, London.

5. AZIZ, K. and HELLUMS, J.D. (1967) "Numerical solution of the three-dimensional equations of motion - convection in fluids heated from below". Physics of Fluids, 10, 2, 314-324.

6. BARAKAT, H.Z. and CLARK, J.A. (1965) "Transient natural convection in flows in closed containers". Univ. of Michigan, Mech. Eng. Dept., Heat Transfer Lab., Tech. Rep. No. 2.

7. BATCHELOR, G.K. (1956) "On steady laminar flow with closed stream-lines at large Reynolds numbers". J. Fluid Mech., 1, 2, 177-190.

8. BIRD, R.B., STEWART, W.E. and LIGHTFOOT, E.N. (1960) Transport Phenomena, John Wiley, New York.

9. BLAIR, A., METROPOLIS, N., TAUB, A.H. and TSINGOU, M. (1957) "A study of a numerical solution to a two-dimensional hydrodynamic problem". Physics & Maths, LA-2165 (TID-4500, 13th Ed. Rev.).

10. BOELTER, L.M.K., YOUNG, G. and IVERSON, H.W. (1948) "An investigation of aircraft heaters XXVII - Distribution of heat transfer rate in the entrance region of a circular tube". NACA TN 1451.

11. BOUSSINESQ, T.V. (1877) Mem. pres. Acad. Sci. Third Edition, Paris XXIII, 46.

12. BRAMBLE, J.H. (1966) Numerical Solution of Partial Differential Equations. Academic Press, London.

13. BURGGRAF, O.R. (1966) "Analytical and numerical studies of steady separated flows". J. Fluid Mech., 24, 1, 113-151.

14. CARLSON, W.O. (1959) "Heat transfer in laminar separated and wake flow regions". Proc. Heat Trans. Fluid Mech. I st., Stanford Univ. Press, 140-155.

15. CHAPMAN, D.R. (1956) "A theoretical analysis of heat transfer in regions of separated flow". NACA TN 3792.

16. CHARWAT, A.F., DEWEY, F.C. Jr., ROOS, J.N. and HITZ, J.A. (1961) "An investigation of separated flows - Part I - The pressure field". J. Aero/Space Sci., 28, 6, 457-470. See also "Part II - Flow in a cavity and Heat transfer". J. Aero/Space Sci., 28, 7, 513-527.

17. CHILCOTT, R.E. (1967) "A review of separated and reattaching flows with heat transfer". Int. J. Heat Mass Transfer, 10, 6, 783-798.

18. CHORIN, A.J. (1967) "The numerical solution of the Navier-Stokes equations for an incompressible fluid". Bull. Am. Math. Soc., 73, 6, 928-931.

19. COURANT, R., ISAACSON, E. and REES, M. (1952). "On the solution of non-linear hyperbolic differential equations by finite-differences". Comm. Pure Appl. Math., 5, 243-255.

20. DIESSLER, R.G. (1955) "Analysis of turbulent heat transfer, mass transfer, and friction in smooth tubes at high Prandtl and Schmidt numbers". NACA Rep. 1210.

21. DUFFIELD, P.L. (1966) "Diffusion-controlled electrolysis at a porous electrode, with gas injection". Ph.D. Thesis, Univ. of London.

22. EDE, A.J., HISLOP, C.I. and MORRIS, R. (1956). "Effect on the local heat transfer coefficient in a pipe of an abrupt disturbance of the fluid flow: abrupt convergence and divergence of diameter ratio 2/1". Proc. Inst. Mech. Engr., 170, 38.

23. EDE, A.J., MORRIS, R. and BIRCH, E.S. (1962) "The effect of abrupt changes of diameter on heat transfer in pipes". NEL Rep. 73.

24. EMMONS, H.W. (1954) "Shear flow turbulence". Proc. 2nd U.S. National Congress. Appl. Mech. ASME, 1.

25. FILETTI, E.G. and KAYS, W.M. (1967) "Heat transfer in separated, reattached and redevelopment regions behind a double step at the entrance to a flat duct" ASME J. Heat Transfer, 89, 2, 163-168.

26. FORSTALL, W. and SHAPIRO, A.H. (1950) "Momentum and mass transfer in coaxial gas jets". J. Appl. Mech. 17, 4, 399-.

27. FORSYTHE, G.E. and WASOW, W.R. (1960) Finite-Difference Methods for Partial Differential Equations John Wiley, New York.

28. FROMM, J.E. and HARLOW, F.H. (1963) "Numerical solutions of the problem of vortex street development" Physics of Fluids, 6, 7, 975-982.

29. GLUSHKO, G.S. (1965) "Turbulent boundary layer on a flat plate in an incompressible fluid". Izv. Akad. Nauk SSSR, Mech. No. 4, 13-. (In Russian).

30. GOSMAN, A.D. (1969) Personal communications. To be published as "Diffusion-controlled electrolysis in two-phase flows" for a Ph.D. Thesis, Univ. of London (1969).

31. GOSMAN, A.D., PUN, W.M., RUNCHAL, A.K., SPALDING, D.B. and WOLFSHTEIN, M. (1968) "Heat and mass transfer in recirculating flows". Imperial College, Mech. Eng. Dept. SF/R/3.

32. GREENSPAN, D. (1967) "Numerical studies of two dimensional steady state Navier-Stokes equations for arbitrary Reynolds numbers". Univ. of Wisconsin, Tech. Rep. No. 9 of the Dept. of Computer Sci.

33. HANSON, F. B. and RICHARDSON, P.D. (1964) "Mechanics of turbulent spearated flows as indicated by heat transfer: A review". Symp. on Fully Separated Flows, ASME, 27-32.

34. HANSON, F.B. and RICHARDSON, P.D. (1968) "The near-wake of a circular cylinder in cross-flow". Fluids Engg. Conference. ASME, Philadelphia, Pa., No. 68-FE-5.

35. HARLOW, F.H. and NAKAYAMA, P.I. (1967) "Turbulence transport equations". Physics of Fluids, 10, 11, 2323-2332.

36. HARLOW, F.H. and WELCH, J.E. (1965) "Numerical calculation of time-dependent viscous incompressible flow of fluid with free surface". Physics of Fluids, 8, 12, 2182-2189.

37. HINZE, J. O. (1959) Turbulence. McGraw-Hill, New York.

38. JAYATILLAKA, C.L.V. (1966) "The influence of Prandtl number and surface roughness on the resistance of the laminar sub-layer to momentum and heat transfer" Ph.D. Thesis, Univ. of London.

39. KAWAGUTI, M. (1961) "Numerical solution of the Navier-Stokes equation for the flow in a two dimensional cavity". J. Phys. Soc. Japan, 16, 11, 2307-.

40. KESTIN, J. and RICHARDSON, P.D. (1963) "Heat transfer across turbulent incompressible boundary layers". Int. J. Heat Mass Transfer, 6, 147-189.

41. KLINE, S.J., REYNOLDS, W.C., SCHRAUB, F.A. and RUNSTADLER, P.W. (1967) "The structure of turbulent boundary layers". J. Fluid Mech., 30, 4, 741-773.

42. KNIGHT, H.R. (1966) "Heat transfer in separated flows". Imperial College, Mech. Eng. Dept. SF/TN/3.

43. KOLMOGOROV, A.N. (1942) "Equations of turbulent motion of an incompressible fluid" (In Russian). Izv. Akad. Nauk SSSR ser. Phys. No. 1-2.

44. KRALL, K.M. and SPARROW, E.M. (1966). "Turbulent heat transfer in the separated, reattached and redevelopment regions of a circular tube". ASME, J. Heat Transfer, 88, 1, 131-136.

45. LARSON, H.K. (1959) "Heat transfer in separated flows". J. Aero/Space Sci., 26, 11, 731-738.

46. LAX, P.D. and RICHTMEYER, R.D. (1956) "Survey of the stability of linear finite-difference equations". Comm. Pure and Appl. Math., 9, 267-293.

47. LEVICH, V.G. (1962) Physico-chemical Hydrodynamics Prentice-Hall, New York.

48. MACAGNO, E.O. and HUNG, T.K. (1967) "Computational and experimental study of a captive annular eddy". J. Fluid Mech., 28, 1, 43-64.

49. MALKUS, W.V.R. (1954) "Discreet transitions in turbulent convection". Proc. Roy. Soc. London, A225, 185-.

50. MARRIS, A.W. (1964) "A review on vortex streets, periodic wakes, and induced vibration phenomena". J. Basic Eng., Trans. ASME, Series D, 86, 2, 185-196.

51. MILLS, R.D. (1961) "Flow in rectangular cavities". Ph.D. Thesis, Univ. of London.

52. MILLS, R.D. (1965) "Numerical solutions of the viscous flow equations for a class of closed flows". J. Roy. Aero. Soc., 69, 714-718.

53. MOFFATT, H.K. (1964) "Viscous and resistive eddies near a sharp corner". J. Fluid Mech., 18, 1, 1-18.

54. MORKOVIN, M.V. (1964) "Flow around circular cylinder - A kaleidoscope of challenging fluid phenomena". Sym. on Fully Separated Flows, ASME, 102-118.

55. MUELLER, T.J. and ROBERTSON, J.M. (1962) "A study of the mean motion and turbulence downstream of a roughness element". Proc. 1st Southeastern Conf. on Theo. and Appl. Mech., Gatlinburgh, Tenn. May 3-4.

56. NIKURADSE, J. (1932) "Gesetzmässigkeiten der turbulenten Strömung in glatten Rohren". Forschungs-Arb. Ing.-Wesen, No. 356.

57. PAN, Y.F. and ACRIVOS, A. (1967a) "Heat transfer at high Peclet number in regions of closed stream-lines" Int. J. Heat Mass Transfer, 10.

58. PAN, F. and ACRIVOS, A. (1967b) "Steady flow in rectangular cavities". J. Fluid Mech., 28, 4, 643-655.

59. PATANKAR, S.V. and SPALDING, D.B. (1967) Heat and Mass Transfer in Boundary Layers. Morgan-Grampian, London.

60. PRANDTL, L. (1904) Proc. 3rd Intern. Math. Cong., Heidelburg, also, NACA TM 452.

61. PRANDTL, L. (1945) "Uber ein neues Formelsystem für die ausgebildete Turbulenz". Nachr. Akad. Wiss., Göttingen, IIA, 6-19.

62. PUN, W.M. and SPALDING, D.B. (1967) "A procedure for predicting the velocity and temperature distributions in a confined, steady, turbulent, gaseous, diffusion flame". Imperial College, Mech. Eng. Dept. SF/TN/11.

63. REIMAN, T.C. (1967) "Laminar flow over transverse rectangular cavities". Ph.D. Thesis. California Inst. of Tech., Univ. Microfilms, Inc. No. 67-17072, Ann Arbor, Mich.

64. REIMAN, T.C. and SABERSKY, R.H. (1968) "Laminar flow over rectangular cavities". Int. J. Heat Mass Transfer, 11, 6, 1083-1085.

65. RICHARDSON, P.D. (1963) "Heat and mass transfer in turbulent separated flows". Chem. Eng. Sci., 18, 3, 149-155.

66. RICHTMEYER, R.D. (1962) "A survey of difference methods for non-steady fluid dynamics". Nat. Centre for Atmospheric Res. Tech. Note 63-2.

67. ROTTA, J. (1951) "Statistische Theorie nichthomogener Turbulenz". Z. für Physik, 131, 51-77.

68. RUNCHAL, A.K., SPALDING, D.B. and WOLFSHTEIN, M. (1967) "The numerical solution of the elliptic equations for the transport of vorticity, heat and matter in two-dimensional flows". Imperial College, Mech. Eng. Dept. SF/TN/2. (In revised form SF/TN/14, 1968).

69. RUNCHAL, A.K. and WOLFSHTEIN, M. (1966) "A finite-difference procedure for the integration of the Navier-Stokes equations". Imperial College, Mech. Eng. Dept. SF/TN/1.

70. RUNCHAL, A.K. and WOLFSHTEIN, M. (1967) "A FORTRAN IV computer programme for the solution of the steady-state, two-dimensional equations of motion, energy and concentration". Imperial College, Mech. Eng. Dept. SF/TN/10.

71. SCHLICHTING, H. (1960) Boundary Layer Theory. McGraw-Hill, New York.

72. SCOTT, C.J. and ECKERT, E.R.G. (1966) "Heat and mass exchange in the supersonic base regions". AGARD, CP, No. 4, Part I, 429-.

73. SIMUNI, L.M. (1964) "The numerical solution of some problems in the flow of a viscous fluid". Inzh. Zhou., 4, 3, 446-450. (In Russian) (NLL Translation, RTS 3634).

74. SPALDING, D.B. (1964) "Contribution to the theory of heat transfer across a turbulent boundary layer". Int. J. Heat Mass Transfer, 7, 743-761.

75. SPALDING, D.B. (1966) "Some recommendations concerning research on separated flow phenomena". Imperial College, Mech. Eng. Dept. ON/1.

76. SPALDING, D. B. (1967a) "Notes on the solution of the Navier-Stokes equations for steady, two-dimensional turbulent flow by finite-difference methods". Imperial College, Mech. Eng. Dept. SF/TN/5.

77. SPALDING, D.B. (1967 b) "Heat transfer from turbulent separated flows". J. Fluid Mech., 27, 1, 97-109.

78. SPALDING, D.B. (1967c) "The calculations of the length scale of turbulence in some boundary layers remote from walls" Imperial College Mech. Eng. Dept. TWF/TN/31.

79. SPALDING, D.B. (1967d) "Monograph on turbulent boundary layers". Imperial College Mech. Eng. Dept. TWF/TN/24,33.

80. SPALDING, D.B. (1968) Personal communications.

81. SPALDING, D.B. and JAYATILLAKA, C.L.V. (1965) "A survey of the theoretical and experimental information on the resistance of the laminar sub-layer. to heat and mass transfer". Proc. 2nd All-Union Conf. on Heat and Mass Transfer, Minsk, USSR, 1964, 2, 234-264 (In Russian) (English Trans. Rand Corp. California 1966).

82. SPRENGER, H. (1959) Unpublished work. Mitt. Inst. Aerodynamic, E.T.H. Zürich.

83. SQUIRE, H.B. (1956) "Note on the motion inside a region of recirculation (Cavity flow)". J. Roy. Aero. Soc., 60, 203-205.

84. TANI, I. (1958) "Experimental investigation of flow separation over a step". Boundary Layer Res., 377-, ed. by H. Göertler Springer-Verlag, Berlin.

85. THOM, A. (1932) "Arithmetical solution of problems in steady viscous flow". A.R.C., R.& M. 1475.

86. THOM, A. (1933) "The flow past circular cylinders at low speeds". Proc. Roy. Soc. London. A141, 651-.

87. THOM, A. and APELT, C.J. (1961) Field Computations in Engineering and Physics. D. van Nostrand Co., London.

88. TOBIAS, C.W., EISENBERG, M. and WILKE, C.R. (1952) "Diffusion and convection in electrolysis - A theoretical review". J. Electrochem. Soc., 99, 12, 359c-.

89. VARGA, R.S. (1962) Matrix Iterative Analysis. Prentice-Hall International,London.

90. WEISS, R.S. and FLORSHEIM, B.H. (1965) "Flow in a cavity at low Reynolds number". Physics of Fluid, 8, 9, 1631-1635.

91. WIEGHARDT, K. (1945) Addendum to Prandtl (1945).

92. WOLFSHTEIN, M. (1967) "Convection processes in turbulent impinging jets". Imperial College, Mech. Eng. Dept. SF/R/2.

Nomenclature

1. Roman characters

Symbol	Meaning	Equation of first mention
A_E, A_W, A_N, A_S	coefficients associated with the convective terms in the finite-difference equation for Ø	(3.2-13)
B_E, B_W, B_N, B_S	coefficients associated with the diffusive terms in the finite-difference equation for Ø	(3.2-19)
c_p	specific heat of a fluid	(4.2-5)
C, C_1 etc.	constants in various equations	
C_E, C_W, C_N, C_S	coefficients associated with the successive-substitution formula for Ø	(3.2-24)
C_D	constant associated with dissipation of k	(4.1-7)
C_ϕ	constant associated with diffusion of k	(4.1-5)
C_μ	constant associated with μ_t	(4.1-6)
g_m	mean mass transfer coefficient	(7.2-1)
G_j	component of the mass-velocity in the direction j	(2.1-1)
G_m	mean mass-velocity in a pipe	(5.2-1)
$J_{\emptyset,j}$	component of the diffusional-flux of Ø, in direction j	(2.1-3)
k	kinetic energy of turbulence	(4.1-1) Table 2.4-1
k_*	non-dimensional k	(4.2-1)
l	characteristic length scale of turbulence	(4.1-5)
m	the mass of a chemical species	Table 2.4-1
p	static pressure	(2.1-2)
p_*	non-dimensional pressure-gradient along a wall	(4.2-1)

Symbol	Meaning	Equation of first mention
Pr	Prandtl number of the fluid (see non-dimensional parameters)	(5.2-1)
q''_s	heat-flux at a wall	(4.2-5)
r	radius - distance from the axis of symmetry	(2.1-1)
R	radius of a pipe	(5.2-1)
Re	Reynolds number of the flow (see non-dimensional parameters)	(5.2-1)
R_t	Reynolds number characterizing turbulence	(4.2-5)
$R_{t,J}$	value of R_t at the junction of laminar and turbulent regions	(4.2-7)
R_{t,J_*}	$\equiv R_{t,J}/R_t$	(4.2-7)
s	non-dimensional skin friction (see non-dimensional parameters)	(4.2-5)
S	source terms in the successive-substitution formula for ϕ	(3.2-24)
Sc	Schmidt number (see non-dimensional parameters)	(7.4-1)
St	Stanton number (see non-dimensional parameters)	(4.2-5)
S_ϕ	source terms for ϕ	(2.1-3)
S_ω	source terms for vorticity	(2.3-2)
T	temperature	Table 2.4-1
T_*	non-dimensional temperature	(4.2-1)
u_i	component of velocity in direction i	(2.1-1)
u_*	non-dimensional velocity	(4.2-1)
V_P	volume of the 'tank' over which the equation for ϕ is integrated	(3.2-21)
x_j	coordinate in direction j	(2.1-1)
y_*	non-dimensional distance normal to a wall	(4.2-1)

Symbol	Meaning	Equation of first mention
z	distance in the axial direction of a pipe	(5.2-1)
Z	non-dimensional distance in a pipe	(5.2-1)

2. Greek characters

α	a coefficient in the general differential equation for ϕ	(2.4-1)
β	a coefficient in the general differential equation for ϕ	(2.4-1)
Γ	a coefficient in the general differential equation for ϕ	(2.4-1)
Γ_ϕ	diffusivity for property ϕ	(5.2-1)
$\Gamma_{\phi,eff}$	effective diffusivity for ϕ	(2.2-2)
δ	a coefficient in the general differential equation for ϕ	(2.4-1)
μ	dynamic viscosity	(4.1-9)
μ_{eff}	effective viscosity	(2.2-1)
μ_t	turbulent viscosity	(4.1-4)
μ_*	non-dimensional effective viscosity	(4.2-1)
ρ	mass-density	(2.3-5)
σ_ϕ	Prandtl-Schmidt number for property ϕ	(4.1-10)
$\sigma_{\phi,t}$	turbulent Prandtl/Schmidt number for ϕ	(4.1-10)
$\sigma_{\phi,eff}$	effective Prandtl/Schmidt number for ϕ	(2.2-3)
τ_{ij}	component of the stress tensor in direction j acting in the plane with its normal in direction i	(2.1-2)
τ_s	shear-stress at a wall	(4.1-12)

Symbol	Meaning	Equation of first mention
τ^*	non-dimensional form of the wall shear-stress	(4.1-15)
ϕ	any dependent variable or conserved property	(2.1-3)
ψ	stream-function	(2.3-4)
ω	vorticity	(2.3-1)

3. Subscripts

B	the bulk value
C	at the edge of a Couette-flow
eff	effective value of the quantity concerned
i	in the direction i
I	at the inlet of a control volume
j	in the direction j
k	pertaining to the kinetic energy of turbulence
m	pertaining to the mass of a chemical species
O	at the outlet of a control volume
r	in the radial direction
S	at the surface
t	turbulent value of the quantity concerned
T	pertaining to temperature
z	in the axial direction
ϕ	pertaining to property ϕ
*	denotes a non-dimensional value of the quantity concerned

Also: P, E, W, N, S, NE, SE, NW, SW and the corresponding lower case letters denote the respective values at the corresponding nodes of the finite-difference grid (see Fig. 3.2-1 for illustration).

4. The non-dimensional parameters

Prandtl number $Pr \equiv \mu/(\rho.\Gamma_T)$

Reynolds number $Re \equiv (\rho.u_1.x_2/\mu)_C$ for Couette flows, and

$\equiv 2.G_m.R/\mu$ for pipe flow.

skin friction coefficient $s \equiv \tau_S/(\rho.u_1^2)_C$ for Couette flows, and

$\equiv \tau_S.\rho/G_m^2$ for pipe flow.

Schmidt number $Sc \equiv \mu/(\rho.\Gamma_m)$

Stanton number $St \equiv \dot{q}''_S/[c_p.\rho_C.u_{1,C}.(T_C-T_S)]$

for Couette flow,

$\equiv \dot{q}''_S/[c_p.G_m.(T_B-T_S)]$

for pipe flow with heat transfer, and

$\equiv g_m/G_m$ for pipe flow with mass transfer.